Naval Research Laboratory

Washington, DC 20375-5320

NRL/MR/6707--94-7462

Theoretical Aspect of Low Pressure Discharges in Simple Gases

WALLACE M. MANHEIMER

Senior Scientist Fundamental Plasma Processes
Plasma Physics Division

March 28, 1994

Approved for public release; distribution unlimited.

REPORT DOCUMENTATION PAGE

Form Approved
OMB No. 0704-0188

1. AGENCY USE ONLY (*Leave Blank*)	2. REPORT DATE	3. REPORT TYPE AND DATES COVERED
	March 28, 1994	Interim

4. TITLE AND SUBTITLE

Theoretical Aspect of Low Pressure Discharges in Simple Gases

5. FUNDING NUMBERS

PE - 61153N

6. AUTHOR(S)

Wallace M. Manheimer

7. PERFORMING ORGANIZATION NAME(S) AND ADDRESS(ES)

Naval Research Laboratory
Washington, DC 20375-5320

8. PERFORMING ORGANIZATION REPORT NUMBER

NRL/MR/6707--94-7462

9. SPONSORING/MONITORING AGENCY NAME(S) AND ADDRESS(ES)

Office of Naval Research
800 North Quincy Street
Arlington, VA 22217-5660

10. SPONSORING/MONITORING AGENCY REPORT NUMBER

11. SUPPLEMENTARY NOTES

12a. DISTRIBUTION/AVAILABILITY STATEMENT

Approved for public release; distribution unlimited.

12b. DISTRIBUTION CODE

13. ABSTRACT (*Maximum 200 words*)

Discharges processing is becoming more and more important in many industries. This paper attempts to bring together, in relatively compact form a basic derivation of the physics of processing discharges including collision theory, kinetic theory, simple chemical reactions, fluid formulations and sheath physics.

14. SUBJECT TERMS

Discharges
Processing
Sheaths

15. NUMBER OF PAGES

132

16. PRICE CODE

17. SECURITY CLASSIFICATION OF REPORT	18. SECURITY CLASSIFICATION OF THIS PAGE	19. SECURITY CLASSIFICATION OF ABSTRACT	20. LIMITATION OF ABSTRACT
UNCLASSIFIED	UNCLASSIFIED	UNCLASSIFIED	UL

NSN 7540-01-280-5500

Standard Form 298 (Rev. 2-89)
Prescribed by ANSI Std 239-18
298-102

CONTENTS

THEORETICAL ASPECTS OF LOW PRESSURE DISCHARGES IN SIMPLE GASES

1. Introduction

Low density discharges have been an important part of plasma processing, which has grown into a tremendously important industrial tool over the last 20 years. Both the National Research Council[1] and Naval Studies Board[2] have recommended that plasma processing be put on a firmer scientific footing, and point to several areas where industrial processes are limited by the plasma itself. Shohet[3,4] points out that the markets and potential markets for materials produced by plasma processing is in the hundreds of billions of dollars. Also he quotes several industrial users as needing a better understanding of the plasmas in their devices to fully exploit the potential. Plasma processing occurs over a huge volume of parameter space and involves many disciplines. As Shohet points out, no one person can summarize all of it now. This paper attempts to set out the basic plasma physics of low density discharges, which is a very important aspect of the overall field of plasma processing.

Another reason for interest in the area regards its recent history[5]. Figure (1.1), from Ref.(5) shows the number of elements on a chip and the scale size for the design rules as a function of time. The authors call the 25 year record of innovation unmatched in all world history. As an illustration, the computer this is typed on contains about ten million transistors, an amazing number of manufactured items for an individual to own. By contrast, ten million paper clips costs about as much as a house. Much of this innovation resulted directly from plasma processing with low density discharges. As the design rules get tighter, the requirements on the low density processing plasma also become more difficult to meet, and it becomes more and more important to understand the plasma itself.

There are a large number of American textbooks in plasma and discharge physics [6,7,8,9,10,11,12,13,14]. However these do not completely cover the aspects of discharge physics most relevant to plasma processing. The two that come closest to what is presented here are two English translations of older Russian texts[15,16] which are probably not very widely available here now. Furthermore there are several other books devoted to plasma processing[17,18,19,20], and a very extensive one is in preparation[21]. This paper hopes to complement these and also to stake out its own

Manuscript approved February 14, 1994.

role as covering important aspects of the theory, along with comparisons with experiment and simulations. It hopes to be an educational resource as well as a review of recent literature.

With the current importance of plasma processing, there are now many attempts at modeling the plasma both with fluid simulations[22,23,24,25,26,27,28,29], Monte-Carlo modeling of particle streams in sheath fields[30,31,32,33,34,35], and full particle simulations[36,37,38,39,40,41,42,43,44,45,46,47]. There is less analytic work, but nevertheless, analytic work is doable and important[48,49,50,51,52,53,54]. In fact analytic work and numerical simulations nicely complement each other. Analytic work can derive scaling laws, elucidate the basic physics, and generally see the forest rather than the trees. As Art Buchwald put it, *War is too important to leave to the computers.* Numerical modeling, of course is the only way of solving the seemingly intractable problems related to the low density discharges.

Now we will very briefly discuss some industrial plasma processes using low density plasma processes, to see what direction they drive the theory. We will start with integrated circuit fabrication, described more fully in the cited books. Typically the challenge is to etch a precise pattern into a substrate, often silicon or silicon dioxide. Atop the wafer is a mask which has the pattern in it. One would like to expose the covered wafer to something that the cover is impervious to, but which etches the silicon. In the early days of integrated circuit fabrication, the etch was usually done chemically. However as characteristic sizes were reduced over the years, chemical etching became less and less satisfactory. For one thing, chemical etching is typically isotropic, so that the mask is undercut by the etch. As tolerances became tighter, this became unsatisfactory since one line etched into the silicon would run into its neighbor. The solution for these narrower line widths, has been to use a plasma etch. The plasma has two advantages, first it produces the etch material in a dry environment, and secondly, the etch is anisotropic, so the trench edge is nearly vertical. One great advantage of the plasma, is that electron collisions produce not only charged particles, but also free radicals. When they strike the workpiece however, they react very strongly. These free radicals, which do not exist long in liquids or high density gases, can be readily produced and maintained in the plasma environment because the electrons of the plasma have more than enough energy to generate them. However the electrons, while energetic compared to

the background, have such low density that they do not appreciably increase the energy content of the entire gas. Thus a plasma gives rise to the possibility of high energy density chemistry at low gas energy density.

Now let us consider the anisotropic nature of the etch[55]. The workpiece is exposed not only to the neutral free radicals, but also to the streaming ions which form the plasma sheath. The ions and fast neutrals impinge perpendicular to the workpiece. Thus the bottom of the trench will be struck by the ion flux, and the side walls will not be. In Fig.(1.2) is shown a schematic of the features of wet and plasma etching along with a microscope photograph of a very deep trench produced by a plasma etch.

While the total process just described involves complicated aspects of surface and gas phase chemistry, the plasma is important also. Specifically we would like a plasma theory to be able to predict the production of free radicals as well as the flux and energy spectrum of fast ions and neutrals to the surface. At low density, the gas chemistry depends greatly on the electron distribution function; and in the cases where a fluid model for the electrons apply, on their density and temperature. The flux and spectrum of fast ions and neutrals to the workpiece depends crucially on how the plasma sheath is set up. Different types of plasma set up different types of sheaths, and the industrial process exploits this. For instance a DC discharge has a cathode sheath with very little flexibility, as we will see. While it is sometimes useful, one has more control over the sheath of a planar RF plasma, and this is the workhorse of low density plasma processing today. As the design rules tighten, one would like still more control as well as lower neutral density. This is forcing the plasma toward electron cyclotron resonance, helicon, or induction reactors. A description of these is still very much in the research phase, this paper concentrates on the dc and rf plasma, where the theory is much better established.

In addition to etching, plasmas are used for deposition also. One of the most spectacular has turned out to be the deposition of thin diamond films[56,57,58,59]. Diamond has remarkable properties regarding hardness, as well as thermal and electrical properties. Until recently, they were available only through natural mining, or high temperature, high pressure compression of carbon. In the last ten years it has been discovered that diamond films could be

deposited on substrates by plasma chemical vapor deposition. Typically the plasma are CH_4-H_2 or other mixtures. The plasma density ranges from the very low to the very high, but low density discharges are used at a number of institutions.

The actual deposition process is very complicated and does not seem to be well understood at this point. If a layer of carbon is deposited on a substrate, the energetically favored form is graphite, not diamond. However since the particle stream impinging on the substrate is quite energetic, there is sufficient energy flux to form the less favorable diamond structure. Typically, a large fraction of the deposited carbon is in graphite form, and a much smaller part of the deposited carbon is in the diamond structure. The idea then is to eat away the graphite as rapidly as it builds up, so that what is left is a diamond film. The deposition rate is typically microns per hour. This is done in two ways, first by heating up the substrate to keep it less hospitable to graphite and more to diamond, and second to have a flux of free radicals on the substrate. The flux of free radicals also eats away at the graphite much faster than it does the diamond.

The plasma then seems to play the role of a source of free radicals and as a source of energy to initially form the diamond crystal. The free radicals come mostly from electron interactions with the background gases. Thus what one needs from a theoretical model is the electron density and temperature (or electron distribution function if the electrons are not Maxwellian) and the free radical production

Finally we will consider the case of Plasma immersed ion implantation (PIII)[3,60]. Often one has a metal, a tool for instance, and one desires to implant guest ions up to a certain depth in the metal, for surface modification. For instance nitrogen is often implanted in steel to harden the surface, and/or to reduce the surface friction. To implant the nitrogen to the necessary depth, it must be driven into the metal at energies of typically 100 keV and higher. At first one might think an ion accelerator would be required. However this has disadvantages in that the ions all are accelerated in one direction and the workpiece might not be planar. An alternative would be to put the workpiece in a plasma and pulse it with a negative voltage pulse. Then ions will be accelerated from the plasma into the workpiece. As long as the object is large compared to the plasma sheath, the ions will be accelerated perpendicular to the surface. We would like a plasma theory to tell

us the ion dose in terms of the plasma and external circuit parameters.

The theory we work out in this report is guided by what appear to be the needs for the plasma processors just described. We begin in Section 2 with a description experimental results on dc and rf discharges. Sections 3-7 review collision and reaction processes in processing discharges. While we emphasize low density discharges here, where thermal equilibrium considerations can be simply included we have occasionally done so, not only for completeness sake, but also because a relevant reaction rate can often be more easily be calculated by first calculating its inverse and then using detailed balance. We assume that cross sections for the appropriate processes are known and the theory we work out will be in terms of these cross sections. Section 3 reviews the basic physics of simple collisions. The next problem is the kinetic theory of a gas of particles with no internal structure, but which interact with each other via binary collisions. This is described in section 4. There, there are relations between each collision process and its inverse which have important implications for the equilibrium theory. For the case of collisions of particles with no internal structure, these relations are not difficult to see from the basic collisional descriptions. The case of particles with internal structure are described first for the case of atoms in Section 5. As the particles have more and more complicated internal structure, relations between the collision and its inverse become less and less obvious. However these relations are still necessary in order for equilibrium statistics to hold.

Section 6 discusses an infinite homogeneous molecular plasma. This gets even more complicated because now there is chemistry as well as excitations and ionizations. In fact one of the most intimidating things about a processing plasma is the very large number of potential reactions, and the necessity of sorting them out. For instance Sommerer and Kushner and others enumerate a large number of reactions for certain simple and more complicated plasmas[61],[62]. We consider a fairly simple molecular plasma, but one still of importance in processing discharges, the oxygen plasma. However even this plasma has a tremendous amount of chemistry potentially occurring. Possible components are O_2, O, O_2^+, O^+, O^-, O_2^-, O_3, O_3^+, O_3^-, electronically excited oxygen, electrons, and possibly clusters. The number possible of reaction channels is huge, and one must keep only the most important. While the chemistry is

very important, it cannot be the whole story of the plasma. As we will see, for the oxygen plasma, there are components which have no reasonable equilibrium in a low density plasma if one considers chemistry alone. For instance at low electron density, recombination is unimportant. Also atomic oxygen can be produced by electron impact dissociation, but since three body reactions are unimportant at low density, it cannot recombine. Thus there are no sinks for electrons or atomic oxygen, and no sources for molecular oxygen. Thus at low density, chemistry alone cannot describe the equilibrium.

Section 7 discusses the solution for the distribution function in a homogeneous plasma in an electric field. The full processing plasma, which is described by the Vlasov equation for all species coupled to Maxwell's equations for the fields is much too complicated to solve, or even simulate. However for plasmas dominated by binary collisions, there are scaling laws, which in some cases can relate solutions to one another. This is described in Section 8.

Solving the Vlasov equation involves following the time dependence a function of 6 variables, three velocity dimensions and three position dimensions. A fluid formulation however has only three spatial dimensions, so if there is any justification for it, it is greatly simpler than a Vlasov formulation. In a multi-dimensional fluid formulation rather than a zero or one dimensional Vlasov formulation, one is essentially trading thermal realism for geometric realism. In processing plasmas where complicated geometry plays an important role, laminar[63,64,65], and turbulent[66] fluid simulations play an important role. The fluid formulation for the charged species in the presence of the neutrals is derived in Section 9. Usually, even for low density plasmas, the fluid equation gives a reasonable approximation for the bulk, although the chemistry often depends on just what the tail of the electron distribution function is.

Typically most of the plasma volume is quasi-neutral so the electron and ion densities are equal. However near walls, the quasi-neutrality approximation breaks down. This breakdown manifests itself in the steady state quasi-neutral fluid solution by the presence of a singularity[67,68,69,70,71]. This singularity signals that the quasi-neutral central part must transition into a non-neutral sheath. This can be a very complicated mathematical problem,

although in the cases discussed here, it turns out to be not too difficult. Typically the sheath width is very small compared to the other lengths in the plasma, including the mean free path. Thus a fluid model is not necessarily valid for the sheath. However there are often other simplifications, for instance the neglect of collisions or a one dimensional structure. This is discussed in Section 10.

Sections 11 discusses the bulk plasma in a DC cylindrical discharge. It shows how the quasi-neutral part couples to the sheath and how mass, momentum and energy are coupled from the external circuit to the plasma. As an example, let us consider again the oxygen plasma in a cylindrical configuration. We pointed out earlier that there was no steady state determined by chemistry alone because there were only sources for electrons and atomic oxygen, but only sinks for molecular oxygen. In the finite cylindrical system however there is a possible equilibrium. The electrons, oxygen atomic and molecular ions, and oxygen atoms are produced in the bulk and diffuse to the wall. The molecules are lost in the bulk. However at the wall the electrons, oxygen atomic and molecular ions, and oxygen atoms recombine to form molecular oxygen, since the wall now acts as the third body for three body collisions. This molecular oxygen then diffuses from the wall back in to the bulk, and allows the formation of a low density steady state. Thus in the oxygen plasma, the low density equilibrium is an interplay between the chemistry, and what might be called the conventional plasma physics. Neither alone is sufficient to form the equilibrium.

Sections 12 discusses the cathode sheath of a DC plasma. This is one of the oldest observations in all plasma physics and still one of the most complicated. Strictly speaking, the sheath is not fluid like, and it is inherently collisional. We discuss both simple and more complicated models of the sheath and compare with experiments. Section 13 discusses both the sheath and bulk of an rf plasma an compares with experiments. To summarize, we will see that there is a good bit of theory that can be done, and that it does not do too bad a job in explaining many of the features observed in low density discharges in simple gases.

2. Measurements on Processing Type Discharges

In this section we will discuss measurements of plasmas of the type used in processing discharges. These are dc and rf discharges. Particularly for dc discharges, basic experiments, regarding both the bulk and sheath regions go back nearly a century and work is still proceeding. To illustrate this, we will cite some early results taken from the oldest textbooks found in the NRL library. The work on rf discharges seems to be much more recent. Most studies of the sheath region in rf plasmas seem to date from about the late sixties.

In a dc plasma which is very weakly ionized, the parameters of the plasma often depend on the electric field E divided by the neutral density N. A large amount of data for this sort of plasma has been summarized by J. Dutton[72] . This data is usually called swarm relations, because it is basically data regarding a swarm of electrons in a gas acted on by an electric field E. The electron density is assumed to be so small compared to the neutral density, that any effect proportional to the square of the electron density (for instance electron electron collisions, electron ion collisions, or collisions of electrons with neutrals excited by electrons) is assumed negligibly small. Calculations of the electron distribution function are then calculations using the Boltzman equation, but the equation is linear in electron density. Typically a background gas temperature is assumed and the electron distribution function is then calculated accounting for the various elastic and inelastic collision processes. We will show a simple example of such a calculation later on. Furthermore, the average properties of the electron swarm (for instance drift velocity, temperature, ionization rate, excitation rate, etc) can often be measured and compared with the theoretical calculations.

One example is for oxygen (O_2), and the data is taken[73]. Shown in Fig.(2.1a) are plots of the momentum and exchange collision frequencies divided by neutral number density as a function of characteristic electron energy (ie electron temperature). Through the graphs are empirical straight lines covering the temperature range characteristic of processing oxygen plasmas, about 0.5 to 5 eV. Although the data does not exactly fit a straight line, each one fits to within about a factor of two over the entire range of interest to processing plasmas, that is energies from about 0.5 to about 5 eV. The slopes of the line for momentum collision frequency is 0.5 and

that for energy exchange is 2.6. Analogous data is given for Nitrogen[74]. The slopes then become 0.7 and 3.4. Since the slope of ν_p (which is the collision cross section times the thermal velocity times the background gas density) versus energy is 0.5 for oxygen, the collision cross section is nearly constant as a function of energy. For nitrogen, the cross section does have a weak dependence on energy, $\sigma_p \propto E^{0.2}$.

Shown in Fig.(2.1b) are plots of electron drift velocity and electron temperature for oxygen as a function of electric field divided by neutral number density. (Hake and Phelps call it average energy, but from the numerical factors used in their definition, it is in fact the temperature.) Again, straight lines are drawn through the data and the slopes are respectively 0.7 and 0.5. For nitrogen, a similar analysis of the data gives slopes of 0.8 and 0.4. Later on, we will develop a theoretical model for the relation between these slopes. For the case of oxygen, the drift velocity versus E/N fits the power law quite well. The agreement is not quite as good for the temperature, and other power law indices between about 0.35 and 0.55 could also give reasonable agreement. The index we chose. 0.5 also gives reasonable agreement to the cathode fall theory we will develop later on.

It is important to realize that the rapid increase of energy exchange collision frequency in Fig 2.1 cannot be sustained for much higher energies than the 5 eV shown. In fact for most simple gases, at energies corresponding to the electron temperatures of processing plasma, the electron momentum exchange collision frequency remains the collision process with the largest cross section. Shown in Fig. 2.2 are the momentum exchange and inelastic cross sections for O_2, N_2, and O as a function of energy.[75] Of particular interest is the peak in the nitrogen elastic and inelastic collision frequency between about 2 and 4 electron volts. This is the excitation of vibrational states of nitrogen at these energies. It is also important to realize that this peak depends on the vibrational temperature of the neutral gas. As the neutral gas heats, energetic vibrationally excited molecules can give energy back to the electrons in a collision and this peak decreases in amplitude. At energies below 100 eV, the momentum exchange cross section is dominant by at least an order of magnitude at nearly all electron energies. Of course at very high electron energy, momentum exchange becomes less important compared to other processes.

We now turn to the classical self sustaining gas discharge. It has a cathode at one end, an anode at the other end, and is surrounded by a cylindrical glass tube. The characteristics of the discharge vary both as a function of distance along the tube z, radius r, and as a function of the Voltage, or what is generally more convenient, the current between the electrodes. Note that the current and Voltage cannot be separately specified, they are related by whatever the Ohm's law is for the plasma.

The typical Voltage versus current curve for a dc discharge is shown in Fig.(2.3) taken from Cohen[76]. This is for air at a pressure of 1 Torr with metal electrodes of 100 cm^2 and separated by 30 cm. At very low current, the Voltage increases very rapidly with current and then levels off. This is the Townsend discharge which is usually not self sustaining. That is it relies on electron emission, typically photo-emission from the cathode. The current densities are so small that vacuum fields are basically unperturbed by the plasma. At a certain current, the discharge is self sustaining and over a large range of currents, the Voltage is constant. This is the normal glow, at which the vacuum fields are strongly perturbed by the plasma. As the current increases, there is second critical current at which the Voltage again begins to increase with current. This is the abnormal glow. In both glow modes, the current near the cathode is sustained by ions streaming into the cathode and being absorbed there. The current is limited by the very small currents ions can carry because of their large mass and low velocity. Within the bulk of the plasma however, the current is always carried by electrons. The question of how ion current near the cathode transitions to electron current in the positive column is very interesting and will be discussed later on. Finally at higher current still, the Voltage decreases again with current and one is in the arc mode. Here one relies on electron emission from the cathode caused by local heating of cathode spots by the discharge itself. We concern ourselves here with the normal and abnormal glow regimes.

We now turn to the axial structure of the plasma. A photograph of such a discharge, along with plots of various parameters, taken from L. Loeb[77],is shown in Fig.(2.4). Actually an earlier photograph of the same sort of thing was shown in A. von Engel and M. Steenbeck[78]. Most of the length of the discharge appears to be a uniform plasma which the authors call the positive column. It is characterized by a uniform electric field and a uniform

luminosity. The current is virtually entirely electron current. Earlier researchers investigated whether the positive column had any inherent length like the cathode and anode sheath regions. Both Brown and Chapman quote Hittorf in an experiment attempting to measure this length. He lengthened a tube until it ran back and forth across his lab. At this stage, a frightened cat pursued by a pack of dogs came through the window. "Until an unfortunate accident terminated my experiment" Hittorf wrote, "the positive column appeared to extend without limit."

Studies of the positive column have been made by Bickerton and von Engel[79]. They show that for an unmagnetized helium plasma, the electron temperature depends on Rp where R is the radius of the discharge and p is the background pressure in torr. Shown in Fig.(2.5a) is some of their data. The curves shown are various theoretical curves which will be discussed in a later section. The presence of a magnetic field parallel to the axis has the effect of reducing the electron temperature. Fig.(2.5b) also shows the temperature as a function pressure for a 1.8 cm radius tube for a magnetic field of 440 Gauss. The curve shown is a theoretical curve to be introduced later on. Actually the positive column is not as simple as this data indicates. Often the positive column is striated, and this is discussed both by Loeb, and von Engel and Steenbeck. Furthermore, for magnetic fields above a critical value, the positive column becomes unstable[80]. This instability was described experimentally and theoretically by Kadomtsev and Nedospasov.

Near the anode there is a sheath region which Fig.(2.4) shows as having increasing potential as one approaches the anode. Actually this is the wrong polarity. Chapman (Fig(4.2)) shows a graph similar to this with the increasing potential. However in his more detailed discussion of the anode sheath, he shows that the potential is decreasing toward the anode (Fig(4.4)). That is the plasma potential is the highest potential, even higher than the anode potential. The electron current to the anode is very small compared to the current from a one sided Maxwellian distribution at the electron density in the positive column. Thus there must be a retarding potential which repels the electrons from the anode. It lowers the electron density until the current from the one sided Maxwellian is equal to the actual electron current. The need to repel the electrons leads to the plasma to be at a higher potential than even the anode.

The cathode sheath is much more complicated still. There is both a much larger potential drop and a more complex structure. In fact, unless the positive column has very long length, almost all of the potential drop is across the cathode sheath region, called the cathode fall. Near the cathode, there is a positive space charge, and most of the current to the cathode is ion current. Typically the cathode is not a strong electron emitter, so that most of the current is ion current. In fact, for each energetic ion impinging on the cathode, γ electrons are back emitted. For cathode materials and energies characteristic of glow discharges, typically $0.1<\gamma<0.3$.

Earlier researchers carefully investigated the structure and scaling of the cathode fall region. Both Loeb and Darrow[81] point out that the width of the cathode fall region, d_n, is inversely proportional to background gas number density N. Furthermore, with some variation, the current scales basically as N^2. One of the most striking scalings to come from this work is the constancy of Voltage over the normal glow regime. As Darrow puts it(p406), "It is one of the dogmas of modern physics that the ordinary cathode fall V_n is determined entirely by the nature of the electrode and the nature of the gas. As some express it, V_n is a "*material constant*" whereas I and d_n are not for they vary with the pressure of the gas". For typical gases and electrode materials, this Voltage V_n varies from about 150 to 300 Volts. Darrow, Loeb and von Engel all tabulate V_n's for various gases and electrode materials.

Actually, what happens in the normal glow regime is that the current density is constant as a function of radius, but the total current increases depending on how much of the cathode surface is covered with the discharge. Fig (2.6a), from Darrow shows the current as a function of the illuminated area of the cathode, showing a linear relation. When the entire cathode is covered by plasma, one then enters the abnormal glow regime where the current then increases with Voltage.

Within the cathode fall, the electric field, to a good approximation is a linear function of distance from the cathode surface. Fig.(2.6b), taken from Darrow shows the linear variation of the electric field as a function of distance. Experiments in planar[82] hollow[83,84] cathodes also show a basic linear variation of electric field with distance. We will see that there are good and reasonably simple analytical models for all of these features.

We now turn to rf discharges. Also we consider only the rf discharges driven at 13.5 MHz so as to reduce the size of the parameter space. This frequency is the principle frequency used in industrial plasma processing. As far as physics regime is concerned, it is much less than the electron plasma frequency and much greater than the ion plasma frequency. Thus the electrons respond to the instantaneous fields (both the rf fields and any induced dc fields), and the ions respond to the average fields which they see. Work on rf discharges, both as fundamental studies and for plasma processing seems to go back to the late sixties and early seventies[85,86,87,88,89,90,91,92,93,94], although some work goes as far back as the mid fifties[95]. V. Godyak has published some of the seminal work in the area[96,97,98,99,100,101].

Radio frequency discharges are like dc discharges in some ways, and are very different in other ways. Typically an rf current is driven between two parallel plates. As in the dc case, there is a central plasma which is reasonably uniform, and at each electrode, there is a sheath. These sheaths are characterized by both dc and rf electric fields. The dc fields accelerate the ions into the electrode, as in the dc discharge. However unlike the dc case, these fields accelerate the ions into both electrodes. Furthermore, unlike the dc case, the electrodes do not necessarily have to be conductors. That is if the electrodes are insulators, the fields can be capacitatively coupled in a rf discharge (in other words, near the electrodes, there can be displacement current instead of conduction current). The fact that the electrodes can be insulators is significant industrially, since the workpiece is not always a metal. Secondly, as we have seen, the Voltage for the dc cathode sheath has to be above a minimum value. For the case of the rf sheath, there is no such minimum.

Godyak enumerates three regimes for the discharge. The first is the collisional regime, where power is put into the bulk plasma by conventional Ohmic heating. At lower density and higher driving currents, the electrons mean free path is comparable to or larger than the length. The discharge can still form, but the heating is now stochastic heating of the electrons, caused by the electrons being reflected from oscillating sheaths. Finally at sufficiently high currents, the dc voltage drop at the electrode becomes larger than that required to sustain the corresponding dc discharge. In this case, secondary electrons emitted from the electrode and

accelerated in the dc fields play an important role. Godyak calls this the γ mode of operation. Here we concentrate mostly on the collisional regime.

Shown in Fig (2.7a) are data from Godyak of probe data for the density and temperature as a function of rf driving current. His system was nearly one dimensional, with 160 cm^2 electrode area and electrode separation of 6.7 cm. Other than the electrical drive parameters, the main additional parameter was the gas pressure. For the data in Fig (2.7a), the gas pressure was 0.3 Torr. The data shown is for argon, and data was taken for both argon and helium. Up to a drive current of about 40 mA/cm^2, the electron temperature is constant at about 4 eV and the density increases linearly with current. Beyond this, the temperature falls and the density rises more rapidly. Godyak attributes this to the transition to the γ mode. Although the temperature falls, the electron distribution begins to sprout a tail on non thermal electrons.

Shown in Fig (2.7b) is a plot of discharge power dissipated versus current for the same discharge parameters. Also drawn in are two straight lines corresponding to linear increase in power with current and also corresponding to an increase with the current to the 2.5 power. As we will see, this data is reasonably consistent with theory of rf discharges in the collisional regime. Finally, in Fig (2.8) is shown an analogous power plot for the collisionless case, where the pressure is 0.003 Torr. The straight lines shown now have slopes 4/3 and 8/3.

3. Particle Collisions in Processing Discharges

Since processing discharges are weakly ionized, the most important gas phase collision processes are those with the background neutral gas. Here we briefly review the basic binary collision processes. Many different types of elastic and inelastic collision processes are important in a processing discharge. First we consider binary collisions between two particles labeled with subscript a and b. The initial velocities are v_a and v_b, and the masses are m_a and m_b. The center of mass velocity is given by

$$v_o = (m_a v_a + m_b v_b)/(m_a + m_b) \qquad (3.1)$$

and the relative velocity is given by

$$v = v_a - v_b \qquad (3.2)$$

Velocities after the collision are denoted by primes. If the energy change in the collision is denoted by ΔE, corresponding to a change of an internal state of one of the colliding particles, conservation of momentum and energy gives the result

$$v_o = v_o', \quad \mu v^2/2 = \mu v'^2/2 + \Delta E. \qquad (3.3)$$

where μ is the reduced mass $m_a m_b/m_a+m_b$. Thus, according to Eq.(3.3), the change of internal energy can come only from the motion about the center of mass. If the two input velocities v_a and v_b are known, conservation of momentum and conservation of energy (assuming ΔE is specified) give four of the six unknown velocity components for the particles after the collision. We define the other two components in terms of two collision angles. These are θ, the scattering angle in the center of mass frame, and ϕ, the angle about the scattering plane. The minimum distance of the linear orbit of, for instance particle a from the center of mass position, defines an impact parameter b. The relation between b and θ defines the scattering cross section as

$$\sigma(\theta,v)\sin\theta d\theta = b db \qquad (3.4)$$

Often published graphs of scattering cross section are integrated over angle, so that what is shown is perhaps $\int\sigma(\theta,v)d\Omega$, for estimates

of total number of collisions, or $\int\sigma(\theta,v)(1-\cos\theta)d\Omega$, for estimates of momentum or energy change. Here Ω denotes solid angle.

In an elastic collision ($\Delta E=0$), Eq.(3.3) shows that the magnitude of the relative velocity of the two particles remains the same before and after the collision so it rotates through the angle θ in the scattering. One can calculate the change in momentum of particle a:

$$\Delta \mathbf{p}_a = -\mu(1-\cos\theta)(\mathbf{v}_a-\mathbf{v}_b) \qquad (3.5)$$

A straightforward calculation of the energy change of particle a gives the result

$$\Delta K_a = -k(1-\cos\theta)[2K_a-2K_b + (m_b-m_a)\mathbf{v}_a\cdot\mathbf{v}_b] \qquad (3.6)$$

where $k = [\mu/(m_a+m_b)]$.

Since the electron is so light compared to the atoms, it loses momentum at about the collision frequency, but loses energy much more slowly. Thus in low density processing plasmas, the equilibrium normally is one in which the electron temperature can be much higher than the gas or ion temperature.

Let us now calculate the force between electrons and atoms in a discharge if they have an average drift with respect to one another. This is

$$\mathbf{F}_e = -\mu\int d^3v_e d^3v_a\, n_e n_a f_e f_a(\mathbf{v}_e-\mathbf{v}_a)v\sigma_p(v) \qquad (3.7)$$

where n_e is the electron number density, f_e is the electron distribution function normalized to unity over velocity, and analogously for atoms. The quantity σ_p is the momentum exchange cross section,

$$\sigma_p(v) = \int d\Omega\sigma(\theta,v)(1-\cos\theta) \qquad (3.8)$$

Analogously for collision frequency, $\nu_p = n_a v\sigma_p$. It is this collision frequency as a function of energy which was plotted in Fig (2.1a) for O_2. Since momentum is conserved, there is an equal and opposite force on the atoms. To evaluate the integrals, one would have to

calculate the magnitude of the relative velocity in terms of $\mathbf{v}_e$ and $\mathbf{v}_a$. We do this in Section 7 where fluid equations are derived, and assuming a fairly simple collision model. A similar calculation for the kinetic energy exchange between isotropic distributions electron and atoms for elastic collisions is given by

$$K_e' = -k\int d^3v_e d^3v_a [2K_a - 2K_e + (m_e - m_a)\mathbf{v_a}\cdot\mathbf{v_b}] n_e n_a v\sigma(v) \qquad (3.9)$$

with an equal and opposite term for the atoms. We evaluate this also in Section 7.

To proceed with a description of a processing plasma, it is necessary to have a knowledge of the collision cross section σ_p as a function of energy. For the processing plasmas which are not simple chemically to begin with, and then which decay into many species of ions and free radicals, this information is not always easy to obtain, and qualitative estimates are often the best one can do. Brown is one place where data is tabulated, and he gives a prescription for how one might obtain various collision data with a computerized library search. For some of the simpler gases, we show some data here taken from Brown. The simplest case is a rare gas plasma because it is atomic. In Fig.(3.1a) is shown the momentum exchange collision cross section for argon as a function of energy. In the regimes of interest to processing plasmas, about 1-10 eV, the cross section is an increasing function of energy, so the collision frequency is an even more rapidly increasing function of energy. Above about 10 eV, the collision cross section is reaonably constant over the energies of interest to processing discharges, and then slowly decreases with energy. The minimum cross section at about 0.3 eV is called a Ramsauer minimum. Shown in Fig (3.1b) is the momentum exchange cross section for helium, also from Brown. This is a decreasing function of energy. In fact since it decreases roughly as $E^{-1/2}$, the collision frequency is approximately constant as a function of energy.

Molecules, but not atoms, have excitations that have energies typically comparable to or less than the electron temperature in processing plasmas. These are the rotational states (excitation energy of typically 10^{-4}-10^{-2} ev) and vibrational states (excitation energy of typically 10^{-2}-2 ev). Often the inelastic collision rate for excitation of these states is quite high, so much so that in molecular plasmas, the energy loss collision frequency of electrons

is much greater than that for atoms, $2(m/M_a)\nu_p$. For the case of molecules, we relate the energy exchange collision frequency to the momentum exchange collision frequency by a factor $\zeta(v)$. The Westinghouse Research Laboratory has measured and calculated many of these cross section in the mid sixties. This is what is shown in Fig.(2.1a) for O_2 as a function of energy.

Shown in Figs.(3.2a and b) are the cross sections for elastic, electronic, vibrational and ionization cross sections of O_2 as a function of energy from Ref.(73). From the cross sections shown, it appears that the $\zeta(v)$ factor will not be grater than about 0.1 at any energy.

We will now consider inelastic processes like ionization, dissociation of molecules, or excitations of electronic states which have a relatively high threshold energy (say 10-20 eV) compared to the the electron temperature in most processing plasmas. Since the electrons are the energetic species in the bulk of a processing discharge, they are the source of all such processes assuming they occur in the bulk. (There are energetic ions in the sheaths which we will consider later.) In Fig (3.3a), from Brown, is shown the ionization cross section as a function of energy for a variety of molecular gases.

Once the cross sections are given, the rate for the process can be calculated. For instance let us say the process of interest is the ionization of background atoms by electron impact.. The impact ionization cross section is then given as some function of v. The rate at which ions are produced by impact ionization is then given by

$$n_e' = \int d^3v n_e n_a v \sigma_i(v) f_e \equiv \alpha_i(T_e) n_e n_a \qquad (3.10)$$

Let us assume that the electron distribution function is Maxwellian and take the relative velocity between the electron and atom to be equal to the electron velocity. The ionization cross section is zero until one is above the threshold energy E_i. Then it increases roughly linearly with energy until is maximizes at a value of σ_o at about four times the threshold energy, at which point it decreases again with energy, generally as $\ln E/E^{-1}$. If $E_i >> T_e$, as is usually the case with processing plasmas, we will approximate the cross section as

$$\sigma_i = \sigma_o(E-E_i)/3E_i \qquad (3.11)$$

Then the expression for $\alpha(T_e)$ can be written as approximately

$$\alpha_i(T_e) \approx [4\sigma_o/3][T_e/2\pi m]^{1/2}\exp-(E_i/T_e), \quad E_i/T_e<<1 \qquad (3.12)$$

with T_e in ergs. Analogous expressions can be written for excitations of electronic states, dissociation of molecules, and any other process having a high excitation energy, as long as the electrons are Maxwellian. The exponential factor is the same factor as appears in the so called Arrhenius form for chemical reaction rates. If the temperature is low compared to the activation energy, this factor gives the dominant temperature dependence. While this formula is not exact, it does give a very useful first approximation to a large variety of rates in a processing plasma.

Now it is worthwhile to discuss the relation between the ionization rate α_i above, and the first Townsend ionization coefficient, which we will denote α_T. The latter is historically defined in terms of an electron swarm experiment, where an electron beam swarms into a gas and ionization is measured as a function of distance from the electron beam input. Typically a very low electron current is injected by the cathode and self fields are unimportant. If the electric field is sufficiently large, the ionization builds up exponentially in space from the cathode. The spacial growth rate of electron density is the Townsend first ionization coefficient α_T. Electron current proceeds towards the anode, and ion current goes back to the cathode. The current is relatively easy to measure as a function of distance, so one can measure this coefficient α_T. However, as we will see, in the self sustaining discharge, the local electric field is not usually equal to the voltage divided by the electrode separation.

Thus the Townsend coefficient is defined in terms of ionization per unit length, and $u\alpha_T = \alpha_i$, where u is the drift velocity of the electrons. To calculate α_T from, say distribution functions, one must know the electron drift velocity. Furthermore, in the older literature, it is rare that the electron temperature was introduced. Typically, when one tried to do a first principles calculation of α_T, T_e never appeared, and the calculation is always in terms of electric field divided by gas pressure, E/P. Not only is this a less direct calculation, there were strong disagreements in the earlier literature over whether the assumptions and calculations were valid

at all. Throughout this paper, we will use only α_i and will not use the older Townsend coefficients.

Along with ionization, there is also electron impact excitation of the electronic states of the atom or molecule. This is more fully discussed in Sec. 5. Generally the excitation energy is quickly radiated awayand is a power loss to the system. In some cases, long lived energetic states called metastables with energy E_M are produced. These can be important because they can be ionized with an electron of lower energy, energy greater than E_i-E_M. Also if $E_M > E_i/2$, metastable-metastable collisions can give rise to ionization also. For instance in the common fluorescent lamp, the discharge is controlled by such two step proceses. However, we generally do not consider metastables here.

Now we consider recombination processes. Since recombination is an inelastic precess, the presence of another particle is required to conserve momentum and energy. In the simplest case, this is a photon, and the process is called radiative recombination. We will discuss this somewhat in Section 5 as an example of how the process can be easily calculated from the photo ionization cross section. However this is not usually very important in processing plasmas. Often the most important recombination is at the wall, where it serves as the third body. In fact, in this paper, we generally assume that the wall recombination is so strong that any ion that gets to the wall recombines and is recycled to the plasma as a neutral.

However there are important two body recombination processes in the bulk. These are processes where all elements to the collision are particles. Schematically, these processes are written as

$$A + BC \rightarrow AB + C \qquad \text{or} \qquad AB + CD \rightarrow AC + BD$$

and generally their cross section is much higher. Thus recombination is almost always much more important in molecular plasmas than in atomic plasmas.

We consider first dissociative recombination, which for oxygen is

$$e + O_2^+ \rightarrow O + O \qquad (3.13)$$

This was recently reviewed by Mitchell, where he called it "one of the most complex and least understood of atomic and molecular collision processes". The theories are difficult to do, and the experiments are difficult to interpret. Accepted values of cross sections have changed by as much as a factor of 5 over the last few years. A typical theoretical curve from Mitchell[102] is shown in Fig (3.3b), and this would be a reasonable approximation for either a nitrogen or oxygen plasma. As a reasonable model, one might consider the cross section to vary as E^{-1} up to a maximum energy of about 1 eV, after which it falls off very quickly.

The next process of importance is dissociative attachment, where an electron attaches itself to a neutral molecule and dissociates the molecule at the same time. For oxygen, this reaction is

$$e + O_2 \rightarrow O + O^- \qquad (3.14)$$

Dissociative attachment is only important in electro negative gases, so it is important in an oxygen plasma, but not a nitrogen plasma. Processing plasmas often have such electronegative gases as chlorine and flourine, so dissociative attachment could be a very important process there. Thus one could expect that negative ions could play an important role here. (If there are many negative ions, one must, of course consider detachment as well as attachment.) The dissociative attachment cross section depends not only on the electron energy, but also on the internal vibrational state of the oxygen molecule, that is on the gas temperature. For a gas vibrational temperature of about 300°K, the minimum energy for dissociative attachment is about 4 eV. As the gas is heated, this minimum energy decreases. Shown in Fig (3.4a), taken from Brown is a plot of dissociative attachment cross section for oxygen at 300°K. Generally here we neglect the effect of gas heating, although at sufficiently high elecron density, it can be important.

Finally we will discuss charge exchange. Here, an ion gives its charge to a neutral. If the ion has high energy, as it might in a plasma sheath, after the charge exchange, one is left with a fast neutral and a slow ion. Typically charge exchange is the dominant ion-ion collision process in a processing plasma. Shown in

Figs.(3.4b) and (3.4c) from Brown are charge exchange cross sections of N_2^+ and O_2^+ in various host gases. The charge exchange maximizes between the ions and the corresponding neutral. In all cases, for the energies shown, the charge exchange cross section is is reasonably independent of energy. At lower energies, corresponding more or less to room temperature, the charge exchange cross section of an ion in its host gas increases from the results in Brown. Shown in Fig.(3d) is a result from Banks and Kockarts[103] of the charge exchange cross section of N_2^+ in its parent gas at very low temperatures (compared to those in Fig 3.b). Note also that Bank's result is for the momentum exchange cross section, which is twice the exchange rate for a collision in which the resulting ion does not change direction. Thus as a general rule, the charge exchange cross section of a fairly simple ion in its host gas is a few time 10^{-15} cm^2 at temperatures of several eV, and is a one or two times 10^{-14} cm^2 at temperatures around room temperature.

For rare gases, the picture is similar. Shown in Figs (3.4e) and (3.4f), also from Brown, are charge exchange cross sections for Helium and Argon in the the parent gases. The argon cross section is reasonably constant, while helium decreases as a function of energy, but not nearly as rapidly as $E^{-1/2}$. Thus constant charge exchange cross section is a reasonalbe approximation for these gases also.

4. Kinetic Theory for Particles with No Internal Structure

Let us assume that the processing discharge we are considering has particles with no internal structure. Thus collisions are elastic and the internuclear force is a central force. The distribution function for each particle species is determined by the Vlasov Equation for that species

$$\partial f_a/\partial t + \mathbf{v}\cdot\nabla f_a + (e_a/m_a)[\mathbf{E}+\mathbf{v}\times B/c]\cdot\nabla_v f_a = C_{aa}+C_{ab}+\ldots \quad (4.1)$$

Where the C's on the right hand side denote the contributions to the change in f_a due to the binary collisions specified.

We concentrate now on the collision terms. When particle b collides elastically with particle a, particles with velocity $\mathbf{v}_b$ are lost from the distribution function f_b. The rate at which particles are lost in a phase space volume $d^3v d^3x$ is

$$\partial f_b/\partial t(\text{out}) = -\int d^3v_a d\Omega \sigma(\theta,v) v f_a f_b \quad (4.2)$$

Note that it is not necessarily obvious from Eq.(4.2) that momentum, energy, or even particle number is conserved.

To show things like conservation of momentum, as well as to complete the description of the collision integral, we must also calculate the rate at which particles are scattered into the velocity cell d^3v centered at $\mathbf{v}_b$. This is

$$\partial f_b/\partial t d^3v_b(\text{in}) = \int d^3v_b' d^3v_a' \sigma'(\theta',v') v' f_a' f_b' \quad (4.3)$$

where we have denoted with primes the value of the velocities of particles a and b before the collision. The integral over $d^3v_b' d^3v_a'$ is over only that three dimensional portion of the six dimensional double velocity interval which places the final velocity of particle b within d^3v_b of $\mathbf{v}_b$.

To proceed, we relate various before and after collision values. The basic collision, which takes a particle out of velocity element $\mathbf{v}_b$ is shown in Fig.(4.1a). Now we relate this collision to another collision which puts particles into the velocity element at $\mathbf{v}_b$. First consider the time reversed collision, shown in Fig (4.1b) which puts the particle into velocity element $-\mathbf{v}_b$ as shown. Then take the mirror image in the plane perpendicular to $\mathbf{v}_b$. This collision is

shown in Fig (4.1c). Note that the final velocity of the particle is now $\mathbf{v_b}$ so that this collision puts particles into the velocity element around $\mathbf{v_b}$.

This collision is related to the original collision by time reversal and reflection. As we saw in the last section, the magnitude of the relative velocity does not change before and after the elastic collision. Thus the time reversed collision will have the same magnitude of relative velocity, and of course so will the reflected collision. Thus $v=v'$. Since the particles have no internal structure, the collision cross section also is the same for the forward and reversed as well as the reflected collision. Thus $\sigma=\sigma'$. The only other quantities to consider are the differential elements of velocity space. The collision arises from a Hamiltonian representing the interaction between the two particles. We know that in any Hamiltonian interaction, phase space is preserved before and after the collision. The collision is assumed instantaneous, so the configuration space volume d^3r is unchanged. However the collision that puts particles into $\mathbf{v_b}$ is related to the time reversed and reflected collisions. These operations do not change the phase space volume either so $d^3v_a d^3v_b = d^3v_a' d^3v_b'$. Thus the expression for the total change of f_b, $\partial f_b/\partial t(\text{in}) - \partial f_b/\partial t(\text{out})$ becomes

$$C_{ba} = -\delta_{ab}\int d^3v_a d\Omega\, \sigma(\theta,v) v [f_a f_b - f_a' f_b'] \qquad (4.4)$$

where $\delta_{ab}=1$ if $a\neq b$ and $\delta_{ab}= 1/2$ us $a=b$. It accounts for the fact that if $a=b$, each collision is counted twice if the factor of 1/2 were not present. In order to simplify the notation, we usually will not specifically include the factor separately unless it is specific ally required to avoid confusion. Equation (4.4) is the Boltzmann collision integral for particles with no internal structure. The prime in the second term in the brackets means particle which collide into velocities $\mathbf{v_a}$ and $\mathbf{v_b}$.

The fact that

$$\sigma(\theta,v) v d^3v_a d^3v_b = \sigma(\theta',v') v' d^3v_a' d^3v_b' \qquad (4.5)$$

is called the principle of detailed balance. For the case of the simple collisions we have been considering, not only is the product of the factors in Eq.(4.5) equal, the individual factors are also. This results from the simplicity of the collision for the case of particles

with no internal structure. As we will see later, for the case of particles with an internal structure, the principle of detailed balance still holds; however the individual factors are themselves no longer equal.

There are several properties of the Boltzmann collision integral which can be easily proved and are reviewed here. First of all, if f is initially positive everywhere, it stays positive. If f_b is positive and were to go negative, it would first have to be zero at some velocity. However if $f_b=0$ at this velocity, Eq.(4.4) shows that C_{ba} is greater than zero, so that f_b would become positive at subsequent times. It is also not difficult to show that the Boltzmann collision integral conserves mass, momentum and energy in the plasma. If Y_b denotes a component of momentum, mass or energy of the particle b, the collisional rate of change of Y is

$$Y' = -\int d^3v_a d^3v_b Y_b d\Omega \sigma(\theta,v) v[f_a f_b - f_a' f_b'] + b \rightarrow a \qquad (4.6)$$

where Y' is the total change of the quantity summed over both colliding species, a and b. If we consider the change within a species, the same logic applies. The integrand is symmetric with respect to changing a and b so the $b \rightarrow a$ term can easily be incorporated into the integral. Now since v_a and v_b are simply variables of integration, we can label then as v_a' and v_b' in Eq.(4.6). Then, using the fact that for the elastic collision between particles having no internal structure, $d^3v_a d^3v_b d\Omega \sigma v = d^3v_a' dv_b' d\Omega' \sigma' v'$, by the principle of detailed balance

$$Y' = -\int d^3v_a d^3v_b d\Omega v \sigma(\theta,v)\{Y_a + Y_b - Y_{a'} - Y_{b'}\}[f_a f_b - f_a' f_b'] \qquad (4.7)$$

However the term in the bracket {} is simply the sum of the mass, momentum or energy before and after the collision in question. Since mass, momentum and energy are conserved in the collision, this bracket vanishes, thereby proving that mass, momentum and energy are conserved for the entire plasma by the Boltzmann collision integral.

Next we prove the Boltzmann H theorem, essentially a proof that entropy increases until the plasma reaches an equilibrium state. We define the quantity H as

$$H = -\Sigma_b \int d^3v_b \, f_b \ln f_b \qquad (4.8)$$

By multiplying the Boltzmann equation by $\ln f_b$ and integrating over velocity and space, one can get an equation for the total change of H over the entire plasma. Let us first consider the convective terms. Since $[\nabla f_b]\ln f_b$ is the gradient of a function of f_b, $Z(f_b)$, ($Z(f) = (1/2)f^2\ln f-(1/4)f^2$), the integral over space vanishes as long as the plasma is isolated so that the boundary terms in the spatial integral vanish. If the terms do not vanish, then there is a flux of H (an entropy flux actually) into the system from the boundary, which we do not consider here. The contribution to dH/dt from the **E** and **B** can be written as divergences in velocity space of vector functions of Z(f). These vanish on integration over velocity.

We now consider the collision terms. By the same logic as was used in the derivation of conservation of mass, momentum and energy, we find that

$$dH/dt = 0.25\Sigma_{ab} \int d^3v_a d^3v_b d\Omega v\sigma(\theta,v)\{\ln[f_a'f_b'/f_af_b]\}[f_a'f_b'-f_af_b] \qquad (4.9)$$

Since the f's are everywhere positive, the integrand is positive everywhere also. Thus the conclusion is that dH/dt is always equal to or greater than zero. Note however that an important step in this proof is the summation over species a and b. The H of one component does not necessarily increase, a decrease of H_a might be balanced by a larger increase of the H of the interacting component H_b. However the total H increases. Correspondingly, the contribution to dH/dt of a species through its self interaction also increases. Of course H cannot increase without limit because f integrates to unity over velocity. Since H increases or remains constant, and is bounded from above, the plasma must evolve toward a state in which H'=0.

Hence the H theorem allows one to derive an equilibrium distribution function for the plasma. For a homogeneous, force free plasma $\partial f/\partial t$ will vanish as long as

$$f_af_b - f_a'f_b' = 0 \qquad (4.10)$$

or as long as

$$\ln f_a + \ln f_b = \ln f_a' + \ln f_b' \qquad (4.11)$$

Recall that a and b denote particle parameters before a binary collision, and a' and b' denote the values after the collision. Thus the natural log of f must be one of the quantities conserved in the collision. There are three and only three such quantities so conserved, the mass, momentum and energy. Thus the equilibrium distribution function must be

$$f_b(v) = n_b(m_b/2\pi T)^{3/2}\exp[-(m_b/2T)|\mathbf{v}-\mathbf{u}|^2] \equiv n_b f_{mb} \qquad (4.12)$$

Notice that T (the temperature or 2/3 of the thermal energy) and **u** (the average velocity) have no subscript. These values must be the same for each species of the plasma if it is to be in thermal equilibrium. The constants in the distribution function are chosen so that when integrating over the velocity, the result is the density n_b. The thermal energy of the species W_b is obtained by integrating $1/2m_b|\mathbf{v}-\mathbf{u}|^2$ over the distribution function, giving $W_b = 3n_bT/2$.

To continue, we consider the equilibrium distribution function for a non flowing species of plasma in an external force. For convenience, we will take the case of charged particles in an electrostatic potential. As we have seen, a local Maxwellian distribution function is a thermal equilibrium distribution function as long as interparticle collisions are the only thing taken into account. We then consider what spatial dependence will render the Maxwellian distribution an equilibrium distribution in the external field. That is we consider a distribution function of the form

$$f_b = n_b(\mathbf{r})f_{mb} \qquad (4.13)$$

Because the velocity distribution is considered to be Maxwellian (with the same temperature for all species), the collision term in the Boltzmann equation vanishes. Thus if a density can be determined so that

$$\mathbf{v}\bullet\nabla n_b f_{mb} - n_n(e_b/m_b)\nabla\Phi\bullet\nabla_v f_{mb} = 0 \qquad (4.14)$$

the equilibrium distribution in the external force can be obtained. One can easily show by direct substitution that an n_b can be found and is

$$n_b = n_{bo}\exp -e_b\Phi/T \qquad (4.15)$$

where n_{bo} is the number density of species b at $\Phi=0$. For a single species, getting the distribution in an externally provided electrostatic potential is not difficult as we have just shown. For a plasma which comprises several species of very different masses and positive and negative charges, the thermal equilibrium distribution function in the external field can be considerably more complex if it exists at all. If the electrostatic field is itself generated by the charge separation in the plasma, and the charged species in the plasma are ions and electrons, we must have

$$\nabla^2\Phi = 4\pi e(n_e-n_i) \qquad (4.16)$$

as well as Eq.(4.15) for thermal equilibrium. Notice that in a falling potential, the electron density decreases while the ion density increases. It is very rare that this describes any aspect of a processing plasma. As we will see later, in non neutral sheaths, where $n_e \neq n_i$, one species or the other is not in thermal equilibrium.

We now consider ion charge exchange collisions. If the collision is that of an ion with its parent neutral, this is like that of a particle with no internal structure. Generally these are the most important ion neutral collision processes. These collisions are particularly important in the sheaths of processing plasmas where the ions are accelerated. In this case, particles are conserved within the ion species. However since we are primarily concerned with the sheath ions, their energy is assumed to be much greater than the energy of the target neutral. Thus we assume that the ion, after the collision is replaced with another ion at zero velocity. Hence if the target neutrals have number density N, the collision integral for charge exchange is

$$C_{in} = -N|v|\sigma_x(v)f_i(v) + N\delta(v)\int d^3v'\sigma_x(v')|v'|f_i(v') \qquad (4.17)$$

In Eq. (4.17) above, all velocities refer to ion velocities; the neutral particles are simply considered to be background targets for the ions. (at least until the neutral becomes an ion). Also σ_x is the charge exchange collision frequency. The first term in C_{in} is the standard term we have used for particles scattering out of a velocity element around v. The second term is different in that the only particle velocity after the collision is assumed to be zero.

Clearly, C_{in} conserves ions, but it does not conserve either ion momentum or energy. Also there is no particular tendency for Eq.(4.17) drive the system toward thermal equilibrium, because the target particles are assumed to be non interacting. The reaction of the neutrals is neglected here. Thus there is no detailed balance, or tendency toward Boltzmann statistics if one considers the ions alone.

5. Kinetic Theory and Rate Equations for Atoms

In this section, we extend the kinetic theory calculations to the cases where the particles do have internal structure. We consider the case of atoms with only electronic excitations and as ionizations. We first consider the case of excitations alone. In the binary collision, particle a has excitation energies E(a,j), where the index j denotes the various atomic excitations. The distribution function now has an additional index j.

To derive the kinetic equation for the case where the particles have internal degrees of freedom, we follow the procedure of the previous section. Specifically, Eq.(4.2) still applies and the rate of particles of species b and internal energy E(b,j) (the unexcited particle is defined as having internal energy of zero) scattered out of the region of velocity space is

$$\partial f_{bj}/\partial t(\text{out}) = -\Sigma_i \int d^3v_a d\Omega \sigma(\theta, v.E(b,j), E(a,i)) v f_a f_b \qquad (5.1)$$

The particles scattered in are given by

$$\partial f_{bj}/\partial t(\text{in}) d^3v_b = \Sigma_{i'j'} \int d^3v_{a'} d^3v_{b'} \sigma'(\theta', v', E(b',j'), E(a',i')) v' f_{a'} f_{b'} \qquad (5.2)$$

The integral over velocity variables and summation over i'j' in Eq.(4.2) is only over those primed velocities which put the final collision products within $d^3v_a d^3v_b$ of v_a and v_b after the collision; and over those i'j' which leave the particle b in energy E(b,j) and particle a in energy E(a,i).

For the case of elastic collisions of particles with no internal structure, the relation between velocity interval, relative velocities and cross sections for the forward and reversed collision provided crucial information which simplified the collision integral and verified Boltzmann statistics. This no longer holds true for the individual factors in the integral for the case where the atoms have internal structure. For instance v (recall it is the magnitude of the relative velocity in the center of mass frame) is no longer constant in an inelastic collision, which implies also that $d^3v = [v^3/v'^3] d^3v'$. However there is a principle, called the principle of detailed balance which says that Eq.(4.5) holds even if the individual factors are not themselves equal. Using the principle of detailed balance to relate

the rates of the forward and reverse processes, we find that the collisional contribution to $\partial f_b/\partial t$ is

$$\partial f_{bj}/\partial t = -\Sigma_i \int d^3v_a d\Omega \sigma(\theta,v,E(b,j),E(a,i))v[f_{ai}f_{bj}-f_{ai}'f_{bj}'] \qquad (5.3)$$

As before, the collisional rate of change of f_{bj} vanishes if $f_{ai}f_{bj}-f_{ai}'f_{bj}'=0$, or if $\ln f_{ai} + \ln f_{bj} = \ln f_{ai}' + \ln f_{bj}'$, and one can still prove the H theorem. Thus, as before, in equilibrium, the logarithm of the distribution function is proportional to quantities conserved in the collision. These are now the momentum and total energy of the particles, the total energy now being the sum of the internal energy and the kinetic energy. Thus the equilibrium distribution function is now given by

$$f_{b,j} = Q(T)^{-1} \exp-[E(b,j)/T]f_b(v) \qquad (5.4)$$

where $f_b(v)$ is the equilibrium velocity distribution given by Eq.(4.12) and

$$Q(T) = \Sigma_j \exp-[E(b,j)/T] \qquad (5.5)$$

where the summation is over the assumed finite number of states. Q(T) is called the partition function and it depends on the temperature as well as on the way the different internal states of the system are distributed. Another way of expressing Q is

$$Q(T) = \Sigma^*{}_j g_j \exp-[E(b,j)/T] \qquad (5.6)$$

where g_j is the number of different states with energy E(b,j) (that is the degeneracy of the state), and the summation (with the star) in Eq.(4.6) is now over distinct energies rather than over distinct states. The quantity g_j is also called the statistical weight of energy state E(b,j). Thus the principle of detailed balance allows us to write the collision integral for the case of inelastic collisions in a way that the Maxwell Boltzmann statistics of the equilibrium can be derived. Alternatively, one might postulate Maxwell Boltzmann statistics for the equilibrium, and use this to derive the principle of detailed balance for the particular kinetic theory studied.

Let us briefly consider Q(T). It is a summation over all of the states or over all of the energy states multiplied by the statistical weight. The energies of the bound states are within some range

from the minimum energy to the ionization energy. However because the Coulomb force is very long range, there are an infinite number of bound states. Thus the summation in Eq.(5.5) diverges if the summation is actually taken over all states. However there is some practical upper limit to the number of states. For instance the hydrogen like atom with energy state n has an energy of E_i/n^2 below the continuum. One possibility is that the atom is thermally ionized when its own thermal motion is above the ionization energy. If the gas has a temperature from room temperature to a few hundred degrees centigrade, the maximum n for distinct ion states is about 15-20. Also, the radius of an atom of principal quantum number n is roughly n^2a_o, where a_o is the Bohr radius, about 5×10^{-9}cm. Thus the cross section becomes large with n, so n's above about this value are probably not of physical interest.

Hence, for states above some maximum level, the excited states become in many ways indistinguishable from ionized states. This is the maximum excited state which the summation in Eq.(5.5) should be carried to. For an energy state n, there are roughly n^2 angular momentum states. The number of n states for which the partition function transitions to that for an ionized gas is denoted by Δn so the upper states do not contribute much to the partition function as long as $\Delta n n_{max}^2 \exp-(E_i/T) << 1$. Thus the truncation of the summation is most valid at low temperature.

We digress briefly to discuss molecular plasmas. Here there are not only electronically excited states, but also rotational and vibrational states of the molecule. The calculation of the partition function and the associated partition of the molecules among these states must also be considered. Unlike the case of electronically excited states, there are only a finite number of rotational and vibrational states. When the rotational energy becomes too high, the rotation begins to interact with the inter nuclear vibration. The binding energy between the nuclei of the molecule is a short range force, so there are only a finite number of excited vibrational states of the molecule. To the extent that rotational, vibrational and electronic states can be regarded as distinct, the partition function can factored into rotational, vibrational and electronic factors. From this, one can determine the thermal equilibrium partition of molecular internal energy into these components.

Let us now consider the ionization of the plasma thermal equilibrium. If the ionized electron ion pair are considered to be an excited state with the ionization energy, an argument entirely analogous to that above, shows that the number of electrons, ions and atoms satisfies the relation:

$$N_e N_i / N_a = [\exp -E_i/T] G_e G_i / G_a \qquad (5.7)$$

where E_i ionization energy and

$$G_a = \Sigma^*_j g_{ja} \exp -\{(E_{ja} - E_{oa})/T\} \qquad (5.8)$$

for atoms and, with identical definitions for electrons and ions. E_o is the ground state energy for the species, and we have used the fact that

$$E_{oi} + E_{oe} - E_{oa} = E_i \qquad (5.9)$$

The key is to get the G factor for the additional free particle produced in the ionization (the electron). The electron has no internal structure, but it does have a spin, so there is a degeneracy factor of 2 from the spin. Since the electron is free, it is highly degenerate and the G_e factor is quite large in nearly all cases. The electron is assumed to be in a system of length L confined in a volume $V = L^3$. It has wave function

$$\psi = \exp 2\pi i \mathbf{p} \cdot \mathbf{r}/h \qquad (5.10)$$

and the boundaries impose the quantitization condition $p_x = nh/L$, where n is an integer, and the number of free electron states within a velocity space volume d^3v is $m^3 d^3v V/h^3$. Integrating over all possible electron velocities with the assumed Boltzmann distribution, and accounting for the spins of the electrons, we find that

$$G_e = 2V(2\pi m T)^{3/2}/h^3 \qquad (5.11)$$

so that

$$n_e n_i / n_a = 2[2\pi m T/h^2]^{3/2} (G_i/G_a) \exp(-E_i/T) \qquad (5.12)$$

using the fact that $N_e/V=n_e$. Equation (5.12) is the Saha Equation and it relates the ionization fraction to the temperature and the internal atomic structure at thermal equilibrium. Since for most atoms and ions, $G_a \approx G_i$, the Saha equation is often written without the G factors.

Now let us consider several of the ionization and recombination processes. Here we will consider only two for atomic systems; impact ionization and the reverse process of three body recombination, and photo ionization and the reverse process of radiative recombination. As we have seen in for instance Eq.(3.12), impact ionization can be written with an ionization rate α_i. Including the two ionization processes and their inverse processes, the equation for electron density can be written as

$$dn_e/dt = \alpha_i n_e n_a - \beta_i n_e^2 n_i + \alpha_p n_a I - \beta_p n_e n_i \qquad (5.13)$$

where the subscripts on the α's and β's denote the impact and photon processes, and I is the photon density. In thermal equilibrium, dn_e/dt must be zero, so this gives a relation between the α and β coefficients. Because there are different functional dependencies on production rate and loss rate depending on the process, in general there is no relation between say the different α's for the different processes. However there is always a relation between the α and the β for the process and its inverse, as would be expected from the principle of detailed balance. This relation must give the same functional relation between the densities. For instance, balancing impact ionization with recombination gives

$$n_e n_i/n_a = \alpha_i/\beta_i \qquad (5.14)$$

while balancing photoionization with radiative recombination gives

$$n_e n_i/n_a = \alpha_p I/\beta_p \qquad (5.15)$$

This is the same relation as long as $\alpha_i/\beta_i = \alpha_p I/\beta_p$. Of course for this to be so, the photons are in thermal equilibrium at temperature T. Thus, at thermal equilibrium, the rate of the ionization process and its inverse are related by the Saha equation for all ionization processes.

To demonstrate the utility of the Saha Equation, we use it to calculate the rate of radiative recombination. The flux of photons at frequency ν incident on an atom is the energy density at frequency ν times c, divided by $h\nu$. The cross section for photoionization maximizes at the ionization energy and then falls off in frequency. We assume a frequency dependence of ionization cross section as $\sigma_i = \sigma_o(\nu_i/\nu)^n$ for $\nu>\nu_i$ and zero otherwise. The energy density of the electromagnetic radiation is given by the Planck spectrum

$$E(\nu) = [8\pi h\nu^3/c^3]\{\exp(h\nu/T)-1\}^{-1} \qquad (5.16)$$

Then one can do an asymptotic approximation to the integral to arrive at this result

$$\alpha_p I = [8\pi\sigma_o E_i^2 T_e/c^2h^3]\exp -E_i/T_e$$

$$= 4x10^{23}T(eV)E_i^2(eV)\sigma_o(cm^2)\exp-(E_i/T_e)\ (s^{-1}) \qquad (5.17)$$

for low values of T_e. Here E_i the ionization energy is $h\nu_i$. Then from the Saha Equation, we can determine that the β_p coefficient for recombination into the ground state is

$$\beta_p = (8\pi\sigma_o E_i^2)/[2(2\pi m)^{3/2}T_e^{1/2}c^2]$$

$$= 65\sigma_o(cm^2)E_i^2(eV)/T_e^{1/2}(eV)\ \ (cm^3/s) \qquad (5.18)$$

Of course recombination is not only to the ground state, but also to all excited states of the atom. Assuming the atom is hydrogen like, each energy state denoted by n has energy below the continuum of E_i/n^2. Also each n has L angular momentum states from zero to n, and each state L has 2L+1 depending on the orientation of the angular momentum vector. Thus the total number of states for each n is about n^2. The summation over energy states then converges rapidly and the expression for recombination to the ground state is approximately correct. If σ_o is taken as approximately 10^{-17} cm^2 and E_i as about 12 ev for oxygen, Eq. (5.18) agrees with the radiative recombination rate as tabulated by Dutton. Hence from the Saha equation and thermal equilibrium considerations, one can estimate the rate of radiation recombination even for the case where the radiation density is far below thermal equilibrium, the case for most non thermal processing plasmas. Coronal equilibrium is

defined as that where impact ionization is balanced by radiative recombination. State populations in coronal equilibrium depend only on electron temperature.

While the ionization rate and recombination rate are, in all cases related by the Saha equation, this can at times be misleading because the most important ionization and recombination processes might not be inverses of each other. Consider the case of three body recombination. Using Eq.(3.12) for the ionization rate and the Saha Equation, one would surmise that the recombination rate coefficient β is proportional to T_e^{-1}. However this three body recombination rate is the rate for recombination directly into the ground state with no intermediate radiative decays. Another reaction path is for the atom to recombine into a highly excited atomic state and then radiatively decay to the ground state. Because the highly excited state has a very large radius, as we have discussed, these cross sections can be very large. (Also the lifetime of these states to radiative decay is very short, so in a nonequilibrium plasma, ionization of these states will not be important.) Let us estimate the β coefficient for this process. At low temperature, two electrons which collide exchange energy of about T_e. The closest these electrons can get to each other is a separation e^2/T_e, and as they approach each other, one of them typically stops. If an ion is within this distance of the electron that nearly stops, the electron can form a highly excited bound state of the atom. The recombination rate then is the two particle collision cross section $\pi e^4/T_e^2$ times the density of electrons n, times the relative electron velocity, $(T_e/m_e)^{1/2}$, times the probability that an ion is within the interaction region, $\pi n(e^2/T_e)^6$. By using the average radius of an excited atomic state, the quantum number squared times the Bohr radius; and the energy of the state compared to the continuum, the Bohr energy divided by the quantum number squared, we see that the state after collision is generally bound. Thus the three body recombination rate into highly excited atomic states is approximately

$$\beta(cm^6/s) \approx e^{10}/(m_e T_e^9)^{1/2} \approx 4\times10^{-27} T_e^{-9/2}(eV) \qquad (5.19)$$

Thus for low temperature plasmas, the three body recombination rate via the formation of highly excited states can greatly exceed the direct three recombination rate into the ground state. Comparing Eqs.(5.18) and (5.19), we see that radiative recombination

dominates three body collisionless/radiative recombination as long as

$$nT_e^{-4} < 10^{12}, \qquad (5.20)$$

the usual condition for processing discharges. To derive Eq.(5.20), we have assumed E_i =10 eV and $\sigma_o \approx 10^{-17}$ cm^2.

6. Homogeneous, Molecular Plasmas

Processing plasmas are not usually atomic plasmas, although atomic argon plasmas are used in sputtering. The fact that the plasma is molecular gives rise to chemistry, as well additional internal states which would figure in the energy equation of the gas species. In this section we will discuss one of the simplest molecular plasmas, an oxygen plasma. We start with a discussion of a low density plasma with hot electrons and cool neutrals and ions; the type usually found in processing discharges; and conclude with brief considerations of thermal equilibrium oxygen plasmas.

One thing about a processing discharge is that the free electrons play a very important part in the chemistry. The reason is that the rate of a chemical process goes as $\alpha = \int \sigma v f(v) d^3v$, so that the electrons, with their lighter mass and higher temperature give rise an α which is $(T_e M/T_g m)^{1/2}$ larger than that of the gas if the cross sections are equal. Thus, even though the overall temperature of the discharge is low, there is chemistry characteristic of very high temperatures going on, because of the presence of the energetic electron species whose temperature may be between about one and ten electron volts.

We also consider low density plasmas, so that the chemistry is mostly through two particle collisions. The typical reaction is then something like

$$A + BC \rightarrow AB + C$$

and these usually have high reaction rate. An alternate possible two body reaction like

$$A + B \rightarrow AB + h\nu$$

is usually less important because radiative recombination rates are small as we have seen in Sec.(5). Another possible chemical reaction, $O + O \rightarrow O_2$ is also typically not important in a processing plasma. The direct radiative rate is very small. The other possible reaction channel is through formation of an excited molecule and its interaction with a third body. This is a three body process, which we assume is negligible at the low densities considered. However if the third body is the wall of the chamber, atomic oxygen can easily

recombine. Thus surface reactions can be a whole new reaction set which we will not consider here.

One of the most complex and intimidating things about the processing plasma is the number and complexity of the possible reactions. Also, as we have seen, there is often disagreement regarding just what the rates and cross sections are. Furthermore, it is not always clear where to find the appropriate reaction rates and cross sections, and to what extent published rates should be trusted. As we have seen, they are often corrected in subsequent research. (Rates given here should not be taken as better than factor of two accurate.) Electron rates should really be obtained from integrating the cross section over the velocity distirbution. However simple expressions like Eq. (3.12) can often give a reasonable qualitative estimate.

Sources of cross sections and rates in the plasma literature include Brown, Guervich, and Talrose and Karachevtsev's chapter[104] in Venugopapans *Reactions Under Plasma Conditions*. Two sources for reaction rates of atmospheric gases are the NIST[105] and DNA[106] Handbooks. Also there is a Journal called *Plasma Chemistry and Plasma Processing*, edited by E. Pfender, and particular articles quote specific reactions rates relevant to the process considered in the article. Finally there are two journals of data, *Atomic Data and Nuclear Data Tables*, and *Journal of Physical and Chemical Reference Data*. Looking through the last fifteen years of publication of these journals, one finds many articles which look potentially useful for particular discharges. In the former, one especially useful article is D.L. Albritton[107], as is Dutton[72] in the latter. Finally, there is one published bibliography of reaction rates, but unfortunately, it is about 25 years old[108]. This lists a tremendous number of reactions and then gives references where they can be found. For instance for dissociative attachment of oxygen, it lists 18 references.

Let us then consider the two body reactions in an oxygen plasma. We first consider a large number of possible reactions, and then make certain approximations to reduce the problem to a smaller and more manageable set. The reactions are

Ionization:

$$e + O_2 \rightarrow 2e + O_2^+ \qquad (6.1)$$

described by Eq.(3.12) with an ionization energy of 12 eV and a maximum ionization cross section of 3×10^{-16} cm^2. This value for ionization coefficient agrees reasonably well with that tabulated by Dutton. Then there is ionization of the oxygen atom,

$$e + O \rightarrow 2e + O^+ \qquad (6.2)$$

with E_i =15 ev, $\sigma_o = 3\times10^{-16}$ cm^2;

Dissociative ionization:

$$e + O_2 \rightarrow 2e + O + O^+ \qquad (6.3)$$

with E_i=20 ev and $\sigma_o = 10^{-16}cm^2$. Cross sections for these processes are given in Ref(104) and agree reasonably well with that from Eq. (3.12).

Dissociation:

$$e + O_2 \rightarrow e + O + O \qquad (6.4)$$

described by Eq.(3.12) with E_i=8ev, $\sigma_o = 10^{-16}$ cm^2. This expression agrees to within about a factor of two to that given in Ref.(104) p80.

Then there is ion chemistry.

$$O^+ + O_2 \rightarrow O_2^+ + O \qquad (6.5)$$

The reaction rate here is given as 1.9×10^{-11} cm^3/s by Albritton for an ion temperature of about 600°K. This agrees reasonably well with that surmised from Brown's expression for charge exchange cross section with an assumed ion thermal velocity of 2×10^4 cm/s. This reaction has a fairly large cross section, so even though the ion velocity is small compared to the electron velocity, its rate is competitive with the electron driven reactions. The inverse reaction is

$$O_2^+ + O \rightarrow O^+ + O_2 \qquad (6.6)$$

with a rate of about 10^{-11} cm^3/s.

The electrons are lost mostly by dissociative recombination.:

$$e + O_2^+ \rightarrow O + O \qquad (6.7)$$

Assuming a dissociative recombination cross section as $\sigma = 4\times10^{-16}/E$ for E<3ev and zero otherwise (here and in all formulae, energies are in ev and lengths are in cm) the dissociative recombination rate is given roughly by $(2.6\times10^{-8}/\sqrt{T_e})[1-\exp-(3/T_e)]$ in cm^3/s. This agrees reasonably well with the DNA reaction rate handbook.

We do not consider excitations separately, but regard these as energy sinks that go into determining the electron temperture. Reference (61) considers the production of metastables as end points for oxygen reactions, but apparently it does not consider secondary processes infolving them. Here we neglect metastables.

These are the main reactions which we will limit ourselves to. We calculate these rates by assuming a particular electron temperature, which we take as 3 ev, a typical electron temperature for an oxygen processing plasma. However there are many other possible reactions. For instance a tremendous Pandora's box is opened up by the generation of negative ions. Since oxygen is an electro-negative gas this is a possible reaction. If only two body reactions are allowed, the most important one is dissociative attachment.

$$e + O_2 \rightarrow O^- + O \qquad (6.8)$$

This depends on the vibrational state of the molecule. For gas vibrational temperatures below about 1000°K, the attachment cross section peaks at about 10^{-19} cm for energies between about 5 and 8 ev as shown in Fig (3.4a). The attachment rate is given by roughly $(6.4\times10^{-12}/\sqrt{T_e})\times[(5/T_e+1)\exp-(5/T_e) - (8/T_e+1)\exp-(8/T_e)]$ Although the rate of dissociative attachment is small, it is the largest production rate for negative oxygen ions. At a temperature of 3 ev, this attachment rate is small, about 10^{-12}. However it can be much larger under a variety of circumstances including higher electron temperature, as is characteristic of electron cyclotron resonance plasmas; higher gas density, so three body attachment is important; and higher neutral temperature so the minimum energy for dissociative attachment gets smaller.

Along with attachment, there are the analogous detachment reactions. First there is electronic detachment:

$$e + O^- \rightarrow 2e + O \qquad (6.9)$$

The minimum electron energy for detachment is about 7 ev and above this energy, the cross section is about 7×10^{-16}. This gives a detachment rate of $3\times10^{-7}T_e^{-1/2}\exp-(7/T_e)$. Then there is associative detachment:

$$O^- + O \rightarrow O_2 + e \qquad (6.10)$$

The rate for this process is given as 3×10^{-10} in ref (104) p.110. If both ions are charged, the reaction rate can be even higher, as in positive-negative charge exchange:

$$O^- + O^+ \rightarrow O + O \qquad (6.11)$$

or

$$O^- + O_2^+ \rightarrow O_2 + O \qquad (6.12)$$

Reference (61) quotes a rate of 3×10^{-7} for the former and 10^{-7} for the latter. We assume that rate here.

The O^- does not appear to be a source of O_2^-. The possible reaction $O^- + O_2 \rightarrow O_2^- + O$ has a reaction rate of only 10^{-22} cm^3/s according to Guerevich. O^- does appear to be the main source of ozone however. For oxygen molecules in the ground state, the reaction is

$$O^- + O_2 \rightarrow O_3 + e \qquad (6.13)$$

with a reaction rate of 3×10^{-15} according to the DNA handbook. However if the oxygen in in an electronically excited state, the reaction rate is much more rapid. In the $a'\Delta g$ excited state the reaction

$$O^- + O_2(a'\Delta g) \rightarrow O_3 + e \qquad (6.14)$$

has a rate of 3×10^{-10}, again according to the DNA handbook. Thus for a more rigorous description, there has to be an entire set of

chemistry for the excited states. Once ozone is produced, there becomes the possibility of positive and negative ions of ozone. A reaction like

$$O_3 + e \rightarrow O_3^+ + 2e \qquad (6.15)$$

can occur with a rate given by Eq. (3.12). There is also the possibility of charge exchange

$$O_3 + O^- \rightarrow O + O_3^- \qquad (6.16)$$

with a rate given by $8x10^{-11}$ according to Albritton. Finally, if ozone is present, there is also neutral chemistry

$$O + O_3 \rightarrow 2O_2 \qquad (6.17)$$

and

$$O_2 + O_3 \rightarrow 2O_2 + O \qquad (6.18)$$

with reaction rates respectively of $2x10^{-11}$ exp-[2300/T(°K)] and $5x10^{-11}$exp-[2850/T(°K)] according to the NIST atmospheric rate handbook.

Clearly, the chemistry is very complicated in the general case. We make the simplifying assumptions that the negative ion production rate is unimportant. For the electron temperature of 3 ev that we consider, the rate is small (Eq.(6.8)), and the rates of the reactions returning the O^- back to O_2, and O, are large (Eqs(6.9-11), the steady state concentration of negative ions is small. We then neglect the O^- and all of its derivative chemistry.

To see the validity of this, let us consider a simple steady state chemistry for O^-. There is only one source, the reaction of Eq.(6.8), which is about 10^{-12}. It is destroyed through many reactins, but we will consider only the positive negative ion recombination, Eq. (6.12). If this determines the equilibrium concentration of O^-, it is given roughly by

$$N(O^-) = 10^{-5} n_e N(O_2)/N(O_2^+)$$

If n_e is about equal to $N(O^+)$, we see that as long as the ionization fractin is significantly larger than 10^{-5}, $N(O^-) << N(O_2^+)$.

However, even for this relatively simple system of oxygen and nothing else, we have identified seven important reactions; Eqs(5.1-5.7). Below we enumerate the processes and the approximate reaction rate in cm^3/s at an electron temperature of 3 ev, a typical temperature for a processing discharge. We denote the reaction rate by α_i where i denotes the equation number 6.1-6.7

Process	Rate in cm^3/s
α_1	$2x10^{-10}$
α_2	$6x10^{-11}$
α_3	$6x10^{-11}$
α_4	$6x10^{-10}$
α_5	$2x10^{-11}$
α_6	10^{-11}
α_7	10^{-8}

In a weakly ionized processing plasma with low gas temperature, and electron temperature in the ev range, all of the reactions proceed only in the forward direction. The reverse reactions, in all cases (except for 5 and 6 which of course are reverse reactions of each other) have an energy threshold that the heavy particles cannot get over, or are three body reactions which do not proceed at low density.

In the simplified set, there are five chemical quantities, O_2, O, O_2^+, O^+ and e, whose number densities will be denoted respectively a,b,c,d and e. The rate of change of the quantities are then determined by the five equations describing the seven reactions.

$$a' = -(\alpha_1+\alpha_3+\alpha_4)ae - \alpha_5 ad + \alpha_6 bc \qquad (6.19)$$

$$b' = (-\alpha_2 b+\alpha_3 a+2\alpha_4 a+2\alpha_7 c)e + \alpha_5 ad - \alpha_6 bc \qquad (6.20)$$

$$c' = (\alpha_1 a-\alpha_7 c)e + \alpha_5 ad - \alpha_6 bc \qquad (6.21)$$

$$d' = (\alpha_2 b+\alpha_3 a)e - \alpha_5 ad + \alpha_6 bc \qquad (6.22)$$

$$e' = (\alpha_1 a+\alpha_2 b+\alpha_3 a-\alpha_7 c)e \qquad (6.23)$$

where a prime indicates a derivative with respect to time. It is simple to verify that the reactions (6.19-6.23) together conserve charge as indeed they must.

Since a processing plasma is in steady state, a natural question is whether the steady state constituents of this non thermal equilibrium processing plasma can be determined from the gas phase chemistry alone once the reaction rates (that is the electron temperature) are specified. Although some quantities may have steady state densities determined through the chemistry, in general the answer is no, or at least not an equilibrium that resembles the weakly ionized equilibrium known to exist in glow discharges. For instance from the equilibrium equation for the electrons, the e' equation, if we assume that $b<<a$, then we find a steady state value of c equal to about 3% of a. However in a steady state glow discharge, the value of the ionization is much less, under 10^{-3}. Thus the equilibrium values resulting from the e' equation does not give an equilibrium consistent with what is observed. Similarly consider the a' equation. If $e \geq d$, as it must since $e=c+d$, then we find that a must be about 3% of b for equilibrium. This is also not the case of a weakly ionized oxygen discharge, for which the neutral gas is almost entirely O_2.

Hence the conclusion is that gas phase chemistry alone does not determine the steady state components of the oxygen discharge. As we will see in a later section, it is gas phase chemistry coupled to the fundamental discharge processes and surface chemistry, which determine the composition. Specifically, there is a much greater electron loss term arising from diffusion to the walls, and a much larger source of O_2 from recombination on the walls (surface chemistry). Thus the geometry and the plasma physics are playing a very important role in determining the chemical composition of the

discharge. This is in contrast to the much lower temperature ionospheric plasma, where Gurevich has shown that gas phase chemistry alone can give the composition of the plasma. The main difference is that the ionization here is photoionization, whose rate is independent of electron density. Thus there is no tendency for avalanche, and the electron driven chemistry rates are all bounded by the photoionization rate.

We now consider briefly the opposite extreme, a molecular plasma at thermal equilibrium. Here, all species (including the radiation) are at a given temperature T. In order for equilibration to occur, the gas density is usually much higher than glow discharge. Because the dense background gas is at the high electron temperature rather than the cooler gas temperatures characteristic of low density processing discharges, the equilibrium plasma is usually much more energetic, even though the temperature is typically less than that of the electrons in a low density discharge. Typical temperatures might be under 1 ev. In thermal equilibrium, the reverse reactions cannot be neglected, in fact thermal equilibrium is defined by a balance between forward and reverse reactions which are satisfied for all possible reactions.

Let us consider the reactions we have just discussed for an oxygen plasma, except let us make the additional simplification of neglecting the O^-. Then there are 6 reactions with forward reaction rate α_1-α_6. However at thermal equilibrium, the reverse reaction can also occur, and we define the rates of the reverse reactions as β_1-β_6. Notice that we redefine α_6 here as β_5 and dissociative recombination and its inverse becomes reaction six. The reactions and the reverse reactions all conserve charge and mass, so e=c+d and a+2b+c+2d=A, the total number of oxygen nuclei. Setting each reaction rate to zero at equilibrium, we find six equilibrium relations

$$\alpha_1 a = \beta_1 ec \qquad (6.24)$$

$$\alpha_2 b = \beta_2 ed \qquad (6.25)$$

$$\alpha_3 a = \beta_3 ebd \qquad (6.26)$$

$$\alpha_4 a = \beta_4 b^2 \qquad (6.27)$$

$$\alpha_5 ad = \beta_5 bc \qquad (6.28)$$

$$\alpha_6 ec = \beta_6 b^2 \qquad (6.29)$$

These six equilibrium conditions specified plus the conservation relations would appear to over specify the system. However this is not so, because the equations are not all independent. For instance a, an oxygen molecule, can go to 2 b's, oxygen atoms, directly via equation (6.27), direct dissociation. However alternatively it can go to 2 b's by first going through an intermediate stage of an e and c, ionization, Eq.(6.24); and then the e and c react to give 2 b's by dissociative recombination, Eq.(6.29). Thus there must be a relationship between the rates of the two reaction channels of getting from the a to the two b's. Specifically, we must have $\beta_1/\alpha_1 = \beta_4\alpha_6/\beta_6\alpha_4$. The other two relations between the rates are $\beta_3\alpha_4/\alpha_3\beta_4 = \beta_2/\alpha_2$, and $\beta_1\alpha_2/\beta_2\alpha_1 = \beta_5/\alpha_5$. This is the principle of detailed balance applied to molecular systems, where it is known that in thermal equilibrium, forward and reverse rates must individually balance, and *not* rates around a cycle[109]. Furthermore, reactions 1, 2 and 4 are just direct ionization and dissociation reactions, so the forward and inverse rates are related by the Saha equation. Hence for the three additional reactions, representing more complicated chemistry, the three additional constraints relate the forward to the inverse reaction rates. If additional reactions between only these five species become possible (for instance multi-body reactions at higher density, or new reaction channels at higher temperature), the new constraints would also be between the forward and backward reaction rates.

Going back to the thermal equilibrium oxygen plasma, we find the three relations for b. c and d, in terms of a given value of A become

$$(c+d)c/(A-2b-c-2d) = \beta_1/\alpha_1 \qquad (6.30)$$

$$b^2/(A-2b-c-2d) = \alpha_4/\beta_4 \qquad (6.31)$$

$$(c+d)d/b = \alpha_2/\beta_2 \qquad (6.32)$$

These three equations then determine b. c and d, and from these, e and a are also determined. It is analogous to the Saha equation for atomic systems.

7. Homogeneous Plasma in an Electric Field

Virtually all processing plasmas exist in the presence of an electric field, either dc, rf or microwave. With an electric field, the distribution function in velocity space is no longer necessarily isotropic. For an anisotropic electron distribution function in a weak electric field, a natural approach is to expand the distribution function in a series of basis functions in angle to the electric field. These are usually taken to be Legendre polynomials. We adopt that approach here, and consider only the first two terms. The main collision process is assumed to be between the electrons and the neutral gas atoms or molecules. These collisions are mostly in angle so that the distribution function has as its main tendency the isotropization of the electron distribution function. However anisotropies and scattering in energy are also very important.

We assume that the background gas atoms are simply fixed scatterers, so the equations are now linear in the electron distribution function. However now that the target atoms decouple, there is no H theorem, so the electrons will not necessarily evolve toward a Maxwellian distribution. As we will see, the distribution will depend on the functional form of the collision frequency.

Let us expand the electron distribution function in the series

$$f(v,\alpha) = f_0(v) + \cos\alpha\, f_1(v) \qquad (7.1)$$

where $\cos\alpha = v_z/v$. Since the distribution function is normalized to unity when integrated over velocity, and only f_0 does not integrate to zero, the normalization is

$$\int_0^\infty 4\pi v^2 f_0 = 1 \qquad (7.2)$$

Similarly, the average velocity in the z direction, u_e is

$$u_e = (4\pi/3)\int_0^\infty v^3 f_1(v)dv$$

If μ is $\cos\alpha$, then we integrate the Boltzmann equation over μ from -1 to 1, and multiply it by μ and do the same. This gives two coupled equations for f_0 and f_1 which are

$$\partial f_o/\partial t - [eE/3mv^2]\partial/\partial v(v^2 f_1) = S_o \qquad (7.3)$$

and

$$\partial f_1/\partial t - (eE/m)\partial f_o/\partial v = S_1 \qquad (7.4)$$

where S_o is one half the collision integral integrated over μ and S_1 is three halves the collision integral times μ integrated over μ.

Now let us consider the collision model for electrons colliding with the heavy particles. The heavy particles are assumed to be fixed scattering centers randomly located. However these may absorb or give some energy to the electron in the binary collision, either because $M \neq \infty$ or because internal energy states get excited. We assume that the collision between the electron and atom is that of a light particle with a fixed scattering center, except that the electron can gain or lose energy in the collision by some prescribed amount.

In this case, in the Boltzmann collision integral, the distribution function for the target atoms simply drops out. In the collision integral, there were integrals over v, from scattering out of a velocity cube of size d^3v centered about v; and also integrals over d^3v' of a particle centered about v' which scatters into the cube about v. As discussed in Section 4, if the collision has an energy change, $d^3v' = (v'/v)^3\, d^3v$. Even for the case of elastic collisions, this factor should still be used if the heavy neutral target particles are simply considered to be target particles which do not otherwise interact. Thus the collision integral is

$$S = (n_a/v^3) \int d\Omega[v'^4\sigma(v',\theta')f(v') - v^4\sigma(v,\theta)f(v)] \qquad (7.5)$$

where Ω is the solid angle denoting the scattering. The next step is to insert f from Eq.(7.1) into Eq.(7.5), multiply by the zeroth and first power of μ and integrate over μ to obtain S_o and S_1.

We start by considering S_1. In the μ integral, only even powers of μ will contribute. These are the terms containing only f_1, so

$$S_1 = -(3n_a/2v^3)\int d\Omega \int_{-1}^{1} d\mu[v'^4\sigma' f'\mu' - v^4\sigma f\mu]\mu \qquad (7.6)$$

Consider first the case where the velocity change is small, as is the case for elastic collisions, and excitations of low energy internal states. Then $v' \approx v$, and the integral is non zero principally because $\mu \neq \mu'$. Now we must obtain the relation between μ and μ'. If the scattering event takes place in the plane defined by v and z, then clearly $\alpha' = \alpha + \theta$ and $\cos\alpha' = \cos\alpha\cos\theta - \sin\alpha\sin\theta$. Now consider the more general case where the scattering is not in the plane. Imagine that the vector v' is rotated by an angle ϕ about the v vector out of the vz plane. Then v' can be decomposed into two vectors parallel and perpendicular to v. The component of the parallel vector in the z direction is $\cos\alpha\cos\theta$ independent of ϕ. The component of the perpendicular vector in the z direction does depend on ϕ and it is $\sin\alpha\sin\theta\cos\phi$. Thus

$$\cos\alpha' = \cos\alpha\cos\theta - \sin\alpha\sin\theta\cos\phi \qquad (7.7)$$

This then allows us to do the integral over μ with the result

$$S_1 = -n_a v f_1 \int d\Omega \sigma(v,\theta)(1-\cos\theta) = -\nu_p(v) f_1 \qquad (7.8)$$

where ν_p is the momentum exchange collision frequency from Eq.(2.8).

Continue now with the evaluation of S_o. The even powers of μ in the μ integral now are only in those terms containing f_o. Thus the μ integral works out trivially. Then assume that v'-v is small in the binary collision, so $v'-v = 0.5v[\Delta K/K]$ where K is the kinetic energy. Thus

$$S_o = (n_a/2v^2)\{\partial/\partial v \int d\Omega(\Delta K/K)\sigma(v,\theta)v^4 f_o\} \equiv 0.5v^{-2}\partial/\partial v(\nu_K v^3 f_o) \qquad (7.9)$$

where ν_K is the angle averaged collision frequency for relative energy exchange. For the case of elastic collisions with heavier atoms, at rest, the energy loss is given by Eq (3.6) with v_b and K_b taken to be zero and with the a species taken to be the electrons. In this case the angular factor is just the same as for momentum change, so

$$\nu_K = 2(m/M_a)\nu_p \qquad (7.10)$$

For the case of inelastic collisions which do not greatly change the energy, the more general expression for $\nu_K = \zeta\nu_p$, discussed in Section 3 must be used.

To summarize, the equations for f_o and f_1 become:

$$\partial f_o/\partial t - [eE/3mv^2]\partial/\partial v(v^2 f_1) = 0.5v^{-2}\partial/\partial v(\nu_K v^3 f_o) \qquad (7.11)$$

$$\partial f_1/\partial t - (eE/m)\partial f_o/\partial v = -\nu_p(v) f_1 \qquad (7.12)$$

Let us solve these for the distribution function for the case in which $E = E_o\cos\omega t$ and ν_K is given by Eq.(7.10) as is appropriate for an atomic plasma such as argon (at least for electron energies less than the lowest electronic excitation energy). Since Eqs.(7.11 and 12) are nonlinear in f and E, f's are generated at all harmonics of ω, with f_1 being a summation over odd harmonics and f_o being a summation over even harmonics. As with the Legendre polynomial expansion over angle α, we retain only the zeroth and first harmonics, so

$$f_1 = [eE_o\partial f_o/\partial v/m(\omega^2+\nu_p^2)]\ (\nu_p\cos\omega t - \omega\sin\omega t) \qquad (7.13)$$

Inserting for f_1 in Eq.(7.11) and setting the time derivative equal to zero because only the zeroth harmonic is considered, we find

$$-e^2E_{or}^2\partial f_o/\partial v/3m(\nu_p^2+\omega^2) = (m/M_a)f_o \qquad (7.14)$$

where E_{or} is the rms value of the electric field. For the dc case, $E_{or}=E_o$, while for the ac case, is is $E_o/\sqrt{2}$. Equation (7.14) can easily be integrated to give

$$f_o(v) = A\ \exp-[3m^3/e^2E_{or}^2M_a]\int_0^v dv\ [-v\ (\nu_p^2+\omega^2)] \qquad (7.15)$$

Where A is chosen so that the distribution function is normalized to unity. If the collision frequency is independent of energy, f_o is a Maxwellian with temperature

$$T_e = M_ae^2E_{or}^2/3m^2(\omega^2+\nu_p)^2. \qquad (7.16)$$

Notice that if $\omega >> \nu_p$, the distribution is Maxwellian even if the momentum exchange collision frequency does depend on particle energy.

For the dc case where the mean free path, rather than the collision frequency is independent of energy, $\nu_p \sim v$, so the distribution function goes as $\exp-(v/v_e)^4$. On the other hand, for a molecular plasma where inelastic collisions are generally more important, and $\nu_K >> (m/M_a)\nu_p$, the energy dependent $\zeta(v)$ must be used inside the velocity integral instead of m/M_a. Since ζ is generally greater than m/M_a , the temperature of a molecular plasma is lower than that of the atomic plasma, and/or the electric field is greater.

The distribution function characteristic of constant mean free path is called a Druyvesteyn distribution and it is very important in gas discharges. The normalized distribution is

$$f(v) = A \exp-(v/v_e)^4, \qquad A = 3/4\pi v_e^3 \Gamma(3/4) \qquad (7.17)$$

where $\Gamma(3/4)$ is given approximately by 1.23. The temperature, defined as 2/3 of the average value of $0.5mv^2$ is given by

$$T = [\Gamma(5/4)/\Gamma(3/4)](1/2)mv_e^2 \approx (1/4)mv_e^2 \qquad (7.18)$$

Notice that at given temperature, the thermal velocity v_e is larger by a factor of $\sqrt{2}$ than it is for the corresponding case of the Maxwellian. Thus while the Druyvesteyn has a 'tail' with much smaller population that the Maxwellian, the 'body' extends out to higher velocity. Finally let us consider the ionization rate for a Druyvesteyn. Assuming that the ionization rate has the functional form given in Eq.(3.11) and $T_e << E_i$, the E_i term in the integral can be integrated analytically, whereas the E term cannot. Making an asymptotic approximation to this integral we find that for the Druyvestyn,

$$\alpha_i = [\sigma_o(T_e/m)^{1/2}\exp-(E_i/2T_e)^2]/[3.7(E_i/2T_e)^2] \qquad (7.19)$$

Note that at very low temperature, the ionization rate of the Druyvesteyn is lower than the Maxwellian, because of the depopulation of the tail. However at somewhat larger temperatures, the ionization rate of the Druyvesteyn can actually be greater, due to the fact that the body extends to higher energy.

There is interesting recent probe data for rf discharges on the distribution functions for different types of collisionality. This is Godyak's data for the argon and helium plasma at a pressure of 0.3 Torr. At this pressure and with a drive frequency of 13 MHz, the electron collision frequency is greater than the drive frequency, so the fact that the discharge is rf rather than dc will not have a large effect on the predicted distribution function. For helium, where as we have seen, the collision frequency is nearly constant, the distribution function at a variety of different drive currents is shown in Fig (7.1a). Up to the largest currents, where the discharge is in the γ regime, the distribution function is Maxwellian. For argon, the case is more complicated due to the Ramsauer minimum. From about 6 to about 25 eV, the energy exchange collision cross section (proportional to σ_p) is reasonably constant,and at higher energies, it slowly decreases. Thus, above about 6 eV, the distribution should be Druyvesteyn like. Below 6 eV, the momentum exchange collision frequency increases sharply with energy. Thus below this energy, the index of the power law in the exponent should be even greater than four. However if the thermal energy is greater than about 4-6 eV, as it must be if there is to be ionization, the difference in the distribution function will not be very noticeable, and the general structure should be Druyvesteyn like. This is found to be the case for argon, and Godyak's data for argon at 0.3 Torr is shown in Fig.(7.1b). Up to the onset of the γ regime, the distribution functions are Druyvesteyn like.

Let us now consider the current in the plasma. As is apparent from Eq.(7.13) for f_1, there is both an in phase and out of phase component. We consider now the dc case, so there is only an in phase component and

$$u_e = (4\pi/3)(eE/m) \int_0^\infty dv(v^3/\nu_p)\partial f_0/\partial v \qquad (7.20)$$

For the simplest case of ν_p independent of velocity, we find that

$$u_e = eE/m\nu_p \qquad (7.21)$$

This might make it appear that u_e would be proportional to E plasma discharges. However this is an oversimplification and is true only if ν_p is independent of v. In the more typical case where the mean free

path is independent of energy (as for instance an oxygen plasma as shown in Fig (2.1a)), we find that

$$u_e \propto E/n_a T_e^{1/2} \tag{7.22}$$

For the dc case, the temperature is itself a function of E/n_a given by Eq (7.16) with $\omega=0$. Instead of m/M_a, we use ζ which is itself a function of T_e when averaged over velocities as is apparent from Fig. (2.1a). Assuming that $\zeta \propto T_e^{\beta}$ and the elastic cross section is independent of energy, we find that

$$T_e \propto (E/n_a)^{2/(2+\beta)} \tag{7.23}$$

and

$$u_e \propto (E/n_a)^{(\beta+1)/(\beta+2)} \tag{7.24}$$

For the oxygen plasma with $\beta=2.6$, we find that the temperature scales as $(E/n_a)^{0.43}$ and the drift velocity scales as $(E/n_a)^{0.78}$. The actual exponents from Fig.(2.1b) and the discussion in Section 2 are 0.5 and 0.7. Thus the predicted values agree reasonably well with the observations. For nitrogen, one gets comparable agreement, but not quite as good agreement.

So far we have considered only the solution for the distribution function where the energy loss from an elastic or inelastic collision is small compared to the electron thermal energy. The dominant effect of these collisions in the f_o equation is now to remove particles from the tail of the distribution function and replace them in the body, but with an energy loss corresponding to the ionization, excitation or dissociation energy. Since f in the tail is so much less than what it is in the body, we will not consider the replacement into the body. Hence there is an additional contribution to S_o which is $-\nu_e f_o$. Also we assume ν_e is zero unless the energy is above a threshold value. Sometimes this is strictly valid, as in the case of an oxygen plasma, where the excitation process is dissociative attachment, and the electrons actually are lost. On the other hand, the vibrational excitations of nitrogen from about 2-4 electron volts constitute a barrier near the thermal energy, so strictly, the repopulation of the body below 2 ev has to be considered for accurate results (see Fig 2.2). The equation for f_o, for the case of the dc electric field, then becomes

$$[e^2E^2/3m]\partial/\partial v[v^2/\nu_p]\partial f_o/\partial v + \partial/\partial v[\nu_K v^3 f_o/2] - v^2\nu_e f_o = 0 \qquad (7.25)$$

If the third term were not present, the solution would be as given in Eq.(7.15), and we will denote this solution now as h(v). If f_o is now denoted by $f_o = g(v)h(v)$, we can reduce Eq.(7.25) to a single second order differential equation for g(v). Making a WKB approximation to the solution, we find that

$$g(v>v_1) = \exp -[(\sqrt{3}\, m\nu_p/eE)\int_{v1}^{v} dv'\zeta^{1/2}(v')] \qquad (7.26)$$

and of course g(v) is unity for $v<v_1$. The factor $\zeta(v')$ is the ratio between energy loss and momentum exchange cross section as a function of velocity, and the factor outside the integral is $\sqrt{3}$ divided by the drift velocity. Clearly the high energy tail of the distribution function is depleted. This in turn reduces the ionization or excitation rate from the approximation based on a Maxwellian given in Eq.(3.12). If there is more than one such process, ν_e is simply a summation over the important processes.

Let us consider this qualitative theory for the case of nitrogen and the vibrational barrier between two and four electron volts. The drift velocity for a 3 ev electron is about $3x10^6$ cm/s if E/N is about $2x10^{-16}$Vcm^2, according to for instance the swarm relations, and $\zeta(v')$ averaged over 2-4 ev is about 0.05 from Fig 2.2. In that case we see that the additional drop in the value of distribution function, as the electrons go from 2-4 ev is about 7 orders of magnitude. Shown in Fig. 7.1 is a plot of the distribution function calculated by Brunet et al[110] calculated from a more accurate modeling of the detailed vibrational excitations. Clearly the drop in log f(u) is roughly correct for the case of room temperature ions, which corresponds to the case of Fig.2.2. As the gas temperature increases, the vibrational states are thermally populated, and become less of an energy sink for the electrons, so that ζ decreases, and so does the drop in f(u). Up to energies of about 10 ev, there is nearly a plateau in f. This corresponds to the very small values of ζ at these energies, also evident from Fig. 2.2.

8. Scaling Laws for Binary Collisional Plasmas

We consider the case of a processing discharge consisting of three components, electrons (index e), ion (i), and neutrals (n) which may have internal structure. The main assumptions we make are that the plasma density is sufficiently low that only binary collisions are included, that the plasma is optically thin so all radiation escapes and has density much less than thermal equilibrium radiation density, and that electron and ion collisions with the neutrals are dominant. Notice that thermal equilibrium ionization densities would occur only by chance since the inverse processes to impact ionization and radiative recombination are not included in the model. However for most low density processing discharges, these assumptions are valid.

The plasma is described by the Vlasov Equation for the three species coupled to Maxwell's Equation.

$$\partial f_a/\partial t + \mathbf{v}\cdot\nabla f_a + (e_a/m_a)[\mathbf{E}+\mathbf{v}\times\mathbf{B}/c]\cdot\nabla_v f = \Sigma_b C_{ab} \quad (8.1)$$

$$\nabla\times\mathbf{B} = (4\pi/c)\Sigma_b n_b e_b \mathbf{v}_b + (1/c)\partial\mathbf{E}/\partial t \quad (8.2)$$

$$\nabla\cdot\mathbf{E} = 4\pi\Sigma_b n_b e_b \quad (8.3)$$

$$\nabla\cdot\mathbf{B} = 0 \quad (8.4)$$

$$\nabla\times\mathbf{E} = -(1/c)\partial\mathbf{B}/\partial t \quad (8.5)$$

The quantities n and nv are the first and second velocity integral of the appropriate distribution function. While these equations cannot be solved analytically there are scaling laws that which allow the solutions in one regime to be extended to another. We consider only scaling within an atomic species. If one goes from species to species, collision cross sections for all the multitude of possible processes depend very much on the atomic species and there is no simple scaling law from one to another. Similarly, we consider only scaling laws that leave particle velocity (and therefore energy and temperature) constant. Cross sections often have complicated velocity dependences for which there is no simple scaling.

Now we consider a scaling transformation of the form

$$f'=p^{a}f,\ t'=p^{b}t,\ x'=p^{c}x,\ v'=v,\ E'=p^{e}E,\ B'=p^{f}B \qquad (8.6)$$

for the electrons and ions. If the plasma is weakly ionized and that the neutral species is regarded as simply a background of density n_n, the right hand side of Eq. (8.1) becomes $n_nC(f_a)$ where a is e or i, and $C(f_a)$ is a linear function of f_a. Here there is a scaling, also valid for a collisionless plasma where $C(f_a)=0$, which is given by

$$a=2,\ e=f=1,\ b=c=-1 \qquad (8.7)$$

If we regard the background density n_n as the scaling parameter, then times and lengths scale as n_n^{-1}, and electric and magnetic fields scale as n_n. The distribution function f_a, and correspondingly the electron and ion densities scale as n_n^2. For dc discharges, we have seen that the current scales as n_n^2 and the sheath cathode fall distance scales as n_n^{-1}. Both these scaling laws are consistent with Eq.(8.7). Also, we have seen that in the positive column, the temperature is constant if Rn_n is constant. This scaling is also consistent. Thus the scaling laws, which can be derived very easily, are capable of predicting many of the features of the dc glow discharge. In the case of collisionless plasmas, the same scaling law applies, except that n_n is obviously no longer appropriate as a scaling parameter. Some other parameter, for instance a length or field could be used.

In most rf driven processing plasmas, the drive frequency is very difficult to vary, but the background neutral density and the input power can be more easily varied. The existence of the scaling for weakly ionized plasmas can then allow one to surmise how a known plasma would scale to different frequencies.

The scaling laws were derived for bulk plasma only. If the plasma is bounded, the presence of the wall might introduce other scaling. For instance the chemistry of the bulk plasma might be affected by the wall. In the simplest cases, of absorbing or reflecting wall, the wall would not affect the scaling, We saw this in the case of the cathode sheath for instance.

9. Fluid Equations for Processing Plasmas

This section derives fluid equations for a processing discharge having three species n,e and i. Three fluid equations for number density, momentum density and energy density are obtained for each species by calculating the first three velocity moments of the Vlaxov Equation. The fundamental difficulty is that each moment is coupled to the next higher moment by the $v\cdot\nabla f$ term in the Vlasov Equation. The hierarchy of fluid equations can only be closed by making some sort of approximation. A typical one, one made in Ref.(5) is that the distribution function of each species is approximately a local Maxwellian. This is not an exact solution to the Vlasov Equation for two reasons; first, the velocities and temperatures of the components may be different, and second, the system can be inhomogeneous and time dependent. The effect of the different velocities and temperatures is an energy and momentum exchange between the components as described in Sec 2. The effect of the inhomogeneity is the introduction of transport. We will consider these two processes separately.

To start, we will work with the electrons and assume its distribution is a Maxwellian. If the fluid velocity is **u**, the particle velocity in Vlasov equation is given by **u+w**, so **w** is the random velocity about the average. Where convenient, to keep the notation as simple as possible, we will delete subscripts denoting species. Where necessary we will return to using them. Then integrating the electron Vlasov Equation over velocity and multiplying by mv and integrating over velocity, we find two equations for electron number density and momentum:

$$\partial n/\partial t + \nabla\cdot n\mathbf{u} = M_c \qquad (9.1)$$

$$\partial nm\mathbf{u}/\partial t + \nabla\cdot[nm\mathbf{uu} + nT] + ne\mathbf{E} + ne[\mathbf{u}\times\mathbf{B}]/c = \mathbf{P}_{en} \qquad (9.2)$$

The charge e by convention is positive. Here, M_c and $\mathbf{P}_c$ are the collisional rates of change of number density and momentum density. The former comes from for instance ionization and recombination, the latter from momentum exchange between the different species as well as ionization and recombination. Often it is convenient to combine Eqs.(7.1 and 7.2) to give an equation for the acceleration of the plasma species:

$$nm\partial \mathbf{u}/\partial t + nm\mathbf{u}\cdot\nabla\mathbf{u} + \nabla nT_e + ne\mathbf{E} + ne[\mathbf{u}\times\mathbf{B}]/c = \mathbf{P}_{en} - mu M_c \qquad (9.3)$$

For the energy equation, multiply the Vlasov Equation by $1/2mv^2$ and integrating over velocity to get

$$\partial/\partial t[1/2nmu^2 + 3/2nT] + \nabla\cdot[1/2nmu^2\mathbf{u} + 5/2nuT_e]$$

$$+ ne\mathbf{u}\cdot\mathbf{E} = W_{en} \qquad (9.4)$$

where W_{en} is the collisional rate of change of energy density from electron neutral collisions. The total electromagnetic energy input into the fluid is the electric field dotted into the current density of the species, as is to be expected. This can also be written as a temperature equation by subtracting $\mathbf{u}$ dotted into the momentum equation and adding $1/2mu^2$ times the number density equation. The result is

$$3/2\partial nT/\partial t + 3/2\mathbf{u}\cdot\nabla nT_e + 5/2nT_e\nabla\cdot\mathbf{u} = W_{en} - \mathbf{u}\cdot\mathbf{P}_{en} + 1/2mu^2M_c \qquad (9.5)$$

Notice that in Eq.(9.5) above, the electric field no longer appears. The Ohmic heating is now expressed as a collisional heating. In equations (9.1-9.5), we emphasize that the assumption has been explicitly made that the species has a Maxwellian velocity distribution with temperature T and velocity $\mathbf{u}$. Thus the collision term for the interaction of the electrons among themselves vanishes; the collision terms M_c, $\mathbf{P}_{en}$ and W_{en} describe changes in number density, momentum and energy from the interaction of the electrons the neutrals, almost always the most important collisional process for weakly ionized processing plasmas.

Let us first discuss the momentum exchange. The average force is given by Eq.(3.7). It is not difficult to show, that the momentum integral of the Boltzmann collision integral can be reduced to this form. For electron neutral collisions, we assume that $w_e >> u_e, u_n, w_n$ and expand relative velocities based on this scaling. Defining $n_n w_e \sigma_p(w_e)$ as the electron momentum exchange collision frequency, $\nu_p(w_e)$, Eq.(3.7) can be expanded in a power series. Keeping only the first few terms, we find

$$\mathbf{P}_{en} = -\mu\int d^3w_n d^3w_e\{\mathbf{w}_e\nu_p(w) + (\mathbf{u}_e-\mathbf{w}_n-\mathbf{u}_n)\nu_p(w_e)$$

$$+ \mathbf{w}_e\partial\nu_p/\partial w_e[\mathbf{u}_e-\mathbf{w}_n-\mathbf{u}_n]\cdot\mathbf{w}_e]/w\}f_e f_n \qquad (9.6)$$

where the notation $\mathbf{P}_{en}$ means the average force, or momentum exchange between electrons and neutrals. The integral of the first term in the brackets is zero because of the assumed Maxwellian nature of f_e. The next term is

$$\mathbf{P}_{en} = -n_e\mu[\mathbf{u}_e-\mathbf{u}_n]\nu_p = -\mathbf{P}_{ne} \qquad (9.7)$$

where by ν_p we now mean the average over the distribution function. Since ν_p is proportional to n_n, the force density has appropriate symmetry between the species. For convenience, we will sometimes use the definition $\nu_p(w_e) \equiv n_n\theta_p(w_e)$. The last term in Eq.(9.6), also proportional to $\mathbf{u}_e-\mathbf{u}_n$ is a correction arising from the variation of ν with energy.

For elastic collisions, the energy density exchange between species is given by Eq.(3.9). Again, one can show that an integral of the Boltzmann collision integral gives this result. Expressing the v's in terms of the w's and u's, we find

$$W_{en} = -k\int d^3w_e d^3w_n n_e n_n f_e f_n \theta_p[mw_e^2+2m\mathbf{w}_e\cdot\mathbf{u}_e+mu_e^2-Mw_n^2-$$

$$2M\mathbf{w}_a\cdot\mathbf{u}_n-Mu_n^2+(m-M)(\mathbf{u}_e+\mathbf{w}_e)\cdot(\mathbf{u}_n+\mathbf{w}_n)] \qquad (9.8)$$

Here we have used m and M for the electron and neutral mass respectively. Also, we have made the simplifying assumption that θ_p is independent of w. The integrals over w can now be done assuming Maxwellian distribution functions. In addition to the elastic collisions, there is a significant energy loss from inelastic collisions. First we consider is impact ionization. This causes a loss of energy E_i from each electron doing the ionizing, and a corresponding gain of internal ion energy of this amount. Secondly, analogous to Eq.(3.11), there is excitation of the electronic states of the atom or molecule. Usually this energy is immediately radiated away, although there are often some long lived excited states (metastables) which can also affect both the energy balance and chemistry. Thirdly, the electron loses energy due to the excitation of rotational and vibrational and electronic states of the neutral. We express the total energy loss as

$$W_{en} = -n_e\nu_p[(3k+\zeta(T_\varepsilon))(T_e-T_n)+ k(mu_e+Mu_n)\cdot(u_e-u_n)]$$

$$-E_iM_c - W_{exc} \qquad (9.9)$$

Included in Eq.(9,9) are temperature equilibration due to elastic collisions, due to the inelastic collisions exciting rotational and vibrational states, energy loss due to drift, which is generally very small, and energy loss due to ionization and excitation of electronic states.

Now consider the fluid equations for the ions. The ions have nearly the same sort of internal energy states as the atom or molecules and are closely coupled them. Nevertheless, since it takes significant energy to ionize the atom, this energy must be accounted for. If the ionization energy is E_i, each ion will be considered to have an internal energy E_i. Then the momentum equation for the ions is given by the obvious analog of Eq. (9.3) and temperature equation is

$$3/2\partial(nT_i+nE_i)/\partial t + 3/2\mathbf{u}\cdot\nabla nT_i + T_i\nabla\cdot n\mathbf{u} + 5/2nT_i\nabla\cdot\mathbf{u} =$$

$$W_{in} - \mathbf{u}\cdot\mathbf{P}_{in} + 1/2mu^2M_c \qquad (9.10)$$

The mass source term, M_c is just the term resulting from ionization of the background gas. We consider here charge exchange, which is often the most important momentum exchange process in simple gases. The main place we will be concerned with the dynamics of the ions are where the ions are accelerated in the sheath. Here they have a large kinetic energy compared to the neutrals. In this case, for constant charge exchange cross section, and for energetic ions with velocity $\mathbf{u}$, streaming through a gas of background neutrals, we have

$$\mathbf{P}_{in} = -n_in_nMu|u|\sigma_x \qquad (9.11)$$

Now let us consider the heating term. There are two conflicting effects. First of all, the particle, when it collides, loses all of its energy, so that there is a significant loss of energy of the ions. However due to the statistical nature of the collisions, a set of ions starting rest from position x=0 will charge exchange at different locations. This manifests itself as a heating. Performing

the collision integrals the heating term in the ion temperature equation is

$$W_{in} - \mathbf{u}_i P_{in} = n_i \nu_x (M u_i^2/2 - 3T_i/2) \qquad (9.12)$$

Once some heating has taken place so that $T > Mu_i^2/3$, the charge exchange gives rise to ion cooling. Thus, often the simplest model is to simply neglect the ion heating and consider the ion streaming as that of a cold fluid. However we must always account for the internal energy, E_i that the ion carries. Whenever the ion recombines, for instance at a wall, this energy is given back to the wall, gas, or is radiated away.

We now consider the case of transport. This gives rise to terms in the fluid equation which result from the fact gradients render f(v) non Maxwellian. A method of deriving an augmented set of fluid equations is to assume that the distribution function consists of a Maxwellian times a summation of various products of velocity. We consider only a single transport coefficient here, thermal electron energy flux. A distribution function can be written which has a non zero energy flux vector, $\mathbf{q} = \int d^3w \, 1/2 m w^2 \mathbf{w} f \neq 0$. For a Maxwellian distribution function, $\mathbf{q}=0$, so no term from q appears in the fluid equations as they have been written so far. If $q \neq 0$, then in the energy density equation, there is an additional term $\nabla \cdot \mathbf{q}$ on the left hand sides of Eq.(9.5). The trick then is to find $\mathbf{q}$ in terms of fluid quantities.

We assume an electron distribution function

$$f = f_m [1 - \mathbf{q} \cdot (m\mathbf{w}/nT^2)(1 - mw^2/5T)] \qquad (9.13)$$

where f_m is a Maxwellian for the electrons with Temperature T and flow velocity $\mathbf{u}$. The additional term does not contribute to the density or the temperature because it is an odd function of w. The coefficients of the two terms in the brackets were chosen so that it does not contribute to the fluid velocity either. The lowest nonzero moment of the assumed distribution function is the thermal energy flux, which comes out to be equal to $\mathbf{q}$.

To determine an equation for $\mathbf{q}$, we take the $1/2mv^2\mathbf{v}$ moment of the Vlasov Equation. The first term (the $\partial/\partial t$ term) is relatively straightforward to calculate. It is $\partial/\partial t [1/2 n m u^2 \mathbf{u} + 5/2 n T \mathbf{u} + \mathbf{q}]$. The

second term (the $v\nabla f$ term) is more complicated. To write the term in simplest form, we assume that $mu^2 << T$ and also that $muq << nT^2$. Making this approximation, we find that this term becomes $5/2\nabla nT^2/m$. Upon several straightforward partial integrations and vector manipulations, the electric field term becomes $-neu(\mathbf{u}\cdot\mathbf{E}) - 1/2neu^2\mathbf{E} - 5/2(eE/m)nT$. The magnetic term is the most burdensome of all to evaluate. It turns out to be $-[5/2(neT/mc) + 1/2(neu^2/c)]\mathbf{u}\times\mathbf{B} - (e/mc)\mathbf{q}\times\mathbf{B}$. This involves a fair number of vector identities and symmetries of f and f_m. In evaluating integrals over cross products in the terms leading to the $\mathbf{q}\times\mathbf{B}$ term, it is often convenient to express cross products in terms of tensor notation $(\mathbf{a}\times\mathbf{b})_i = \varepsilon_{ijk}a_jb_k$ where ε_{ijk} is the completely antisymmetric third rank tensor having ±1 as the nonzero elements.

Thus the energy flux equation becomes

$$\partial/\partial t[1/2nmu^2\mathbf{u} + 5/2nT\mathbf{u} + \mathbf{q}] + 5/2\nabla nT^2/m$$

$$-neu(\mathbf{u}\cdot\mathbf{E}) - 1/2neu^2\mathbf{E} - 5/2(eE/m)nT -$$

$$[5/2(neT/mc)+1/2(neu^2/c)]\mathbf{u}\times\mathbf{B} - (e/mc)\mathbf{q}\times\mathbf{B} = \mathbf{Q}_c \quad (9.14)$$

where $\mathbf{Q}_c$ is the energy flux integral of the Boltzmann collision term. This can be simplified further by using the mass, momentum and energy equations to manipulate the left hand side of Eq.(9.14) into a form in which the terms that do not involve $\mathbf{q}$ are subtracted out from the left hand side. The result is

$$\partial\mathbf{q}/\partial t + 5/2(nT/m)\nabla T - (e/mc)\mathbf{q}\times\mathbf{B} = \mathbf{Q}_c - \mathbf{P}_c[5/2T/m+1/2u^2]$$

$$- 5/3\mathbf{u}(\mathbf{u}\cdot\mathbf{P}_c) + 5/3\mathbf{u}W_c + M_c[5/2\mathbf{u}T - 1/6mu^2\mathbf{u}] \quad (9.15)$$

In arriving at Eq.(9.15), it is necessary to drop terms in the spatial gradient term which are small by factors like mu^2/T or muq/nT^2. That is the flow velocity and energy flux velocity are all assumed small compared to the electron thermal velocity.

In a weakly ionized plasma, the main electron collision process is with the background neutrals. We assume that the background gas consists of atoms of infinite mass compared to the electrons which are at rest. Then we approximate $\mathbf{P}_c = nmu_e\nu_c$, and

w_e is multiplied by an energy exchange collision frequency smaller by either m/M or ζ and therefore negligible.

If we further neglect the effect of the ionization on the energy flux, we have the result that the right hand side of the flux equation becomes $\mathbf{Q}_c$-5/2T$\mathbf{P}_c$. Now let us look at $\mathbf{Q}_c$ as gotten from the Boltzmann collision integrals for stationary, infinite mass ions. It is

$$\mathbf{Q}_c = \int d^3v d\Omega 1/2mv^2 \mathbf{v} n_a n_e \sigma(v,\Omega) v(f_e' - f_e) \qquad (9.16)$$

where as before, a primed variable denotes the velocity of an electron which ends up at velocity **v** after a collision of angle Ω. In writing Eq.(9.16), we have used the principle of detailed balance. Thus, using these relations, and the fact that v is a variable of integration which can be relabeled as v' in the integral, one can derive the result

$$\mathbf{Q}_c = -\int d'v d\Omega 1/2mv^2(\mathbf{v}-\mathbf{v}')n_a \sigma(v,\Omega) v f_e \qquad (9.17)$$

Now for a scattering angle of θ, we can write $\mathbf{v}' = \mathbf{i}_v v\cos\theta + \mathbf{i}_v \times \mathbf{i}_n v\sin\theta$, where $\mathbf{i}_n$ is a unit vector perpendicular to the plane of the collision. The perpendicular part then integrates to zero over angle, and the parallel part is related to the momentum exchange cross section. We find $\mathbf{Q}_c = -\int d^3v 1/2mv^2 \mathbf{v} \nu_c(v) f_e$. Expressing **v** as **u+w**, and assuming that ν_c is independent of v, we find that $\mathbf{Q}_c = -\nu_p \mathbf{q} + 5/2T_e\mathbf{P}_c$, so the equation for q becomes

$$[\partial/\partial t + \nu_p]\mathbf{q} - (\mathbf{q}\times\Omega_c) + 5/2(nT_e/m)\nabla T_e = 0 \qquad (9.18)$$

where Ω_c is the vector electron cyclotron frequency. Generally, for equilibrium conditions, we neglect the time dependence of **q**. Then the value of **q** depends greatly on the magnitude and direction of the magnetic field. Specifically,

$$q_B = -5/2(nT_e/m\nu_p)(i_B \cdot \nabla T_e) \qquad (9.19)$$

and

$$q_T = -5/2(nT_e/m)[\nu_c^2 + \Omega_c^2]^{-1}\{\nu_c \nabla_T T_e - i_B \times \nabla T_e\} \qquad (9.20)$$

where the subscripts B and T mean parallel to and transverse to the magnetic field. In all cases, the temperature gradient drives the thermal conduction. If $\nu_p >> \Omega_c$, the thermal flux is parallel to the negative temperature gradient and is proportional to the reciprocal of the collision frequency as is conventional in kinetic theory. Here however the collisions are with the atom background rather than within the species being considered. If the magnetic field is large, $\nu_p << \Omega_c$, the thermal flux is anisotropic in the three directions of magnetic field, temperature gradient perpendicular to the field, and cross product of the two. The thermal conduction perpendicular to the magnetic field is greatly reduced from its unmagnetized value.

10. Quasi-Neutrality and Sheaths in Plasmas

Far from walls, plasmas are electrostatically neutral. This is called quasi-neutrality, or ambi-polarity. We have seen in Sec.(4), Eqs.(4.15 and 16), that if strong electric fields are set up, they have length scale of the Debye length $(T/4\pi ne^2)^{1/2}$. This is an extremely small length, less than 100μm for a plasma with density 10^{10} cm^{-3} and temperature 1 eV. Notice that quasi-neutrality does not mean exact neutrality; the plasma, for one reason or another may require small electrostatic fields, and these can come only from small differences in electron and ion density. As we will see, the properties of quasi neutral plasmas are calculated using $n_i=n_e$ as an approximate solution of Poisson's equation and then calculating the electric field from the remaining equations.

The plasma bulk will almost always be quasi-neutral over distances large compared to the Debye length. However, there are Debye scale potential and density variations about any plasma boundary. It is interesting to note that the feature scale on the workpiece (an integrated circuit for instance) can be much smaller than the Debye length. Thus once the workpiece is etched into patterns, there may be effects of charge separation in the plasma local to the pattern.

Let us consider in more detail the formation of the sheath. Consider a Maxwellian electron plasma of density n and electron temperature T, but with cold ions, to be in contact with a wall. The boundary condition on the wall is that it absorbs all particles incident on it. This electron flux is $n(T/2\pi m)^{1/2}$. Thus the velocity into the wall is about the electron thermal velocity, and the electrons within a Debye length of the wall are cleared out within about a plasma period. The wall charges up negative and begins to accelerate the ions toward the wall. Thus there is a flux of particles toward the wall, and this flux is assumed to be absorbed.

Since the sheath has Debye length scale, which is assumed to be much smaller than mean free path or geometric scale length, a collisionless one dimensional model is valid. The sheath is at the right hand edge of a collisionless plasma. The electrons have temperature T and the ions are cold. Both have number density n_o far from the sheath where the potential is defined to be zero, the sheath is described by Poisson's Equation

$$d^2\phi/dx^2 = -4\pi e(n_i-n_e) \qquad (10.1)$$

To solve this, we need the electron and ion density in terms of ϕ, starting from the edge of the sheath where by definition $\phi=0$. The electron density is $= n_o \exp e\phi/T$. At $x=-\infty$, far from the sheath, the ion velocity is u_o. Since $nu=n_o u_o$, the ion density in terms of the potential is $n_i = n_o u_o/[u_o^2-2e\phi/M]^{1/2}$.

We expect the ions to accelerate through the sheath, so we expect $\phi<0$, that is we expect the plasma to have a higher positive potential than the bounding surfaces in contact with it. Also, we expect the sheath to have higher ion density than electron density, since the ions are following the electrons out. For small ϕ the electron and ion densities follow by linearization, $n_i = n_o(1+e\phi/Mu_o^2)$ and $n_e = n_o(1+e\phi/T)$. For $\phi<0$, the ion density in the sheath is greater than the electron density only if $Mu_o^2>T$. Also from Eq.(10.1) it is clear that if this is so, the sheath is exponentially decaying into the plasma, otherwise Eq.(10.1) has a solution which is oscillatory in x and the solution does not have the character of a sheath, but rather of a wave. Thus in order for a sheath to be formed, we must have

$$u_o>[T/M]^{1/2} \qquad (10.2)$$

For the case of an equality in Eq.(10.2), this is called the Bohm criterion. The Bohm criterion is often used as a condition separating the plasma from the sheath, and in general this is correct. However the situation is complicated in general, and to determine the actual condition, one must look at the fluid solution both near and far from the wall. The case we have been considering, a semi-infinite one dimensional collisionless plasma in contact with a wall is under specified. To satisfy the sheath condition, any incident ion velocity greater than $\sqrt{T/M}$ will suffice and smaller velocities will not.

To come up with a simple specified system, we will consider a spherical instead of planar wall. We will assume that the spherical radius is small compared to any other physical size characterizing the plasma, but large compared to the Debye length. This then will become the theory of a plasma probe, a common diagnostic. There is an outer quasi-neutral region of size characteristic of the radius, and a Debye length scale inner region, right near the sphere which is

nearly planar. The boundary condition on the sphere is that it absorbs every charged particle impinging on it. These recombine on the surface and are recycled as neutrals back into the plasma. Far from the sphere, the outer region is assumed to be an infinite homogeneous plasma with cold ions, electrons of temperature T, and number density n_o. Thus there is both a particle flux and an electric current to the sphere, and we wish to relate these to the potential of the sphere. The potential of the plasma far from the sphere is zero, and this is defined as the plasma potential.

Using the relation between the potential (and electric field) and electron density, we find that the steady state collisionless ion momentum equation becomes $Mudu/dr = -(T/n)dn/dr$, where we have assumed quasi-neutrality, $n_e=n_i=n$. The steady state mass conservation equation, in spherical geometry becomes $d/dr(r^2nu) = 0$. Combining these, we find a single equation for u,

$$du/dr = -2u/r[1-Mu^2/T] \qquad (10.3)$$

Notice that this equation is singular at $u^2=T/M$, the precise velocity defined by the Bohm criterion. However the singularity is only a singularity of the slope, u itself is defined by Eq.(10.3) right up to the singularity. In fact the equation can be integrated analytically. To specify the outer solution, we need only integrate it subject to the appropriate boundary condition.

The appropriate boundary condition for the outer solution is that the singularity is at $r=r_o$, the surface of the sphere. To see this, note that at the singularity, the infinite slope means that quasi-neutrality has broken down and that Poisson's equation must be used instead of the quasi-neutrality condition. However Poisson's equation has no singularity, but it has a higher derivative, $d^2\phi/dx^2$, which introduces a much smaller length scale where it is needed. Thus the singularity is really the mathematical treatment begging for inclusion of the shorter length scale, or higher derivative. Since the Debye length is assumed to be much less than the radius of the sphere, the singularity is at the spherical surface (or actually a few Debye lengths away). The outer solution, determined by integrating Eq.(10.3), subject to the boundary condition that the $u=\sqrt{T/M}$ at $r=r_o$ is

$$r^2u\exp-[Mu^2/2T] = r_o^2(\sqrt{T/M})\exp-1/2 \qquad (10.4)$$

This solution is also consistent with the boundary condition at $r=\infty$, $u=\phi=0$. At the singular point, the electrostatic potential is given by $e\phi/T = -1/2$, so the density is given by $n=n_0 \exp -1/2$. Thus the mass flux into the sphere is

$$dM/dt = 4\pi r_0^2 n_0 M(\sqrt{T/M})\exp -1/2 \qquad (10.5)$$

and it is specified entirely by the outer solution.

The singular point near the spherical surface marks the beginning of the inner solution. To actually determine the total solution, one must in general do a matching of the inner and outer solutions. Typically this is complicated and involves intermediate solutions with scale lengths that are some fractional power of products of the scale length of the inner and outer solution. In many cases the information desired depends in detail on this matching. The most famous case in the plasma physics literature is a tearing mode, where the growth rate depends on precisely how the inner and outer solutions are matched[111,112]. Just patching them together at the singularity will not give the growth rate of the mode.

Fortunately, the case we are discussing here is much simpler, like some others involving shocks with multiple structure[113], and the main information required, the current as a function of sphere Voltage can be obtained with a simple patch. We are not here interested in the precise structure of the transition region for its own sake, so we will not look into the more complicated problem of the detailed matching. However other sheath problems in processing discharges may require this procedure.

The equation for the nonneutral sheath region is Poisson's Equation

$$d^2\phi/dx^2 = -4\pi e n_0[(-T/2e\phi)^{1/2}\exp -1/2 - \exp(e\phi/T)] \qquad (10.6)$$

where we have assumed as initial values, the parameters at the outer singular point. If this equation is initialized with $e\phi=-T/2$ and a small negative slope, a sheath solution with a Debye length scale will result. Since the sphere is assumed to simply absorb all incident particles, and since the electron density is known as a function of ϕ, we can calculate the current as a function of the

sphere Voltage ϕ_o. Of course the ion current to the sphere is simply e/M times the ion mass accumulation independent of ϕ. The electron current density is that from half a Maxwellian at the electron density of the wall. Thus the electric current is

$$I = -4\pi e r_o^2 n_o[(T/2\pi m)^{1/2}\exp(e\phi_o/T) - (\sqrt{T}/M)\exp -1/2] \qquad (10.7)$$

For this solution to be meaningful, the potential of the sphere must be less than -T/2e, or the outer solution will be non singular. At this potential, the current to the sphere is large and negative, it is nearly the full electron current of a half Maxwellian electron distribution. As the potential is lowered, the magnitude current decreases until it vanishes at a potential ϕ_f

$$e\phi_f/T = 0.5[\ln(2\pi m/M) - 1] \qquad (10.8)$$

This is called the floating potential and is the potential a small foreign body will float to if it is inserted into the plasma, but cannot draw current. For potentials much below this virtually all of the electron current is cut off, and the current to the sphere is positive current from the ion flux, independent of the inner solution.

Thus for the case of the absorbing sphere, the Bohm criterion is correct, but the justification lies in the singular nature of the outer solution. In fact the inclusion of ion inertia will nearly always generate a fluid singularity where the flow speed is equal to the sound speed. The singular nature of the outer solution, at just the Bohm velocity, is then what usually justifies Bohm criterion.

We next consider another type of sheath at higher Voltage and longer scale length, like the cathode fall of a dc discharge. Then electrons from the plasma are virtually excluded from these regions of the sheath according to Eq.(4.15). The edge of the electron region will be the source of nonneutral ion flux, and the current will be purely ion current from the edge of the electron boundary to the workpiece. Since the ion current emerges from the sheath region at low Voltage, the ion region is a planar ion diode.

There are various possible laws for the ion diode depending on the collisionality of the ions. If they are collisionless, the relation between Voltage, current and thickness s is given by the Child-Langmiur space charge limited current equation

$$J_{LC}(A/cm^2)=10^{-8}(M_a/M)^{1/2}V^{3/2}(volts)/s^2(cm) \qquad (10.9)$$

where M_a is the mass of an argon atom and the electric field as a function of distance from the sheath edge varies as $E \sim x^{1/3}$. For instance for a kilovolt across a centimeter in an argon plasma, the ion current is about $3x10^{-4}A/cm^2$. Thus the ion diode thickness is generally much greater than the Debye length which characterizes the electron-ion sheath we have just discussed.

If the ions are collisional, the diode law depends on the collision cross section a function of energy. We consider two idealized cases. First assume the mean free path is constant. Then the ion diode law becomes

$$J_\lambda = 2.3(\lambda/s)^{1/2}J_{LC} \qquad (10.10)$$

and $E \sim x^{2/3}$. Of course this is only valid if $\lambda<s$. Second, assume the ions are collisional with a constant collision frequency ν; then the ion diode law becomes

$$J_\nu = (64/81)[(2eV/M)^{1/2}/s\nu]J_{LC} \qquad (10.11)$$

and $E \sim x^{1/2}$. This is valid only if $J_\nu < J_{LC}$. Thus in the absence of electrons, the collisionless ion diode represents the maximum current that can be drawn to the cathode.

Note that none of the laws give an electric field which is linear in x, as is usually measured. However the law for constant ion mean free path is closest. Furthermore, for the parameters of the discharges discussed in Section 2 and the collisionality laws discussed in Section 3, the constant ion mean free path is a reasonable assumption for the ions if they are governed by dominant charge exchange process. Furthermore, the ion mean free path is small compared to the sheath width. Thus our conclusion is that the collisional ion diode with constant λ gives the best approximation to the cathode fall in the dc glow discharge.

However this does not completely specify the sheath. In a plasma, the Voltage and current are not simultaneously s ed; only one is given, and the other is derived from the Ohm's or the plasma or its equivalent. Thus one additional relation is requ ed to

determine the ion sheath parameters. In the next sections we will see how this determination can be made for dc and rf discharges.

For now, we will consider the simpler case of plasma immersed ion implantation (PIII)[114,115]. In this case a workpiece is inserted in the plasma of number density n_o, and is pulsed with a large negative Voltage, a Voltage we will assume to be much greater than T/e. Before the Voltage is turned on, the workpiece will be bombarded with a low energy ion flux as we have just described. Then at time t=0, a Voltage pulse V(t) is imposed. Then the plasma electrons begin to be excluded from a region of width s near the workpiece. We will assume that s is changing with time very slowly compared to the ion flight time across the sheath region. Then the sheath behaves instantaneously like an ion diode. However the current density is simply the rate that the sheath eats its way into the plasma (The current in the sheath is displacement current). That is

$$-J = n_o e ds/dt \qquad (10.12)$$

where for the configuration we envision, the plasma on the left of the workpiece, so J>0 and ds/dt<0. Equating the current to the collisionless ion diode result, we find a single equation for s (now interpreted as the magnitude of the sheath width) in terms of the Voltage pulse

$$ds/dt = 6x10^{12}(M_a/M)^{1/2}V^{3/2}(t)/n_o s^2 \qquad (10.13)$$

where n_o is in cm^{-3}. From Eq.(10.13), one can integrate and calculate the current pulse and therefore the charge dose as a function of energy which is embedded in the workpiece.

So far we have considered only the flux of energetic charged particles to the workpiece, those generated in the sheath. However in processing discharges, there are also energetic neutrals impinging on the workpiece. The only apparent source of these neutrals is ion charge exchange collisions in the sheath. If we assume that the collision rate is small enough that ion collisions are a small perturbation on the overall ion flux through the sheath, one can calculate the flux of fast neutrals from the charge exchange cross section $\sigma_{ex}(E)$ where E is the ion energy. If the ion density and velocity at a position x in the sheath are $n_i(x)$ and v(x), then the flux of neutrals dF, produced in region dx of the sheath is given by

$$dF = n_i(x)v(x)n_a\sigma(E)dx \qquad (10.14)$$

where n_a is the atom number density. The relation between ion energy (or velocity) and position in the sheath completes the description. Thus from a knowledge of the charge exchange cross section and sheath parameters, one can calculate the flux of energetic neutrals onto the workpiece for the case where it is a small perturbation of the ion flux.

11. Infinite DC Discharges in Cylindrical Geometry

Let us assume that the steady state, magnetized, infinitely long cylindrical plasma is produced by a dc current. We assume that there is a central part, containing virtually all of the plasma volume which is quasi-neutral. Also we will neglect electron inertia and ion inertia in the axial and azimuthal direction. Near the wall, the radial ion inertia is important in that it is responsible for the singular behavior, so we will start by including it, and then show how the problem might be simplified by approximating it away. The quasi-neutral region is described by the number density equation for electrons, the momentum equation for electrons and ions, and the energy equation for electrons. As far as the ion energy goes, we account only for the ionization energy which the ions are defined as having.

We start with the momentum equation in the z direction

$$-eE_z = mu_{ez}\nu_e \qquad (11.1)$$

where ν_e is the electron momentum exchange collision frequency assumed to depend linearly on gas density, but otherwise is a constant. In steady state, curl $\mathbf{E} = 0$, so that in the plasma, E_z is constant and cannot have any radial variation. Since the current in the positive column is electron current one can easily calculate

$$I = \{\int d^2r n(r)\} e^2 E_z / m\nu_e \qquad (11.2)$$

The total power input into the electron thermal energy, from Eq.(9.5) is $nm\nu_e u_{ez}^2$ where u_e can be related to the electric field or total current through Eqs.(11.1 and 11.2). Generally we regard the total current as the specified quantity. In terms of it, the power input per unit length is

$$dP/dz = mI^2\nu_e / e^2 \int n(r) d^2r \qquad (11.3)$$

These then describe the Ohms law and energy input to the plasma. We now consider the radial particle flux. We neglect all inertia except radial ion inertia, which is responsible for the singular nature of the quasi-neutral solution. Then the steady state density and momentum equations become

$$(1/r)d/dr(rnu_r) = \alpha_i n N \qquad (11.4)$$

$$Mu_r du_r/dr = e(E_r + u_{i\theta}B/c) - Mu_r\nu_i \qquad (11.5)$$

$$0 = -eu_rB/c - Mu_{i\theta}\nu_i \qquad (11.6)$$

$$0 = -e(E_r + u_{e\theta}B/c) - m\nu_e u_r - (1/n)d/dr(nT_e) \qquad (11.7)$$

$$0 = eu_rB/c - mu_{e\theta}\nu_e \qquad (11.8)$$

where N is the neutral density and the right hand side of Eq.(11.4) is the ionization rate, where α_i depends strongly on electron temperature as discussed in the section on impact ionization. The ν's also depend linearly in N, but this dependence is not explicitly shown. Also T_e is the electron temperature, the only significant temperature in our discussion.

Equations (11.5-11.8) can be reduced to the single equation for u_r and n

$$Mu_r du_r/dr = -\{A_e+A_i\}u_r-(1/n)d/dr(nT_e) \qquad (11.9)$$

Here $A_e = m\nu_e[1+\Omega_e^2/\nu_e]$, with an analogous expression for A_i, where Ω is the appropriate cyclotron frequency. This and Eq. (11.4) for n are two of the equations for the density, radial velocity and temperature. By solving individually for the density and velocity derivative, one can determine that the solution becomes singular, in that the derivatives approach infinity, when the radial velocity is the ion sound speed.

Let us now discuss a way in which an approximate solution can be obtained without involving the detailed singular structure of the quasi-neutral solution. Neglecting ion inertia, we see that the ion radial velocity is given by

$$u_r = -[n(A_e+A_i)]^{-1}d/dr(nT_e) \qquad (11.10)$$

Notice that the velocity is determined by the magnetic field as well as collisionality of both species. For an unmagnetized plasma typically $A_e << A_i$ so the radial velocity controlled is by the ions. However it does not take a large magnetic field to increase A_e until, it is larger than A_i, thereby making the electrons the dominant

species in controlling the drift radial velocity. As r increases, dn/dr increases and n decreases so the velocity will approach the ion sound speed. The actual value of the density where this occurs is denoted by n_s.

The equation for the density then becomes

$$(1/r)d/dr\{r[A_e+A_i]^{-1}d/dr(nT_e)\} = -\alpha_i(T_e)Nn \qquad (11.11)$$

This must satisfy the boundary condition that $n=n_s\approx 0$ at the plasma edge. For given temperature profile, Eq.(11.11) is a linear equation for n, so that it does not specify the magnitude of the density, but only specifies the relative density profile as well as an eigenvalue insuring the boundary conditions are satisfied at both the center and edge. Also n_s is linearly proportional to n_o, the central density. Since the electric field is uniform in r and the heating rate is proportional to n, so we approximate the temperature as constant. Hence

$$n(r) = n_o J_o(\kappa r) \qquad (11.12)$$

where $\kappa^2 = \alpha_i(T)N[A_e+A_i]/T_e$. At the plasma wall r=a, the eigenvalue is determined approximately by $\kappa a=2.4$, the first zero of the Bessel function. Thus we have determined the relative density profile and the temperature. Notice that for a low temperature plasma, α_i is a very rapidly varying function of T. Thus large changes in things like wall radius will have only a small effect on the temperature.

In practice, the electron temperature then turns our to be one of the easiest quantities to predict. The electron density is much more difficult to calculate accurately. This is particularly so because typically secondary ionization processes and/or ionization from nonthermal energetic electrons can be important.

It is particularly interesting that the magnetic field has little effect on the plasma solution as well. Although the particle flux may be greatly reduced, this is compensated for in steady state, by a relatively small reduction of the plasma temperature. Thus we have many characteristics of the quasi-neutral solution. At the singular point, the quasi-neutral solution joins smoothly to sheath region as discussed in the previous section. Since the wall is assumed to draw no current, the wall is at the floating potential.

The sheath solution in the previous section was derived for the case of an unmagnetized plasma. Here we will show that as long as $\omega_{pe}>>\Omega_e$, (the usual condition in processing plasmas) the sheath is unaffected by the magnetic field. The sheath is assumed to be collisionless, so that here, magnetic deflection of electrons must be balanced by electron inertia. Solving the electron momentum equation in the y direction (corresponding to the θ direction in the cylindrical configuration) and substituting in x, we find that the electron momentum equation is integrable, and integrates to

$$1/2m(u_{ex}^2-u_{exs}^2) = -1/2m\Omega_e^2(x-x_s)^2 + e(\phi-\phi_s) - T\ln(n/n_s) \quad (11.13)$$

where a subscript s denotes a quantity at the sheath edge. Since the sheath velocity is typically $\sqrt{T_e/M}$, the left hand side can be neglected. If the sheath width is of order λ_{de}, the size of the magnetic field term is of order $(\Omega_e/\omega_{pe})^2$ as compared to the other terms, so it too can be neglected. Thus for sufficiently weak magnetic fields, the relation between density and electrostatic potential is as in the unmagnetized case.

Now we will calculate the density by considering the one remaining relation not yet considered, the energy balance relation. We will discuss the qualitative features of the energy relation. Then we will show how the swarm relations can often give a short cut.

The energy input to the plasma per unit length is given by Eq.(11.3). The energy losses are either through charged particles or through other channels. We will consider first the charged particle channel. Every charged particle flows out of the plasma and takes its energy with it. As before, the wall is assumed to be a perfect absorber of charged particles. With the ion flux goes the ionization energy and the ion kinetic energy that it has when it strikes the wall. The ion mass flux into the sheath is given by $n_s\sqrt{T_e/M}$. Thus the ionization energy convected out is $E_i n_s\sqrt{T_e/M}$. As the ion convects through out the sheath, it falls through a potential corresponding to the difference between the floating potential and the potential at the sheath edge given in Eq.(10.8). Thus the ion energy flux convected out is $(n_s\sqrt{T_e/M})(T_e/2)[1+\ln(M/m)]$. Next we consider the electron energy flux out of the plasma. The energy flux

of half a Maxwellian, is $2nT_e(T_e/2\pi m)^{1/2}$. As we have derived in the previous section, the electron density at the floating potential is $(m/M)^{1/2}$ times the density at the sheath edge. Thus the surface power convected out per unit length is

$$dP_s/dz=2\pi r n_s(T_e/M)^{1/2}[E_i +(T_e/2)(1+\ln(M/m)) + 2T_e(T_e/2\pi M)^{1/2}] \qquad (11.14)$$

In addition to the surface flux out, there is a volumetric power loss from radiation, ionization, as well as from heating the neutral gas. This volumetric power loss is

$$dP_v/dz = \int d^2r[(3m/M)\nu_e n T_e + n\Sigma_k \nu_k E_k] \qquad (11.15)$$

where the summation over k is the summation over all excitations. As a rough rule of thumb, these excitations fall into three categories which might be considered seperately. First there are rotational and vibrational excitations. These generally heat the background gas and we have occasionally denoted this as as an additional energy loss $\zeta(T_e)\nu_e n T_e$. Secondly there are electronic transitions which decay almost immediately and radiate their energy away. We can denote this power loss as a radiated power nP_r. Finally there are excitations of long lived states (metastables) which can be the seeds for secondary ionization processes. We can dennote this power loss as nP_m, The steady state energy lost to ionization is accounted for in the surface loss, Eq. (11.14)

Note that the volume power loss is proportional to N while the surface power loss is not, so there is no simple scaling with N. However the total power loss is proportional to the electron density; to the density at the singular surface for the surface loss; and to the average density for the volume loss. The power input per unit length is given by Eq.(11.3). Notice that this is proportional to the reciprocal of the average electron density. Equating the power in to the power out gives us an expression for the overall electron and ion density of the plasma. We find that the electron density is proportional to the total current I.

The swarm relations can often give a short cut. If the swarm relations are valid, the electron energy losses are assumed to be strictly volumetric. Take the case of the oxygen plasma, and say

that the eigenfunction equation for the electron density gave an eigenvalue of a temperature of 2 ev. Then from the swarm relation, Fig. 2.1b, we see this means that E/N is about 10^{15} Vcm^2 and the drift velocity is $w=10^7$ cm/s. The electron density is then given by J/ew. As we have seen, the electron temperature is not a very strong function of the parameters (radius, current or magnetic field for instance), so that if this is reasonably constant, varying from perhaps 1.5-2.5 eV, then there is little variation of drift velocity. This means that the swarm relations predict that the electron density is nearly proportional to current, as we found from energy relations.

Let us now recall the molecular oxygen plasma discussed in Section 6. For the low density plasma, it was pointed out that there was no sensible equilibrium. For instance for the O_2 species, there were only loss terms, while for electrons there were only production terms. We see now that the other part of the issue is the electrodynamics of the plasma itself. The loss of electrons as well as positive ions to the walls now allows equilibria to form as we have just calculated here. As far as the O_2 is concerned, from low density chemistry alone, there were only loss terms. However as the O_2^+, O^+, O and the associated electrons reach the walls of the discharge, they recombine. We have assumed for a boundary condition that the wall absorbs all particles impinging upon it. However once these particles are absorbed, it is likely that, for a totally inert wall, they recombine to the energetically favored species, O_2 in this case. Thus the wall is a source of O_2 which allows an equilibrium to form regarding this species as well.

For neutral atomic oxygen the reverse is the case, there are volumetric production mechanisms leading to a steady state flux to the walls where the it recombines to form O_2. Thus the steady state number density equations for O_2 and O are

$$(1/r)d/dr(rF_a) = S_a, \qquad (1/r)d/dr(rF_b) = S_b \qquad (11.16)$$

where we have used the notation of Section 5 where a corresponds to O_2 and b corresponds to O, and F is a number density flux and S is a source. For O_2, S_a is negative in the bulk, but there is a source at the wall. so the flux is inward, and just balances the volumetric loss. If O_2 is the predominant species, then $F_a = au_a$ where a is the equilibrium density. Thus the velocity as well as the flux can be obtained. For O the opposite is true, and there is an outward flux to

the wall. This atomic oxygen is of course the free radical and often the plasma is used simply to produce it so that it can react with the wall material and chemically affect it. In fact more realistic models of the processing discharge would have to account for the reactions at the wall and not simply assume that everything just recombines to form the initial products.

Let us now see how well this theory matches up with the experiments on magnetized and unmagnetized positive column by Bickerton and von Engel. Their experiments were done in helium. Ion neutral collisions are dominated by charge exchange, and the collision cross section is about 3×10^{-15} cm^2 according to Fig.(3.4e) Thus at room temperature, the ion thermal velocity is about 10^5 cm/s, so the ion collision frequency is $\nu_i(\text{sec}^{-1}) = 2\times10^{-10}N$. In terms of the gas pressure in Torr, $N(\text{cm}^{-3}) = 2.5\times10^{16}P(\text{Torr})$. Helium has a fairly high ionization energy of about 25 eV and a maximum cross section of about 4×10^{-17} cm^2. Thus the ionization rate α_i, from Eq. (3.12) is given by

$$\alpha_i = 1.6\times10^{-9}T_e^{1/2}\exp-[25/T_e] \qquad (11.17)$$

where T_e is given in eV. We will first consider the unmagnetized positive column. The simplest theory is to just use $\kappa a=2.4$ so that the density vanishes at the wall. Inserting for A_i, which is the dominant contribution to A for the unmagnetized case, and expressing the results in terms of pressure P, we find the temperature relation is

$$Pa = 0.086 \times (T_e^{1/4}) \times \exp(12.5/T_e) \qquad (11.18)$$

This is plotted as curve A on Fig.(2.5a). Clearly it only agrees at the very highest densities. One difficulty is that the actual condition is not that the density vanishes at the wall, but (assuming the Debye length is very small compared to the wall radius) rather that the radial velocity at r=a is the sound speed v_s. The radial velocity is given by Eq.(11.10). Using the Bessel function model for the density, the modified boundary condition is

$$v_s = (\kappa v_s^2/\nu_i)[J_1(\kappa a)/J_0(\kappa a)] \qquad (11.19)$$

This relation is plotted as curve B in Fig (2.5a). It shows better agreement with the data, but it still does not agree well for small pressure.

At small pressure, the mean ion charge exchange mean free path becomes comparable to the wall radius. At $aP = 5x10^{-2}$, they are about equal. Instead of collisional ions, one can use a collisionless model for the ions. To simplify the treatment, we use a planar model rather than a cylindrical one. The ion continuity equation is unchanged

$$d/dx(nv) = \alpha_i n N \qquad (11.20)$$

but the equations for velocity and density are now directly expressed in terms of the radial electrostatic potential $v = (-2e\phi/M)^{1/2}$ and $n = n_o \exp(e\phi/T_e)$. Here the potential is defined as zero at the center, x=0, and the density is defined as being n_o there. The wall is at the position where the velocity is equal to the ion acoustic speed, or at potential $e\phi/T_e = 0.5$. Then Eq (11.20) can be reduced to a single nonlinear equation for $\zeta = -e\phi/T_e$. It is

$$\zeta^{-1/2}(1-2\zeta)d\zeta/dx = N\alpha_i/(T_e/2M)^{1/2} \qquad (11.21)$$

This can be integrated. Setting $\zeta = 0.5$ at x=a, and using Eq.(11.17) for α_i and expressing N in terms of P, we find the relation is

$$6x10^{-3} \exp\ (25/T_e) = Pa \qquad (11.22)$$

This is plotted as curve C in Fig.(2.5a). This agrees much better for small P, but does not agree as well for large P. This then illustrates a basic dilemma in trying to explain experimental results in discharge physics. The theory is often developed for one set of approximations, while the experiment crosses over into several different regimes as parameters are varied. In this case however, where both ion inertia and diffusion are both retained, analytic solutions have been obtained in slab geometry. In cylindrical geometry however, one must solve the total fluid equations numerically[116]

Now let us consider the magnetized case. For the case of 440 Gauss used in the experiment, for pressures under about 1 Torr, the transport is dominated by the magnetized electrons. Since the

radial velocities are now much smaller than they were in the unmagnetized case, the transport perpendicular to the field is fluid like even when the mean free path is long. The velocity can now become equal to the ion sound speed only if the denominator of Eq.(11.10) nearly vanishes. Using as a condition for the temperature $\kappa a=2.4$, but where κ is reduced due to the field, we find the relation for temperature as a function of pressure is given by the curve in Fig (2.5b). This fits the data reasonably well in all pressure regimes. Thus the discharge is basically fluid like perpendicular to B, even at low collisionality.

12. Electrode Sheaths in dc Discharges

The previous section considered the infinite cylindrical plasma. Now let us consider the boundaries at the electrodes. As before, our assumption is that the boundaries absorb all incident charged particles and recycle them as neutrals. The anode boundary condition is relatively straightforward. There is an electron and ion flow into the anode, and its potential is determined so that the electron current density is just J, the current density of the discharge. This is analogous to the calculation for the cylinder wall except that now the potential is somewhat higher than the floating potential because the anode draws a net electron current. In terms of J one calculates the anode potential relative to the sheath edge and from that, the various energy fluxes. The sheath width is several Debye lengths.

Now let us consider the cathode. By the assumed boundary condition, the cathode does not emit particles (we will slightly modify this condition shortly), so the only way it can draw the appropriate current is if a flux of ions is absorbed there. However there is an immediate problem with this scenario, if one assumes the same type of sheath as on the anode or cylindrical wall. As the potential is lowered, electrons are all excluded and ultimately the cathode will draw the ion saturation current density $n_s e\sqrt{T/M}$. The problem is that the discharge current density is considerably greater than the ion saturation current in almost all cases.

The solution is a very different type of cathode sheath, and a much more complicated one. The actual sheath is particularly complicated because the one dimensional sheath in x, must transition to the glow discharge which is one dimensional in r. This is a complicated two dimensional problem involving the singular nature of the quasi-neutral regime and the charge separation in the sheath. Fortunately, the qualitative features of the sheath, and the corresponding Ohms law of the discharge can be discerned with only a one dimensional model of the sheath. The scaling of the current and sheath width with neutral density, as pointed out in Sec(2) was discussed in the section on scaling. The nearly linear relation between electric field and distance from the cathode was discussed in Sec.(10) where it was pointed out that a collisional sheath with ions having constant mean free path gave the best agreement, although it did not give the exact power law index. We intend to

describe here the qualitative nature of the increase of current with Voltage in the abnormal glow regime, and also the more striking result of the constancy of Voltage with current in the normal glow regime. We make no attempt to give a discussion, quantitative or otherwise of the various bright and dark spots in the cathode sheath region.

The key is that the current is much larger than the ion saturation current. The only way this can be is if electron current is converted to ion current in the sheath region. This can only occur collisionally through the ionization term in the steady state electron and ion density equation. Thus the cathode sheath is inherently collisional, and therefore is of much greater length than the collisionless anode or wall sheath. The conservation equations for electron and ion number density in steady state are

$$[\partial/\partial x]J_e = \alpha_i(T_e)NJ_e/u_e = -[\partial/\partial x]J_i \qquad (12.1)$$

Thus electron and ion currents are not themselves conserved, but ionization gives rise to coupling from one to another. The total current is, of course conserved. However near the cathode, the current is nearly all ion current. As one proceeds toward the positive column, the ionization in the cathode fall converts the current to electron current.

As the ions strike the cathode, each ion is assumed liberate γ electrons from the cathode. Typical values of γ for common electrode materials, impinging ion energy, and gases vary from about 0.1 to about 0.2. Thus the electron current near the cathode is small compared to the ion current, but is non zero. These electrons are accelerated in the glow, and ionization there converts this initially small current into the dominant electron current in the positive column.

The detailed structure of the cathode fall is complicated and not necessarily fluid like. Therefore the fluid calculations here will be rather approximate in nature. However, we will see that all in all, they do not do too bad a job. We do not attempt to calculate the detailed structure of the cathode fall, but only averaged quantities. Therefore we will deal with approximate integrals of the equations only. The first relation is of course the ion diode relation for the collisional ion diode with constant mean free path

$$J_\lambda(A/cm) = 2.3\times10^{-8}(\lambda M_a/M)^{1/2}V^{3/2}(volts)/s^{5/2}(cm) \qquad (12.2)$$

However as we pointed out earlier, this is not sufficient to specify the current as a function of Voltage because it involves a still unknown parameter, the sheath width s. The other relation is the ionization balance which converts the ion to electron current. Notice that the first equation in Eq.(12.1) predicts very nearly exponential increase of the current with distance. For γ's of about 0.15, it will take about 2 e foldings until the current is converted to electron current. Thus another relation between the cathode fall width s and the ionization is

$$s = 2u_e/N\alpha_i(T_e) \qquad (12.3)$$

The expression for $\alpha_i(T_e)$ is given in for instance Eq.(7.19), as one might expect for a gas with constant collision cross section, or a Ramsauer gas with temperature not much below the maximum cross section. For oxygen, we take the maximum cross section as $\sigma_o = 2\times10^{-16}$ cm^2 and the ionization energy E_i = 12 eV.

However the temperature and the drift velocities are now themselves functions of electric field. We use the empirical results presented in Sec.(2), which, as we have seen, agree reasonably well with theory.

$$T_e(eV) = A[(V/Ns)/10^{-14}\ Vcm^2]^{0.5} \qquad (12.4)$$

and

$$u_e(cm/s) = B[(V/Ns)/10^{-14}\ Vcm^2]^{0.7} \qquad (12.5)$$

where for oxygen, A = 8 eV and B = 6×10^7cm/s and also the ionization potential E_i=12 eV. In Eqs.(12.4 and 5), instead of writing the electric field on the right hand side, we used voltage divided by sheath width.

Now write the expressions for α_i, u_e, and T_e, as functions of V/s, and Eq.(12.3) becomes

$$V = 1.1\times10^2Q^{0.45}\exp-[9/16Q] \qquad (12.6)$$

where $Q = 10^{14}V/Ns$. Equation (12.6) above, and the ion diode relation, Eq.(12.2) are two equations relating the Voltage V, current density J and sheath width s. Let us first examine Eq.(12.6) which involves only V and Q. As Q approaches both zero and infinity, the right hand side approaches infinity. Thus there are two possible solutions to V from Eq.(12.6). The physical solution is the one that has voltage increasing as diode width s decreases, as this is consistent with the diode relation.

Let us now envision the solution to Eq.(12.6) at high Voltage. It gives a relation between V and s. Inserting this solution for s into Eq.(12.2), gives us J in terms of V. It predicts a rapidly increasing J as V increases, both because J increases rapidly with V according to the diode relation, and also because d decreases with V, and J is an even more rapidly increasing function of s^{-1}. This is the abnormal glow mode, where J increases with V. At some maximum current density, the heating of the cathode will get so great that one transitions to the arc mode. However let us envision starting in the abnormal glow mode and decreasing the Voltage. The current density then decreases. However this cannot be done indefinitely. The right hand side of Eq.(12.6) has a minimum, and the Voltage cannot be lowered to less than this value. For the parameters given, this minimum voltage is about 190 Volts. When the Voltage is lower, there is no solution to Eq.(12.6). Furthermore, at the particular value of N, the current density also reaches a certain minimum value. (Recall however that J scales as N^2, but Voltage is independent of N.) However while the Voltage and current density cannot be lowered, the total current, controlled by the external circuit can be lowered. The discharge can lower its total current simply by reducing the cathode area which draws current. This then is normal glow mode; constant Voltage and current density, but emitting area on the cathode proportional to total current. The predicted Voltage, 190 Volts for an oxygen plasma, is also reasonably close to that measured. For instance von Engel, p 229 gives the result that the cathode fall potential for an oxygen plasma with an iron electrode is 290 Volts. Thus the simple theory gives good qualitative agreement. From the value of Q at the minimum and also from the Voltage, we find that the value of the distance is given by $sN = 1.5x10^{16}$, or in terms of the pressure in Torr,

$$sP \text{ (cm torr)} = 0.6 \qquad (12.7)$$

The actual value is about 0.31, according to von Engel (1956) p 230

for an oxygen plasma with an iron cathode. This is also in reasonable qualitative agreement with theory. Other exponents in the temperature relation give qualitatively similar results. A Maxwellian distribution instead of a Druyvesteyn gives somewhat worse agreement for sP. The current density does not agree as well however. The fact that the voltage is a too small by about a factor of 30% and the gap width s is too large by about a factor of 2, means that the current as given by the ion diode relation is too small by almost an order of magnitude if one uses the collisional ion diode relation. The reason is that the current scales as these parameters to fairly high powers. However if one uses the actual experimental values for the voltage and sP, the current is reasonably well predicted by the ion diode relation. Thus simple theory gives reasonable values for V and sP; it also confirms the ion diode relations if actual values are used. This is an example of the fact that, as Hitcheon pointed out[40], even if a simple analytic theory gets some parameters right, it has a hard time getting everything, because the parametric dependences can involve power laws with fairly high powers.

The fact that the predicted value of sP is too large means that the ionization rate used here is too low. In the actual system it may be larger for several reasons. First of all, there may be a small population of energetic electrons from the direct acceleration of a few non-colliding electrons in the cathode fall potential. However, different Monte-Carlo simulations do not always agree as we will see. Secondly, the large sink of electron energy from exciting rotational and vibrational states may fill up if the gas heats up. If the neutral gas in the cathode fall heats up, the ζ's may be smaller, the electrons hotter, and the α_i's larger.

Finally it is interesting that the qualitative theory of the constant voltage limit for the normal glow, like that presented here, was given in von Engel and Steenbeck's original book, but there appears to be no modern rederivation or discussion of it.

To get better quantitative agreement, Monte Carlo simulations are often used. By integrating a random set of colliding test particles from the cathode, a distribution function at the plasma edge of a steady state cathode fall can be generated. It is interesting that the techniques developed, while particle in nature are not particle in cell simulations and are inherently steady state.

The earliest Monte Carlo simulations used fixed fields to calculate the electron distribution function[30]. Self consistent calculations then were done by iterating over a series of fixed field calculations of both electrons and ions[82,117.,118] Sometimes these calculations show nonthermal electrons, and sometimes they do not. Furthermore, these calculations so far have apparently been done only for rare gases. Even here, perhaps only half a dozen excited states are used. Generally these papers do not comment on the dilemma, discussed in Sec 5 of what maximum value to take for the excited state energy. Published Monte-Carlo calculations do not seem to have been done for molecular gases, and these would of course be much more complicated to do. Even in the rare gases however, a large number of atomic and collisional processes have to be taken into account to give good agreement with experiments. Even where the agreement is good, the constant Voltage nature of the normal glow and the shrinkage of the plasma covered part of the cathode with decreasing current is not discussed because of the one dimensional nature of the simulations.

Other models approximate the streaming plasma as a single beam[119] or series of beams. As we have seen, for oxygen, at 1 torr, the sheath width is about 0.3 cm. The electron momentum exchange collision cross section, up to about 100 ev, is about 10^{-15} cm^2, so that the sheath is about 10 mean free paths across. However above 100 ev, the momentum exchange cross section begins to decrease and is down by at least an order of magnitude at about a kilovolt. Thus of the electrons which can free stream about 5 mean free paths, a fraction of about e^{-5}, or something under 1% of them, many of them will be freely accelerated the rest of the way across the sheath. Thus we would also typically expect that something above 0.1% of the electrons would be freely accelerated across the sheath and form a beam at the cathode sheath potential. As this beam itself causes ionization, secondaries would be produced, and parts of the beam would also be at energies less than the full sheath potential. Clearly the basic properties of the sheath are very complicated and not strictly fluid like. However a fluid formulation does reproduce many of the qualitative features.

Finally the Ohm's law for the plasma is given entirely in terms of the sheath because in most cases, the Voltage across the positive column is much less than that across the sheath. For example, take a 0.1 torr plasma. If E/N is 10^{-15} Vcm^2, then this corresponds to a voltage drop of only 3 V/cm. It would be a fairly long plasma before

the voltage drop across the positive column would equal the 300 or so volts across the cathode sheath.

13. RF Discharges in Planar Geometry

In processing discharges, power at an rf frequency $f = \omega/2\pi$, typically 13 Mhz, is often used instead of dc power. For the dc discharge, the cathode sheath was inherently collisional. In the case of the rf plasma, the sheath may be collisionless, and it is the presence of the oscillating current that allows this. The fact that the sheath can be collisionless would appear to allow for rf discharges at neutral pressures less than the minimum required for dc discharges. (In fact Godyak ran at a minimum pressure of 0.003 Torr with a discharge length of 6.7 cm where dc discharge sheath could not form.) Furthermore, we have seen that dc sheaths need a minimum voltage to exist, while rf sheaths can exist below this voltage. Also, as we have mentioned, since the current to the workpiece can be displacement current rather than conduction current, the electrode does not necessarily have to be a conductor. Thus rf driven plasmas have considerably more flexibility than dc discharges, and find more use in industrial processing.

To model the rf discharges in planar geometry, we assume that in the central, quasi-neutral region, each fluid quantity has an average value, and a value oscillating at the rf drive frequency. The idea then is to write the fluid equations as two separate sets of fluid equations, one for the dc quantities, and one for the quantities oscillating at frequency ω. Since the equations are nonlinear, there will be coupling from one set to the other.

We denote the rf quantities with an underline, and generally we assume that these are small compared to the dc quantities, so that a perturbation theory can be applied. This central quasi-neutral region then attaches itself to a sheath near the boundary. This sheath is not neutral, and furthermore, the separation of the rf and dc components becomes rather complicated there.

The rf momentum equation for the central quasi-neutral part then becomes

$$\underline{u_e} = e\underline{E}/m(-i\omega+\nu_e) = -\underline{J}/ne \qquad (13.1)$$

which is also the rf Ohm's law for this portion of the plasma. In applying Ohm's law, it is necessary to keep in mind that $\underline{J}$ has no x dependence due to quasi-neutrality, while the x dependence of $\underline{E}$ is

as specified by Eq.(13.1), that is for constant ν_e, $\underline{E}$ is proportional to the reciprocal of the density. Thus $\underline{E}$ increases near the edge of the plasma where the density decreases, so that we expect the temperature to be larger near the plasma edges. This is in contrast to the dc cylindrical case where E was constant as a function of radius so that the temperature was also.

We now consider the dc part of the momentum and density equations. Recall that in the dc case for the radial dependence, the temperature equation decoupled. The momentum and density equation gave the temperature which was constant as a function of radius, and the relative density profile. In the rf discharge case, the decoupling is not complete because the temperature is now a function of x. We will proceed by approximating the temperature as constant and then discuss qualitatively the effect of non constant temperature. If the temperature is constant, α_i is also, and just as in the cylindrical case, one solves for the relative density profile subject to the boundary condition that the velocity is the sound speed at the plasma boundary. The boundary condition determines the eigenvalue α_i, which in turn determines the temperature, just as for the radial configuration dc flow discharge. Thus the relative density profile and average temperature is determined by the momentum and density equation.

Now let us discuss the effect of a temperature profile in x. As we have seen the electron heating is larger near the electrodes, so the temperature will be larger there also. The actual temperature profile will depend on the thermal conductivity among other things. However, α will be an increasing function of x as one approaches the electrode. This causes the density profile to be broader in the center and more rapidly decreasing near the edges. If we regard the spatial profile of α_i as being specified up to an overall coefficient, the eigenvalue is then that coefficient, or an average temperature. Thus the average temperature depends on the geometry alone and not on the current. This is consistent with Godyak's probe measurements shown in Fig.(2.7), which show the average temperature in the argon rf discharge as independent of current at low current, that is until one reaches the γ regime, which we will discuss shortly.

Let us digress briefly to review the parameters of Godyak's experiment. From our plots of ion charge exchange cross section,

the charge exchange mean free path length in centimeters is given roughly by 1/100P(Torr). The electron collision frequency, in sec^{-1} at 10 eV is given by $5x10^9P$, and at 1 eV is given by $2x10^8P$. Thus for our example of a pressure of 0.3 Torr, $\omega/\nu_p < 1$ for both electron energies, so the electrons are collisional. Also, the ion mean free path is considerably less that the sheath width, so the sheaths near the electrodes are collisional also.

Godyak describes three physics regimes of the discharge. At low current and high neutral density, the bulk heating of the electrons is mostly conventional Ohmic heating. At low neutral density, stochastic heating is dominant. This is the heating the electrons encounter by reflecting from the oscillating sheaths. In all cases a dc sheath also forms at each electrode. At low rf current (the dc current is zero even though there are dc fields), the dc sheath Voltage is less than V_{cr}, that required for a dc cathode fall like that was described in the previous section. As the rf current increases, the dc sheath Voltage becomes comparable to V_{cr} and emission from the cathode becomes important. This is the γ regime.

We now turn to the dc electron temperature equation. There is a power input from the Ohmic heating. If $\underline{J}=-J_o\sin\omega t$ then the average power input into the central region of the neutral plasmas is

$$dP_{OH}/dz = 0.5Am\nu_pJ_o^2/ne^2 \qquad (13.2)$$

where A is the area of the plasma. The fact that the power input goes as n^{-1} is due to the concentration of rf electric fields in the low density region which we have discussed. Also we have assumed no dc current, so there is no power input from dc fields. Now let us consider the sheath region. The total power into the sheath region will be denoted P_s and this depends on the sheath physics, which we will discuss shortly. An additional power input is the stochastic heating of the electrons P_{st}. This is the energy the electrons pick up as the reflect from the oscillating sheath. We will also discuss this power input later. However for the regime where the electrons are moderately collisional, it is small.

Now let us turn to the power dissipated by the plasma. First, and simplest, we consider the sheath. We assume that all of the power put into the sheath is dissipated there also. This dissipation may be in the form of either fast ions or neutrals streaming into the

electrode, or else heating of the gas in the sheath region. In any case, we assume that the power P_s is locally dissipated there. To continue, turn to the power dissipation in the central region of the plasma. The electrons there gain energy from the ohmic heating, and lose it to heating of the neutral gas and also to radiation and ionization. The power loss per unit length from these two mechanisms is

$$dP_L/dz = A[\zeta(T)T\nu_p + P_r + E_i\alpha_i N]n \qquad (13.3)$$

where ζ relates momentum and temperature equilibration collision rates, and P_r is the power radiated per electron as per the discussion after Eq. (11.15). In addition to the volumetric power loses, there is also the energy convected into the sheath. Assuming that the ionization energy is much greater than the electron temperature, as we have typically done here, this is given by

$$P_c = n_s A E_i [T_e/M]^{1/2} \qquad (13.4)$$

where in our convention, the ionization energy is carried by the ion. Also, n_s is the electron density at the sheath edge, the point where the ion velocity is $[T_e/M]^{1/2}$.

Thus the power balance equation is

$$\int dz\ (dP_{OH}/dz) = \int dz (dP_L/dz) + P_c \qquad (13.5)$$

where we have canceled P_s from each side and assumed P_{st} is small,. which Godyak finds to be true for the more collisional plasma. Now recall that in our approximation of fixed temperature profile (or constant temperature), the relative density profile was obtained with the density and momentum equations. Thus the density profile will be denoted $n_o f(x)$ where f is some known function and $f(x=0)=1$. Then the left hand side of Eq.(13.5) scales as n_o^{-1} and the right as n_o, so

$$n_o = \chi J_o \qquad (13.6)$$

Thus the electron density scales linearly with the rf current. This is consistent with Godyak's probe data shown in Fig.(2.7a). At high current, the discharge is in the γ mode and secondary electrons

emitted from the electrodes play an important role and the density appears to increase more rapidly with current. However in the regime of low current and of a reasonably collisional plasma, the theoretical results of temperature independent of current (i.e scaling only with geometry) and density linear with current are borne out by the experimental data. While the density scales linearly with the rf current, its scaling with neutral density is not necessarily simple because dP_L/dz and dP_{OH}/dz scale with N (the neutral number density), but P_c is independent of N.

As we saw in the previous sections, dc ion sheaths either involve Voltage drops of a few times the electron temperature and had a Debye length scale; or else, if the ion current is larger than the ion saturation current, is inherently collisional and had a much longer length scale. However the time dependent nature of the rf sheath allows additional flexibility in the nature of the sheath. It is somewhat analogous to PIII (Plasma Imersed Ion Implantation) except the time dependence is now oscillatory.

We make the approximation that the rf frequency is much greater than the ion plasma frequency, so that the ions, even in the sheath do not respond to the rf fields, but react only to the dc fields set up. (Recall that the boundary condition is that there is no dc current; however as we will see, there are still large dc electric fields in the sheath.) The frequency is low enough that the electrons respond to the instantaneous fields. We assume further, that the dc potential drop across the sheath is very large compared to the electron temperature.

We begin by considering the collisionless sheath. Let us say that the singular point of the quasi-neutral solution is at $x=0$ and $\phi=0$, and the wall is at $x=s_m$ at which point, there is a large negative dc potential. The actual time dependent potential between $x=0$ and $x=s_m$ is complicated due to the fact that the electrons oscillate back and forth between these positions. As the electrons oscillate between $x=0$ and s_m, the position at which $\phi=0$ moves back and forth. If the oscillating and dc potentials are large compared to T/e, as in fact we assume, the electron density is equal to the ion density to the left of the position where the instantaneous potential is zero, and is zero to the right. Thus the picture of the sheath is that of an electron density whose edge oscillates between $0<x<s_m$ as the current oscillates through a cycle. The position of the sheath is at

the instantaneous place where $\phi=0$. However, one can also define a potential averaged over an rf period; this is the potential that the ions respond to. If there were no electrons at all present in the sheath, the current, voltage and sheath width s_m would be related by the collisionless ion diode Langmuir-Child's law, Eq.(10.9). Because there are electrons in the diode region, the ion current is actually somewhat greater than this. However this does not specify the problem, because the specified quantities are J_o, n_s, T and the incident ion flow speed $u_s=\sqrt{(T/M)}$, the first of which is specified, the others all come from the outer, quasi-neutral solution. Thus the dc ion current density is specified by the quasi-neutral solution, but not the Voltage or gap spacing. Furthermore, since there is no dc current, this ion current must be cancelled by an equal and opposite dc electron current.

The actual solution for the collisionless rf sheath was derived by Lieberman by breaking the equations up into a time averaged potential which the ions respond to, and an exact part which the electrons respond to. We will not go through the nonlinear analysis here, but will give a very simple, but approximate solution which demonstrates the basic physics and scaling calculated by Lieberman. If the position of the sheath edge is denoted by s, then

$$J_o \sin\omega t = ne\,ds/dt \qquad (13.7)$$

as in Eq.(10.13). At $t=0$, $ds/dt=0$ and $d^2s/dt^2>0$, so the sheath is at plasma edge, the minimum value of s. Similarly, at $t=\pi/\omega$, the sheath is at the maximum position, $s=s_m$. In terms of the dc potential, the ion density as a function of ϕ is given by $n = n_s(1-2e\phi/T)^{-1/2}$ assuming $u_i = u_s$ at $\phi=0$. Inserting this value of n into Eq.(13.7), and assuming that the potential is large compared to the temperature, we find that an approximate relation between s_m and ϕ_m is

$$s_m \approx (e\phi_m/T)^{1/2} J_o/n_s e\omega \qquad (13.8)$$

which serves as one relation between potential drop, sheath width and plasma parameters. The other relation is simply the ion diode relation, Eq.(10.9). These two relations then specify the scaling laws for the sheath in terms of the oscillating current and the plasma parameters at the singular point of the quasi-neutral

solution. The actual solutions that Lieberman finds from solving the nonlinear equations specifying the rf sheath are

$$J_i=1.8J_{LC} \qquad (13.9)$$

where $J_i=n_s e(T_e/M)^{1/2}$, and J_{LC} is the current of the ion diode given by Eq.(10.9) but with diode Voltage given by ϕ_m, and gap by s_m, and

$$s_m = (e\phi/1.6T)^{1/2}J_o/n_s e\omega \qquad (13.10)$$

Except for numerical factors of order unity, Lieberman's solution is equivalent to the approximated one we have derived here. This then allows us to calculate both the ion energy striking the surface. From Eqs.(13.9 and 10), the Voltage drop across the sheath is given by

$$\phi_m(V)=0.6J_o^4(mA/cm^2)/\{T(eV)[n_s(cm^{-3})/10^{10}]^2[f/13MHz]^4\} \qquad (13.11)$$

Since n is typically proportional to J_o, as specified by the quasi-neutral solution, the dependence of ϕ on J_o is not as rapid as it appears in Eq.(13.11). In fact assuming that n_s scales linearly with J_o we find

$$\phi_m \propto J_o^2/f^4 \qquad s_m \propto J_o/f^3 \qquad (13.12)$$

This is still a rapid scaling with J, and as the current is increased in a regime where the sheath is collisionless, one would expect that power dissipation in the sheath would begin to exceed the power dissipation in the plasma. We will discuss this more fully shortly.

We have calculated the dc ion current in terms of the plasma and circuit parameters. In order to insure that there is no net dc current, the dc ion current must be balanced an opposite dc electron current. Note that at time $t=\pi/\omega$, the electron sheath is in contact with the wall. Although the time of contact is short, the electron current to the wall during this time can be large because the electron thermal velocity is so much larger than the ion streaming velocity. Thus dc current is preserved at its zero value by the electrode drawing the necessary electron current for the time that the electron sheath is in contact with the electrode.

At time π/ω, the actual Voltage across the sheath is equal to the dc potential ϕ_m. Also, J is an odd function of time, and V is an even function of time, so the sheath is capacitive. If we define a sheath capacitance by

$$-AJ_o\sin\omega t = C_s dV/dt \qquad (13.13)$$

where A is the area of the electrode, and if V is approximated as $\phi_m(1+\cos\omega t)/2$, we can obtain the sheath capacitance, roughly equal to A/s_m, in terms of the plasma parameters.

In addition to the capacitive nature of the sheath, there is also a resistive part due to the fact that an individual electron incident on the sheath with velocity v_x bounces off with velocity v_x+2ds/dt, where ds/dt is the velocity of the sheath. However the time for the electron to bounce off the oscillating sheath must be small compared to the collision time. Thus this is a more important heating mechanism for low pressure discharges. In calculating the energy flux bouncing off the sheath, we will only consider even powers of ds/dt since these are the portions that will not average to zero over an oscillation period. If we approximate the time average value of $(ds/dt)^2$ to be $0.5\omega^2 s_m^2$, we find that the additional power input into the plasma is

$$P_{os} = 3An_s[e\phi_m/T]^{-1/2}m\omega^2 s_m^2(T/2\pi m)^{1/2} \qquad (13.14)$$

where in estimating the power input, we have assumed the average density of the sheath is $n_s/(e\phi_m/T)^{1/2}$ to account for the density reduction as the ions accelerate through the sheath. This is the density reduction characteristic of a collisionless sheath. This gives rise to a resistive part of the sheath response. Often this heating is called stochastic heating, since it is not related to plasma collisionality. This power input into the plasma must be added to the bulk resistive power input when calculating the energy balance. Notice however that this power comes in as an energy flux near each electrode. If the stochastic heating is expressed in terms of J_o, n_s and ω only, the result is that the power input scales as $J_o^4/n_s^2\omega^2$.

Let us now briefly consider the very low pressure case, where stochastic heating dominates Ohmic heating. Energy is put in at the edges, but since the electron mean free path is long, the thermal

conduction is high and the temperature profile should once again be reasonably uniform along the length of the discharge. Thus the density profile should have the normal shape, rounded in the middle and not particularly sharp at the edges. Balancing stochastic heating input power with the output power, the result is that the electron density scales as $J_o^{4/3}$.

We now consider the collisional sheath[120] for the case in which the ion mean free path is a constant λ. As we have seen this is a reasonable approximation for both argon and helium; the mean free path has some variation with energy, but the collision frequency has a greater variation with energy. Equation (13.7) still relates the current to the oscillating boundary. Within the sheath, we still have $n=n_s(T/M)^{1/2}/v$, but now $v= [e\phi\lambda/Ms]^{1/2}$ for collisional ions with constant mean free path λ. Then we find the scaling law

$$\phi_m \propto \lambda^{1/2} J_o^{5/2}/f^{5/2} n_s T^{1/2} \qquad (13.15)$$

Making the assumption that T is determined by the geometry and n_s is proportional to J_o, as determined by the external quasi-neutral solution, we find the scaling:

$$\phi_m \propto \lambda^{1/2} J_o^{3/2}/f^{5/2} \quad \text{and} \quad s_m \propto \lambda^{1/2} J_o^{1/2}/f^{3/2} \qquad (13.16)$$

To continue, we calculate the power dissipated by the plasma in the collisional regime. Using our scaling that $n \propto J_o$, the Ohmic power dissipation scales linearly in J_o. The sheath power on the other hand, scales as ϕ_m times the dc ion current. The dc ion current is simply $n_s A(T_e/M)^{1/2}$, which scales as J_o, since n_s scales as J_o and T_e is independent of J_o. Thus the sheath power input scales as $J_o^{5/2}$. Hence if an rf discharge in the collisional regime is run at constant pressure, but the current increases, at low current the power input scales as J_o. As the current increases, the sheath power begins to dominate because it scales as a higher power of J_o. Thus at some current, the scaling will switch to a $J^{5/2}$ law. These are just the sorts of scaling laws that Godyak typically found. Figure (2.7b) here shows some of this data, where the scaling law of power with current is linear with current for low current, but switches to a 5/2 power law at higher current. In the collisional regime at high current, only a small part of the power is dissipated as fast ions striking the electrode. The ion energy of an ion striking the

electrode is typically $\phi_m(\lambda/s_m)^{1/2}$. The remaining energy is dissipated either as fast neutrals striking the electrode or else as heating of the gas in the sheath region.

Now consider the collisionless regime. Using the scalings for ϕ, s_m, and n_s in terms of J_o, we find that if the stochastic heating is dominant, $P_{st} \propto J_o^{4/3}$. At higher input power, the dissipation due to ions in the sheath scales as $J_o^{8/3}$. Thus at higher current, the sheath power dominates. Shown in Fig.(2.7c) is Godyak's data for his lowest pressure, P= 0.003 Torr, where the plasma is collisionless. The straight lines sketched in have slopes 4/3 and 8/3. Again there is reasonable agreement.

Now let us consider the rf response of a symmetric planar discharge. There are two equivalent sheaths on the two equal area electrodes. The rf current is the same through out the plasma. Thus while the sheath is moving towards one electrode, it is moving away from the other. For instance, while the sheath is in contact with the right hand electrode, and the voltage drop to the plasma zero; the sheath has maximum separation from the left electrode and the voltage drop is at its maximum value, the full dc voltage drop. If the voltage drop across the sheath on the right is denoted $V_r(t)$, then the Voltage on the left hand sheath is given by $V_l(t)=V_r(t-\pi/\omega)$, so the total voltage drop across the plasma (assuming the sheath Voltage drops dominate) as a function of time is $V_r(t)-V_r(t-\pi/\omega)$.

To conclude, we briefly discuss the case of an asymmetric discharge for which the areas of the two electrodes are not equal. The total rf current through the electrodes must be equal to one another. Thus $J_o A$ is constant for each electrode. Then, according to Eq.(13.11), the potential drop across a collisionless sheath at an electrode of area A scales as A^{-4}, as long as the electron densities and temperatures are equal at each sheath. On the other hand, the potential drop in the collisional regime scales as $A^{-5/2}$. This rapid variation with area is typically not observed in experiments. One reason is that the densities are not the same at each electrode. This has been examined by Lieberman[121], and depending on what the collisional law is (ie constant collision frequency, constant mean free path etc), there are different area scalings of Voltage. The collisionless, uniform density case has the most rapid scaling with electrode area. Also there are geometric factors. One would expect the density to be larger at the smaller electrode because the current

density is higher there. If the density is taken to scale as the local current density, the collisional sheath would give a scaling of $\phi_m \propto A^{-3/2}$, which is closer to what is observed experimentally. Lieberman has investigated this, within the framework of a one dimensional model, by using cylindrical or spherical coordinates.

Summarizing, we have discussed a variety of theories of rf discharges and compared them with recent data. At least some of the features of the data can be explained with the theories reviewed and developed here.

Acknowledgements: The author wishes to thank James Butler, Martin Peckerar and A.E Robson, all of NRL for a number of useful discussions. This work was supported by the Office of Naval Research.

References

[1] *Plasma Procesing of Materials, Scientific Opportunities and Techicological Challenges, Plasma* Science Committee, National Research Council, National Academy Press, Washington, DC, (1991)

[2] *ONR Research Opprotunities in Physics*, Naval Studies Board, National Academy Press, Washington, DC (1991)

[3] J.L. Shohet, Plasma Aideed Manufacturing, IEEE Trans. Plasma .Sci. 19, 725-733 (1991)

[4] J.L. Shohet, Plasma Aided Manufacturing, Phys. Fluids B 2, 1474-7, 1990

[5] D.L. Flamm and G.K. Herb, Plasma Etch Technology- An Overview, Chapter 1, p1-90, in D. Manos and D. Flamm (ed), *Plasma Etching*, Academic Press, (1988)

[6] M. Venugopapan (ed), *Reactions Under Plasma Conditions*, Wiley Interscience, (1971)

[7] S.C. Haydon (ed) *An Introduction to Discharge and Plasma Physics*, University of New England Press, NSW, Austraila, (1964)

[8] E. Nasser, Fundamentals of Gaseous Ionization and Plasma Electronics, Wiley Interscience, (1971)

[9] G. Marr, *Plasma Spectroscopy*, Elsevier, (1968)

[10] S.C. Brown, *Basic Data of Plasma Physics*, 1966, MIT Press, (1967)

[11] S.C. Brown, in Gaseous Electronics, ed J. McGowan and P John, North Holland, Amsterdam, 1974

[12] A. von Engel, Ionized Gases, Oxford Press, 1965

[13] A. von Engel, Electric Plasmas and Their Use, Taylor and Francis, New York, 1983

[14] Ya. Zeldovich and Yu. Razier, *Physics of Shock Waves and High Temperature Hydrodynamic Phenomena*, Academic Press, (1966)

[15] V.E. Golant, A.P. Zhilinsky, and I.E. Sakharov, *Fundamentals of Plasma Physics*, Wiley and Sons, (1980)

[16] A. Gurevich, *Nonlinear Phenomena in the Ionosphere*, Springer-Verlag, (1978)

[17] D. Manos and D. Flamm (ed), *Plasma Etching*, Academic Press, (1988)

[18] B. Chapman, *Glow Discharge Processing*, wiley and Sons, (1980)

[19] J. Vossen and W. Kerr (ed), *Thin Film Processes*, Academic Press, (1978)

[20] A. van Roosmalen, J. Baggerman, and S. Brader, *Dry Etching for VLSI*, Plenum Press, Hew York, 1991

[21] J. Reece Roth, *Industrial Plasma Engineering*, to be published.

[22] D.B. Graves and K.F. Jensen, *A Continuum Model of DC and RF Discharges* IEEE Trans. Plasma .Sci. PS 14, 78-91, (1986)

[23] J.P. Boeuf, Phys. *Numerical Model of RF Glow discharges*, Rev. A 36, 2782-92 (1987)

[24] N. Sato and H. Tagashira, *A Hybrid Monte Carlo/Fluid Model of RF Plasmas in SiH_4/H_2 Mixtures* IEEE Trans. Plasma .Sci. 19, 102-112, (1991)

[25] M. Meyyappana, *Modeling of Electro-Negative RF Discharges*, IEEE Trans. Plasma .Sci. 19, 122-129, (1991)

[26] P. Meijer and W. Goedheer, IEEE Trans. Plasma .Sci. 19, 170, (1991)

[27] S. Pirooz, P. Ramachandran, B. Abraham-Schrauner, Two Region Computational Model for DC Glow Discharge Plasma, IEEE Trans. Plasma Sci. 19, 408-418, (1991)

[28] M. Talaat, A Two Electron Group Model for RF Ionization of Noble Gases with Turbulent Flow, IEEE Trans. Plasma .Sci. 19, 176, (1991)

[29] P. Meijer and W. Goedheer, *Calculation of Auto-bias Voltage for RF Frequencies well above the Ion Plasma Frequency*, IEEE Trans. Plasma .Sci. 19, 170-175, (1991)

[30] J.Boeuf and E. Marode, *A Monte Carlo Analysis of an Electron Swarm in a Non Uniform Field: The Cathode Region of a Glow discharge in Helium*, J. Phys D, 15, 2169-2187, (1982)

[31] M. Kushner, *Monte-Carlo Simulations of Electron Properties in RF Parallel Plate Capacitively Coupled Discharges* J. Appl Phys, 54, 4958-64, (1983)

[32] M. Goeckner, J. Goree and T. Sheridan, *Monte-Carlo Simulations of Ions in a Magnetron Plasma*, IEEE Trans. Plasma .Sci. 19, 301-308, (1991)

[33] M.J. Brennan, *Optimization of Monte Carlo Codes Using Null Collision Techniques for Experimental Simulation at Low E/N*, IEEE Trans. Plasma .Sci. 19, 256-261, (1991)

[34] T. Sommerer, W. Hitcheon, and J. Lawler, Self Consistent Model of the Cathode Fall of a Glow Discharge, Phys. Rev. A, 39, 6356-66, 1989

[35] Z. Donko and M. Janossy, *Model of the Cathode Dark space in Noble Gas Mixture Discharges*, J. Phys D. 25, 1329-29, (1991)

[36] C.K. Birsdall and A.B. Langdon, *Plasma Physics by Computer Simulation, McGraw Hill*, (1985)

[37] C.K. Birdsall, *Particle in Cell Charged-Particle Simulation Plus Monte-Carlo Collisions with Neutral Atoms, PIC-MCC*, IEEE Trans. Plasma .Sci. 19, 65-85 (1991)

[38] J. DiCarlo and M.J. Kushner, *Aolving the Spatially Dependent Boltzman's Equation for the Electron Velocity Distribution Using Flux Corrected Transport*, J. Appl. Phys. 66, 5763-71, (1989)

[39] M. Surendra and D.B. Graves, *Electron Acoustic Waves in Capacitively Coupled, Low Pressure rf Glow Discharges*, Phys Rev Lett, 66, 1469-72, (1991)

[40] W. Hitcheon, T. Sommer and J. Lawler, *A Self Consistent Kinetic plasma Model with Rapid convergence*, IEEE Trans. Plasma .Sci. 19, 113-121, (1991)

[41] M. Surendra and D.B. Graves, *Particle Simulations of RF Glow Discharges*, IEEE Trans. Plasma .Sci. 19, 144-157, (1991)

[42] R.K Porteous and D.B. Graves, *Modeling and Simulation of Magnetically Confined Low Pressure Plasmas in Two Dimensions*, IEEE Trans. Plasma .Sci. 19, 204-213 (1991)

[43] R. Procassini, C. Birdsall, and E. Morse, *A Fully Kinetic, Self Consistent Particle Simulation Model of the Collisionless Plasma Sheath Region*, Phys Fluids, B2, 3191-3205, (1990)

[44] M. Surrenda and D. Graves, *Capacitively Coupled Glow Discharges at Frequencies above 13.56 MHz*, Appl Phys Let, 59, 2091-3, 1991

[45] M. Alves, M. Lieberman, V. Vahedi, C. Birdsall, Sheath Voltage Ratio for Asymetric rf Discharges, J. Appl Phys, 69, 3823-29, 1991

[46] W. Lawson, Particle Simulation of Bounded 1D Plasma Systems, J. Comp Phys, 80, 253-76, (1989)

[47] M. Surrenda, D. Graves, and I. Morey, Electron Heating in Low Pressure RF Glow Discharges, Appl. Phys. Lett. 56, 1022-4, (1990)

[48] V. Godyak and A. Khanneh, *Ion Bombardment Secondary Electron Maintenance of Steady RF Discharges*, IEEE Trans. Plasma .Sci. PS 14, 112-123, (1986)

[49] M. Lieberman, *Analytic Solution for a Capacative RF Sheath*, IEEE Trans. Plasma .Sci. 16, 638, (1988)

[50] G. Lister, *Low Pressure Gas Discharge Modeling*, J. Phys D, 25, 1649-79, (1992)

[51] D. Economou, D. Evans and R. Alkire, *A Time Average Model of the RF Plasma Sheath*, J. Electrochem Soc 135, 756 (1988)

[52] A. Metze, D. Ernie and H. Oskam, *The Energy Distributrion of Ions Bombarding Electrode Surfacesin RF Plasma Reactors*, J. Appl. Phys. 65, 993, (1989)

[53] K. Riemann, *Theoretical Analysis of Electrode Sheath in RF Discharges*, J. Appl Phys. 65, 993, (1989)

[54] S. Biehler, *Theory of Rf Sheath in the Regime Between Electron and Ion Plamsa Frequency*, Appl. Phys . Lett 54, 316, (1987)

[55] C. Zarowin, *Plasma Etch Anisotropy, Theory and Some Verifying Experiments Relating to Ion Transport, Ion energy and Etch Profiles*, J. Electrochem. Soc.: Solid State Sci and Tech. 130, 1144-52, (1983)

[56] F.G.Celii and J.E. Butler, *Diamond Chemical Vapor Deposition*, Annu. Rev. Phys. Chem. 42, 643-684, (1991)

[57] A Inspektor,T. McKenna, Y. Liou, L. Bourget, K. Spear and R. Messier, *Plasma Chemistry in Diamond Deposition* in *Diamond and Diamind Like Films*, J Dismukes ed, p 342-352 Electrochemical Soc, Pennington, NJ

[58] A. Badzian, T. Bodzian, and D. Pickrell, *Crystalization of Diamonds by Microwave Plasma Assisted Chemical Vapor Deposition*, SPIE Vol 969, p 14-20

[59] M. Kamada, S. Arai, A. Sawabe, T. Murikami, T. Inuzuka, *Thick Diamond Films Grown by DC Discharge Plasma Chemical Vapor Deposition*, in Science and Technology of New Diamond, S. Saito ed, p 55-58, Terra Scientific Publishing, (1990)

[60] J.R. Conrad, J. Radtke, R. Dodd, F. Worzala, N. Tran, *Plasma Source Ion Implantation Technique for Surface Modification of Materials*, J. Appl. Phys., 62, 4591-96, (1987)

[61] T. Somerer and M. Kushner *Numerical Investigation of the Kinetics and Chemistry of RF Glow Discharge Plasmas Sustained in HE, N_2, O_2, He/N_2/O_2, He/CF_4/O_2, and SiH_4/NH_3 Using Monte Carlo fluid Hybrid Model*, J. Appl. Phys 71, 1654-1673, (1992)

[62] I.C. Plumb and K.R. Ryan *A Model of Chemical Processes Occurring in CF_4/O_2 Discharges*, Plasma Chem and Plasma Processing, 6, 205-231, 1986

[63] E. Hyman, K. Tsang, I. Lottati, A. Drobot, B. Lane, R. Post and H. Sawin, *Plasma Enhanced Chemical Vapor Deposition Modeling*, Surface and Coatings Tech, 49, 387-393, (1991)

[64] P. Huang and E. Pfender, *Study of a Transferred-Arc Plasma Reactor with a Converging Wall and Flow Through a Hollow Cathode*, Plasma Chemistry and Plasma Processing, 11, 129-150, (1991)

[65] C. Chang and E. Pfender, *Nonequilibrium Modeling of Low Pressure Argon Plasma Jets, Part I: Laminar Flow*, Plasma Chemistry and Plasma Processing, 10, 473-491, (1990)

[66] C. Chang and E. Pfender, *Nonequilibrium Modeling of Low Pressure Argon Plasma Jets, Part II: Turbulent Flow*, Plasma Chemistry and Plasma Processing, 10, 493-500, (1990)

[67] Ref 18, p 68

[68] K. Riemann, *The Bohm Criterion and Sheath Formation* J. Phys. D, 24, 493-518 (1991)

[69] P. Meijer and W. Goedheer, *The Bohm Criterion for RF Sheaths*, Phys Fluids, B3, 1804-06, (1991)

[70] J. Scheuer and G. Emmert, *A Fluid Treatment of the Plasma Presheath for Collisional and Collisionless Plasmas*, Phys Fluids, B2, 445-451, (1990)

[71] M. Cho, N. Hershkowitz, and T. Intractor, *Temporal Evolution of collisionless Plasma Sheaths*, J. Vac. Sci and Tech A, 6, 2978-86, (1988)

[72] J. Dutton, *Survey of Electron Swarm Data*, Journal of Physical and Chemical Reference Data, 4, 577-673, 1975

[73] R. Hake and A. Phelps, *Momentum Transfer and Inelastic Collision Cross Sections for Electrons in O_2, CO, and CO_2.* Phys Rev, 158, 70-84, (1967)

[74] A, Englehardt, A. Phelps, and C. Risk, *Determination of Momentum Transfer and Inelastic Cross Sections for Electrons in Nitrogen Using Transport Coefficients*, Physical Review A 135, 1566-74, 1964.

[75] P. Banks and G. Kockarts, *Aeronomy, Part A*, Academic Press, New York, 1973, page 202,

[76] S. Cohen, *An Introduction to Plasma Processing*, Chapter 3, in D. Manos and D. Flamm (ed), *Plasma Etching*, Academic Press, (1988)

[77] L. Loeb, *Fundamental Processes of Electrical Discharges in Gases*, Wiley and Sons, New York, 1939

[78] A. von Engel and M Steenbeck *Elektrische Gasentladungen*, Springer, Berlin, 1934.

[79] R. Bickerton and A. von Engel, *The Positive Column in a Longitudinal Magnetic Field*, Proc. Phys. Soc London, 69, 468-481, (1956)

[80] B. Kadomtsev, *Convection of the Plasma of a Positive Column in a Magnetic Field*, Sov. Phys. Tech Phys. 6, 927-933, (1962)

[81] K. Darrow, *Electrical Phenomena in Gases*, Williams and Wilkins, Baltimore, 1932

[82] E. Den Hartog, D. Doughty, and J. Lawler, *Laser Optigalvanic and Fluorescence Studies of the Cathode Region of a Glow Discharge*, Phys. Rev. A, 38, 2471-91, (1988)

[83] P. Little and A von Engel, *The Hollow Cathode Effect and the Theory of Glow Discharges*, Proc. Royal Soc. London, A 224, 209-227, (1954)

[84] K. Takiyama, T. Usui, Y. Kamiura, T. Fujita, T. Oda, and K. Kawasaki, *Measurement of Intensity and Polarization of HeI Forbidd3n Lines for Diagnostics of Electric Fields in a Plasma*, Jap. J. Appl. Phys. 25, 455-457, (1986)

[85] J. S. Logan, N.M. Mazza and P.D. Davidse, *Electrical Characterization of Radio Frequency Sputtering Discharges*, J. Vac. Sci. and Tech, 6, 120, (1969)

[86] J.W. Coburn, *A system for Determining the Mass and Energy of Particles Incident on a Substrait in a Planar Diode Sputtering System*, Rev. Sci. Instrum. 41, 1219 (1970)

[87] D. L. Flamm, *A Model and Apparatus for Electrical Discharge Experiments,* Ind. Eng. Chem Fund. 14, 263, (1975)

[88] J. Tallet, *Resonance Sustained Radio Frequency Discharges,* J. Phys. 5, 227, (1975)

[89] J. W. Coburn and E. Kay, *Positive Ion Bombardment of of Substraits in RF Glow discharge Sputtering*, J. Appl. Phys. 43, 4965, (1972)

[90] H. Koenig an L. Maissel, *Application of RF Discharges to Sputtering,* IBM J. Res. and Devel. 14, 168, (1970)

[91] V. Donnoly, D. Flamm and G. Collins, *Laser diagnostics of Plasma Etching: Measurements of CL_2^+ in a Chlorind Descharge*, J. Vac. Sci. Technol. 21, 817 (1982)

[92] D. Flamm, *Frequency Effects in Plasma Etching,* J. Vac. Sci. Technol. A4, 729, (1986)

[93] R. Gottscho and C. Gaebe, *Negative ion Kinetics in a Radio Frequency Glow Discharges,* J. Vac. Sci. Technol. A4 1795, (1986)

[94] A. J. Roosmalen, *Plasma Parameter Estimation ffrom RF Impedance Measurements in a Dry Etching System*, Appl. Phys. Lett. 42, 416, (1983)

[95] F. Schneider, The *Mechanism of High Frequency Discharge Between Level Plates*, Z. Agnew. Phys. 6, 456, (1954)

[96] V. Godyak, *Statistical Heating of Electrons at an Oscillating Plasma Boundary*, Sov Phys Tech Phys., 16, 1073-76, 1972

[97] V. Godyak, *Steady State Low Pressure RF Discharge*, Sov. J. Plasma Phys. 2, 78-84, 1976

[98] V. Godyak and A. Ganna, Influence of Self Field on the Saptial Distribution of a Plasma of an RF discharge, Sov. J. Plamsa Phys. 5, 376-380, (1979)

[99] V. Donnelly, D. Flamm, and R. Bruce, *Effects of Frequency on Optical Emission, Electrical, Ion, and Etching characteristics of an RF Chlorine Plasma*, J. Appl. Phys. 58, 2135-44, (1985)

[100] V. Godyak, R. Piejak, and B. Alexandrovich, *Electrical Characteristics of Parallel Plate RF Discharges in Argon*, IEEE Trans Plasma Sci, 19, 660-676, (1991)

[101] V. Godyak, R. Piejak, and B. Alexandrovich, *Measurements of Electron Energy Distribution in Low Pressure RF Discharges*, Plasma Sources Sci. Technol. 1, 36-58, (1992)

[102] J. Mitchell, *The Dissociative Recombination of Molecular Ions*, Phys. Reports, 186, 217-241, (1990)

[103] Ref 71 page 221

[104] V.Talrose and G. Karachevtsev *Elementary Reactions in Low Temperature Plasma*, Chapter 12 of Ref 6.

[105] *Reaction Rate and Photochemical Data for Atmospheric Chemistry*, Publiched by NIST, R. Hampson and D. Garvin ed, 1978

[106] *Defense Nuclear Agency Reaction Rate Handbook*, edited by M. Bortner and T. Baurer, 1972, published by the Defense Nuclear Agency (DNA 1948H)

[107] D. Albritton, *Ion-Neutral Reaction Rate Constants Measured in Flow Reactors Through 1977*, Atomic Data and Nuclear Data Tables, 22, 1-101, 1978.

[108] *Bibliography of Chemical Kinetics and Collision Processes*, Adolph R. Hochstein, ed, IFI Plenum, New York, 1969

[109] G.L. Pratt, *Gas Kinetics*, Wiley and Son, New York, 1969, p 26

[110] Brunet, Vincnet and Rocca Serra J. Appl. Phys. 54, 4952, (1983)

[111] H. Furth, J. Kileen and M. Rosenbluth, *Finite Resistive Instabilities of a Sheet Pinch, Phys. Fluids*, 6, 459-484, (1963)

[112] W. Manheimer and C. Lashmore Davies, *MHD and Microisnatbiliteis in Simple Plasma Configurations*, Chapter 7, Adam Hilger, (1989)

[113] W. Manheimer and D. Spicer, *Longitudinal Friction and Intermediate Mach Number Collisionless Transverse Magnetosonic Shocks*, Phys. Fluids, 28, 652-665, (1985)

[114] M. Lieberman, *Model of Plasma Immersion Ion Implantation*, J. Appl. Phys. 66, 2926-29, (1989)

[115] M. Widner, I. Alexeff, W. Jones and K. Lonngren, *Ion Acoustic Wave Excitation and Ion sheath Evolution, Phys. Fluids*, 13, 2532-40, (1970)

[116] S. Self and N. Ewald, *Static Theory of a Discharge Column at Intermediate Pressure*, Phys, Fluids, 12, 2486, (1966)

[117] T. Sommerer, W. Hitcheon and J. Lawler, *A Self Consistent Model of the Cathode Fall of a Glow Discharge*, Phys. Rev. A, 39, 6356-66, 1989

[118] Z. Donko and M. Janossy, *Model of the Cathode Dark Space in a Nobel Gas Mixture Discharge*, J. Phys. D, 25, 1329-39, 1991

[119] T. Sommerer, J. Lawler, and W. Hitcheon, *A Framework fot Modeling the Cathode Fall Illustrated with a Single Beam Model*, J. Appl. Phys. 64, 1774-1780, (1988)

[120] M. Lieberman, *Dynamics of a Collisional Capacitive RF Sheath*, IEEE Trans. Plasma Sci. 17, 338-341, (1989)

[121] M. Lieberman, *Spherical Shell Model of an Assymetric RF Discharge*, J. Appl Phys. 65, 4186-91, (1989)

Figure Captions:

1.1 a) The number of components on a circuit as a function of year, b) The design rules for integrated circuit manufacture.

1.2 a) A trench 0.2 microns wide by 4 microns deep in crystaline silicon. Only with plasmas can such features be fabricated economically. b) A schematic of the characteristics of anisotropic plasma and isotropic wet etches.

2.1 a) Swarm data for momentum an energy trnasfer collision frequency in oxygen. b) Data for drift velocity and characteristic energy (temperature) as a function of E/N.

2.2 Elastic (dashed) and total excitation (solid) cross section as a function of energy for electron collisions with O_2, N_2, and O.

2.3 The various regimes of a dc glow discharge.

2.4 1939 Photo of the qualitative structure of a dc glow discharge.

2.5 a) Electron temperature as a function of radius times pressure for the positive column in an unmagnetized helium discharge. The lines are various theoretical results. b) The temperature as a function of pressure for a positive column in a magnetic field of 440 Gauss. The curve is a theoretical result.

2.6 1932 data showing a) the current as a function of emitting area of the cathode, and b) the electric field as a function of distance from the cathode, both for a dc discharge.

2.7 a) Data for density and temperature as a function of current density in an argon rf discharge. b) Data for power as a function of current for the same discharge. The lines drawn are various theoretical scaling laws. The pressure is 0.3 Torr.

2.8 Input power as a function of current for an argon rf discharge at very low density (P=0.003 Torr). The lines are theoretical scaling laws.

3.1 Electron momentum exchange collision frequency in a) helium, and b) argon as a function of energy.

3.2 a) The momentum exchange collision cross section, the ionization cross section, and various electronic excitation cross sections for oxygen as a function of energy. b) Cross sections for vibrational excitations for oxygen.

3,3 a) Ionization cross sections as a function of energy for a variety of gases. b) Dissociative recombination cross section as a function of energy for typical diatomic gases.

3.4 a) Dissociative attachment coefficient for oxygen as a functionof energy. The area unit is 0.88 square angstroms. Charge exchange cross sections as a function of energy in a variety of gases for b) nitrogen and c) oxygen. d) Charge exchange cross section for N_2^+ in N_2 at much lower energy. Charge exchange cross sections for e) helium and f) argon.

4.1 a) The forward collision. b) The time reversed collision. c) the time reversed collision reflected in a plane perpendicular to the velocity of particle b.

7.1 a) Data for distribution functions in an rf discharge for a) helium and b) argon.

7.2 The distribution function calculated for nitrogen from Ref.(110) showing the drop in f as one crosses the vibrational excitation barrier.

a

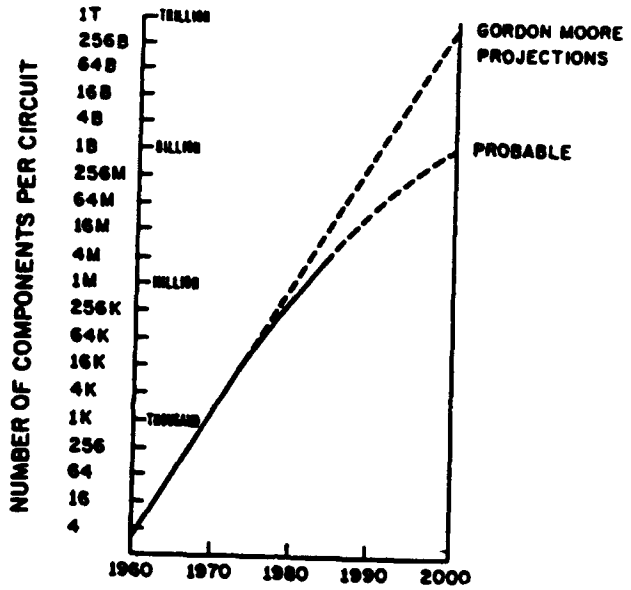
NUMBER OF COMPONENTS PER CIRCUIT
1T
256B
64B
16B
4B
1B
256M
64M
16M
4M
1M
256K
64K
16K
4K
1K
256
64
16
4
1960
1970
1980
1990
2000
GORDON MOORE PROJECTIONS
PROBABLE

b

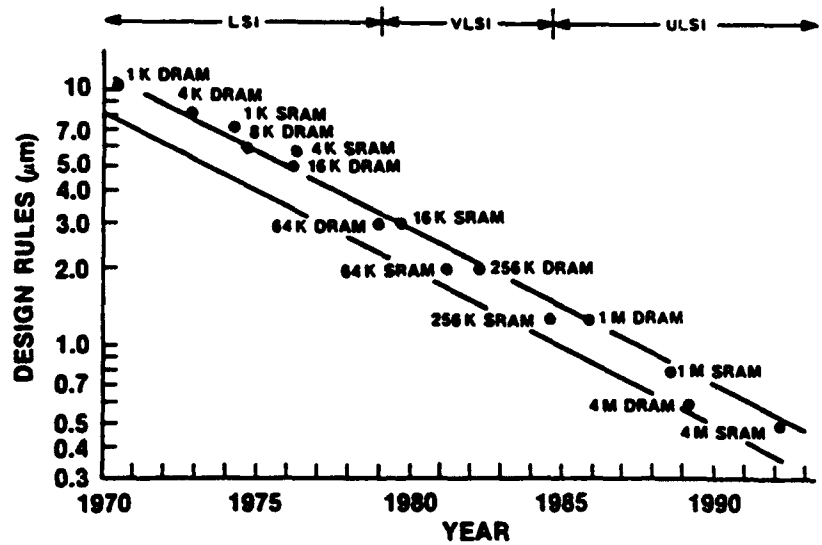
LSI
VLSI
ULSI
DESIGN RULES (μm)
10
7.0
5.0
4.0
3.0
2.0
1.0
0.7
0.5
0.4
0.3
1970
1975
1980
1985
1990
YEAR
1K DRAM
4K DRAM
1K SRAM
8K DRAM
4K SRAM
16K DRAM
64K DRAM
16K SRAM
64K SRAM
256K DRAM
256K SRAM
1M DRAM
1M SRAM
4M DRAM
4M SRAM

Figure 1.1

a

b

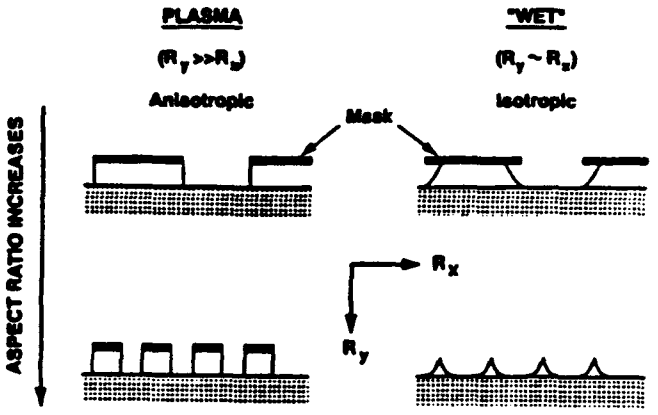
PLASMA
($R_y >> R_x$)
Anisotropic
"WET"
($R_y \sim R_x$)
Isotropic
Mask
ASPECT RATIO INCREASES
R_x
R_y

Figure 1.2

a

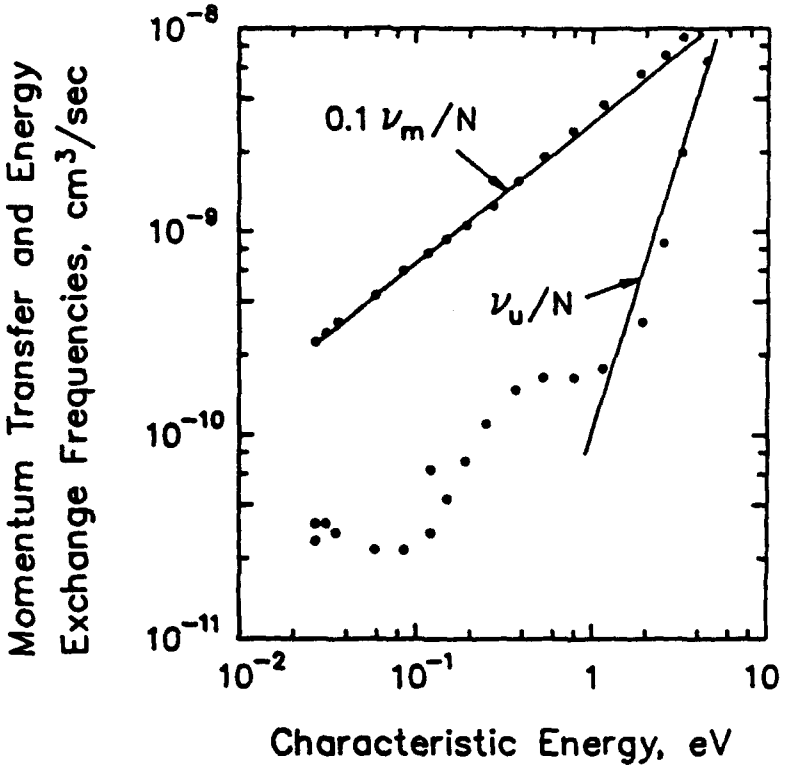
Momentum Transfer and Energy Exchange Frequencies, cm³/sec
0.1 ν_m/N
ν_u/N
Characteristic Energy, eV

b

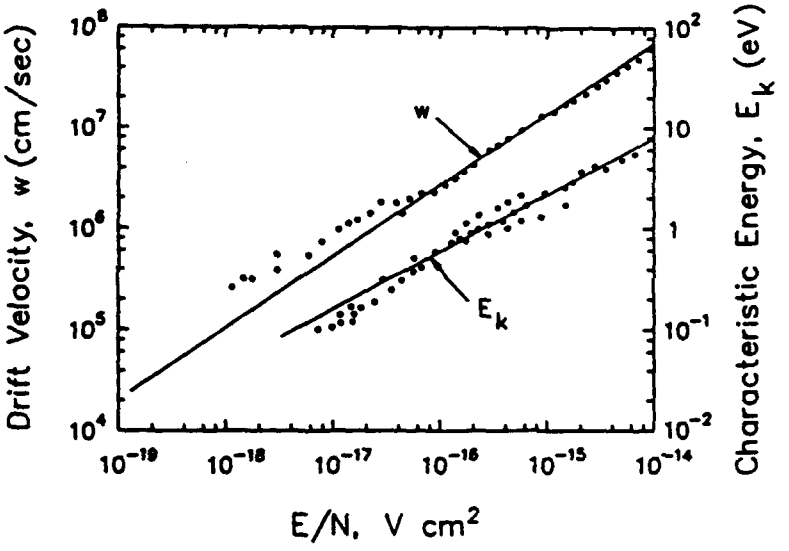
Drift Velocity, w (cm/sec)
w
E_k
Characteristic Energy, E_k (eV)
E/N, V cm²

Figure 2.1

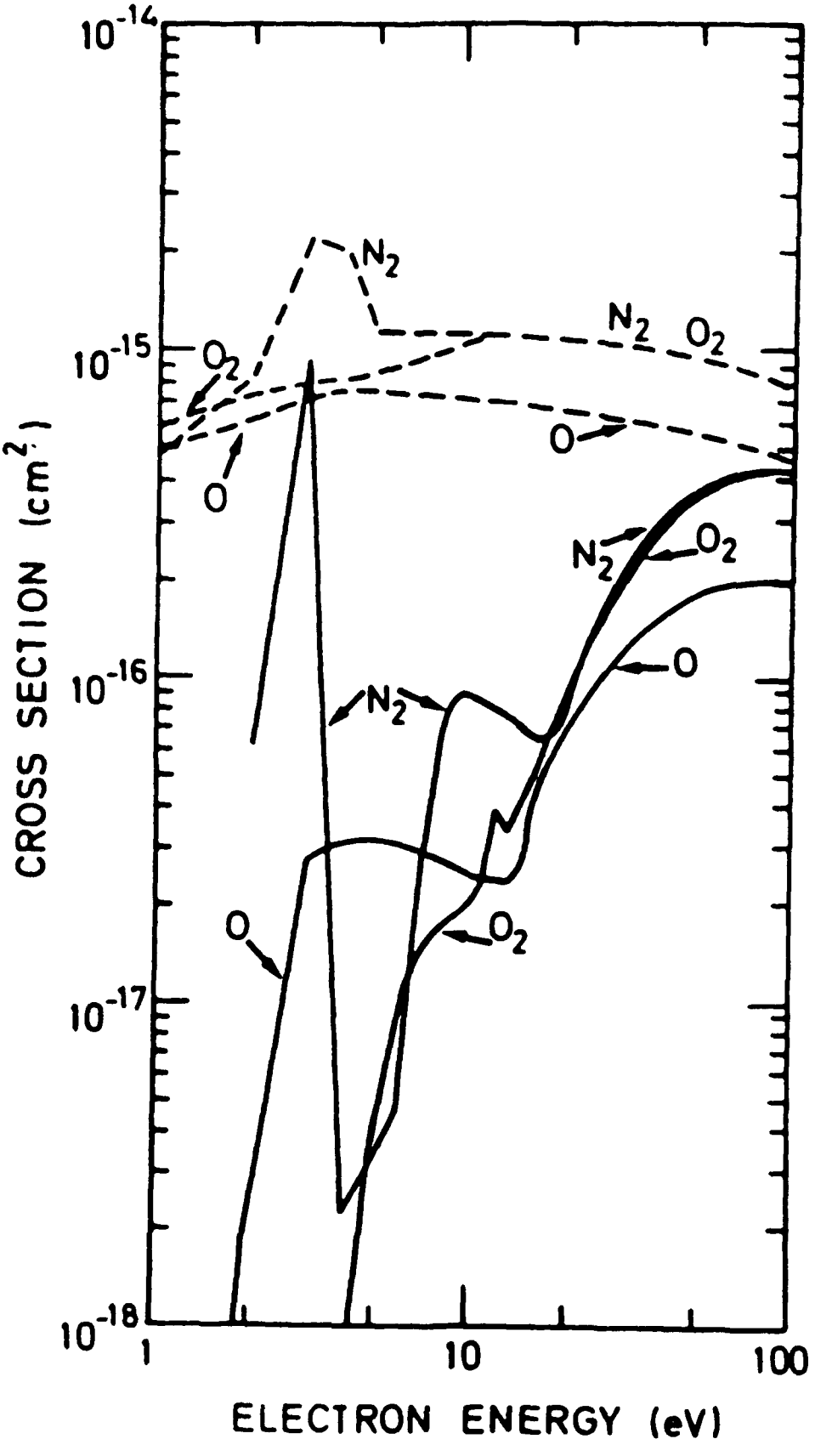
10^{-14}
10^{-15}
10^{-16}
10^{-17}
10^{-18}
CROSS SECTION (cm^2)
N_2
O_2
O
N_2 O_2
O
N_2
O_2
N_2
O
O
O_2
1
10
100
ELECTRON ENERGY (eV)

Figure 2.2

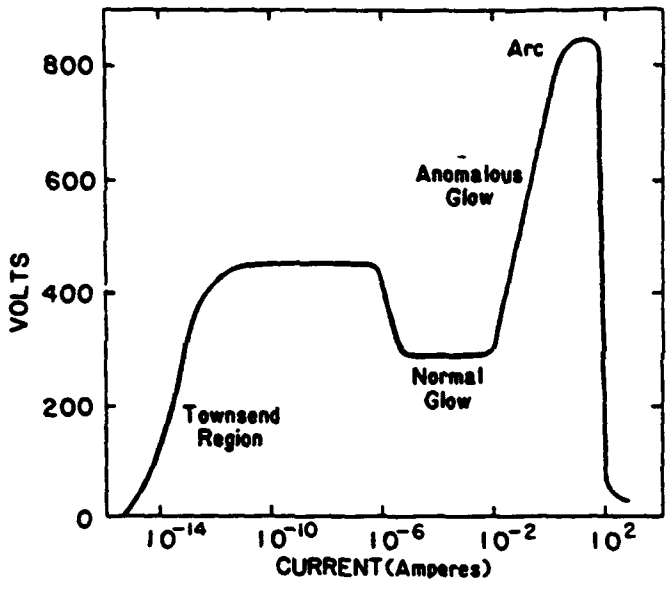
800
600
400
200
0
VOLTS
Arc
Anomalous
Glow
Normal
Glow
Townsend
Region
10^{-14}
10^{-10}
10^{-6}
10^{-2}
10^{2}
CURRENT(Amperes)

Figure 2.3

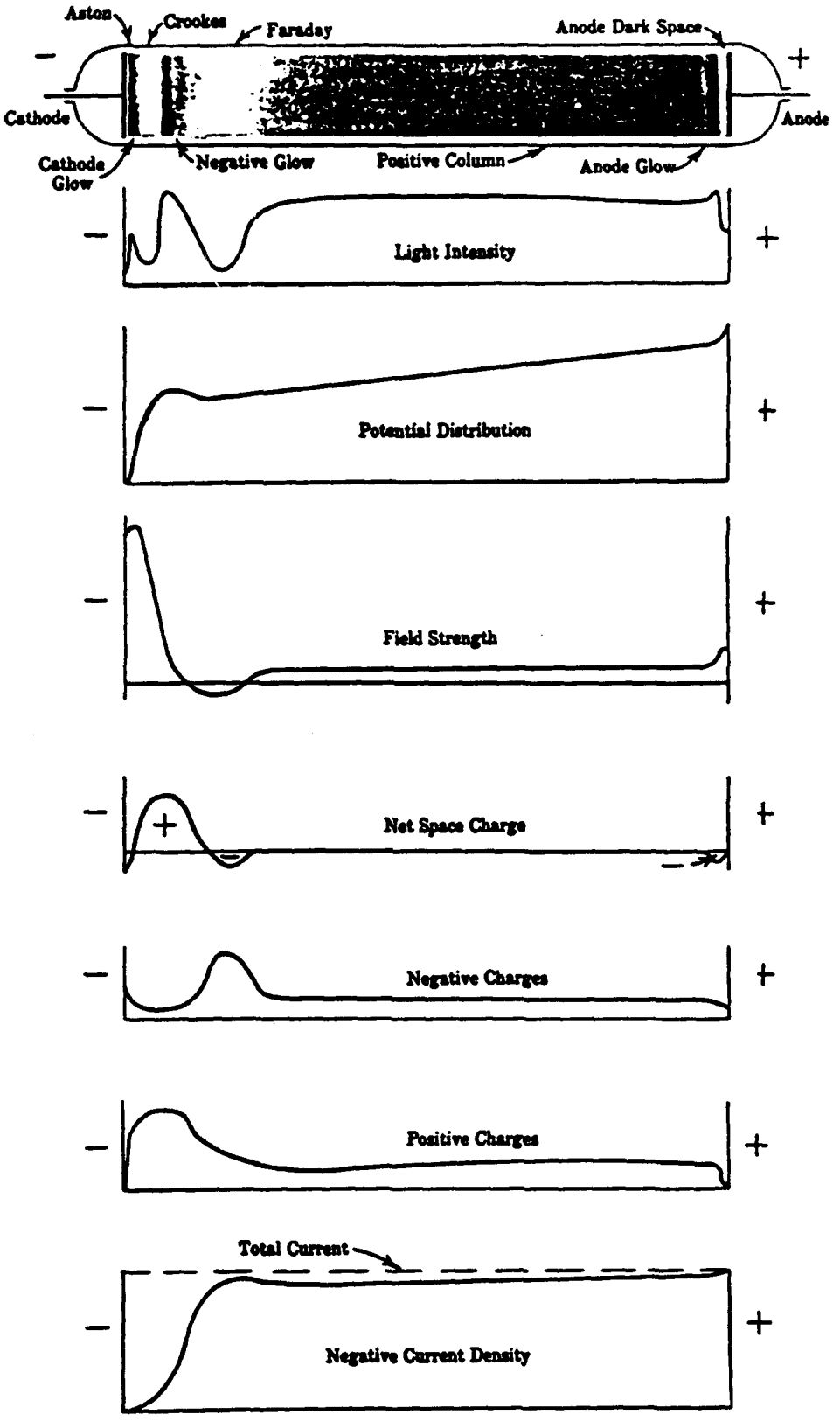
Aston
Crookes
Faraday
Anode Dark Space
−
+
Cathode
Anode
Cathode Glow
Negative Glow
Positive Column
Anode Glow
Light Intensity
Potential Distribution
Field Strength
Net Space Charge
Negative Charges
Positive Charges
Total Current
Negative Current Density

Figure 2.4

a

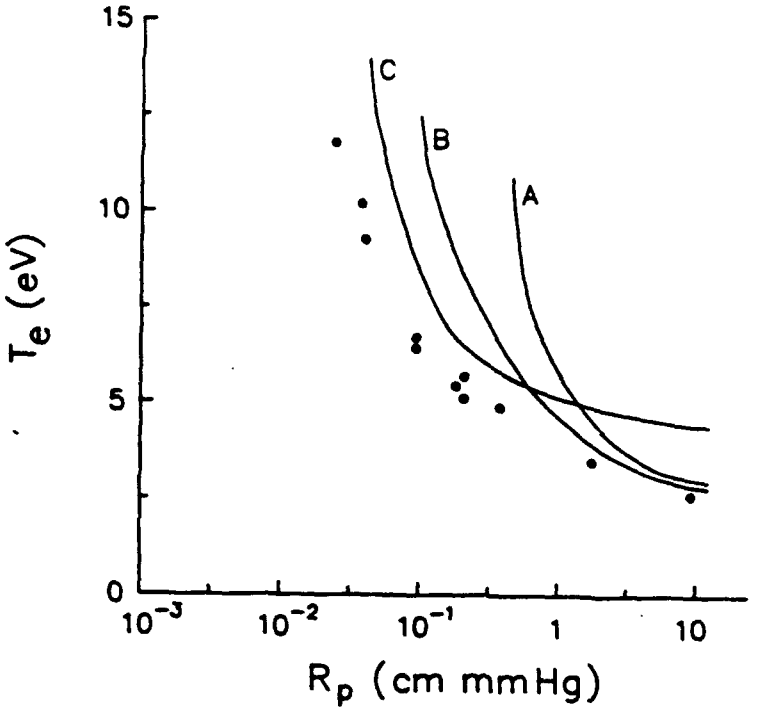
15
10
5
0
T_e (eV)
C
B
A
10^{-3}
10^{-2}
10^{-1}
1
10
R_p (cm mmHg)

b

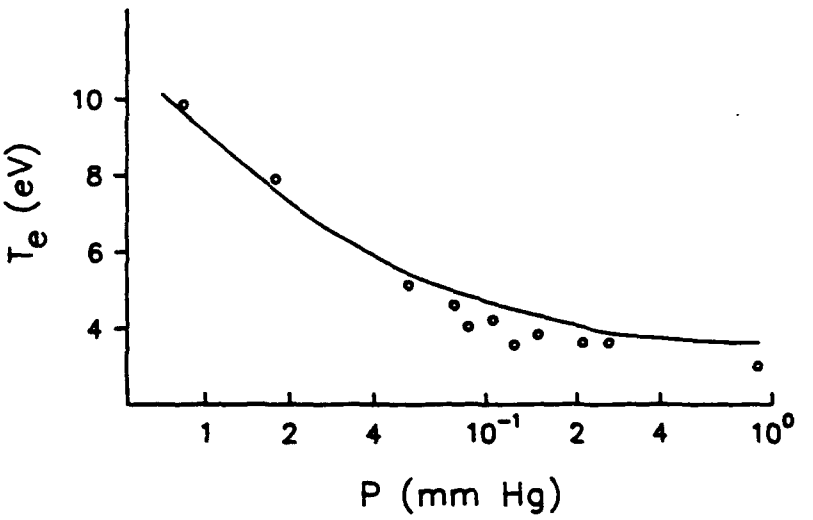
10
8
6
4
T_e (eV)
1
2
4
10^{-1}
2
4
10^0
P (mm Hg)

Figure 2.5

a

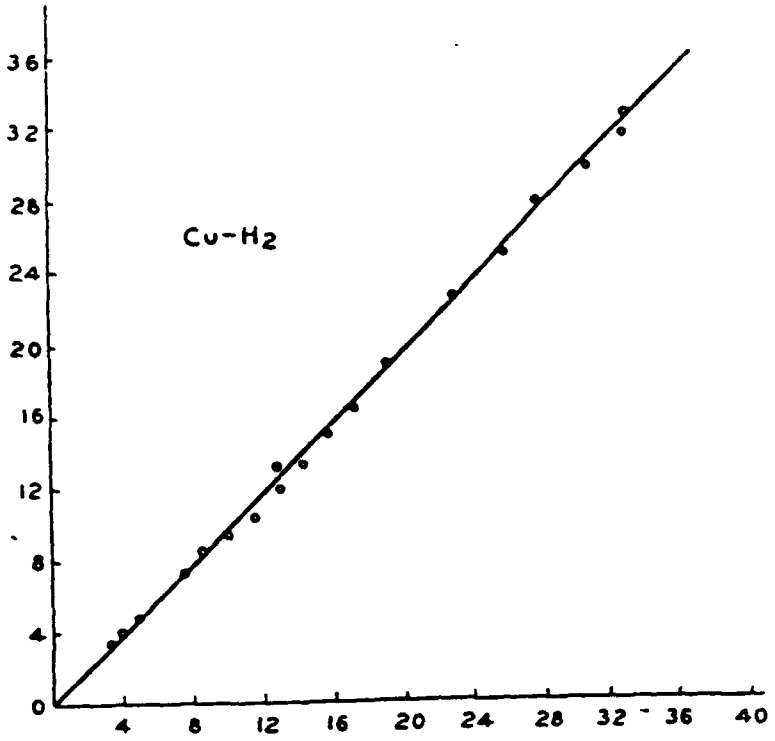
Cu-H2
0
4
8
12
16
20
24
28
32
36
40

b

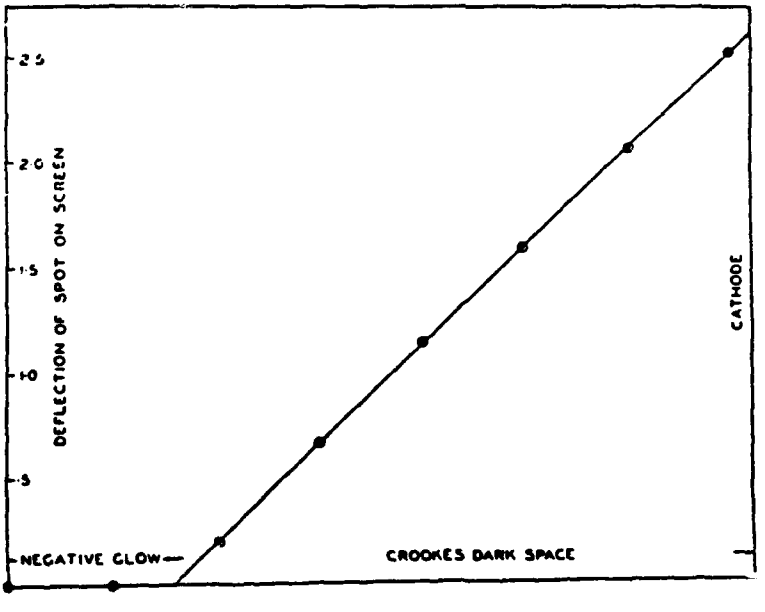
DEFLECTION OF SPOT ON SCREEN
NEGATIVE GLOW
CROOKES DARK SPACE
CATHODE

Figure 2.6

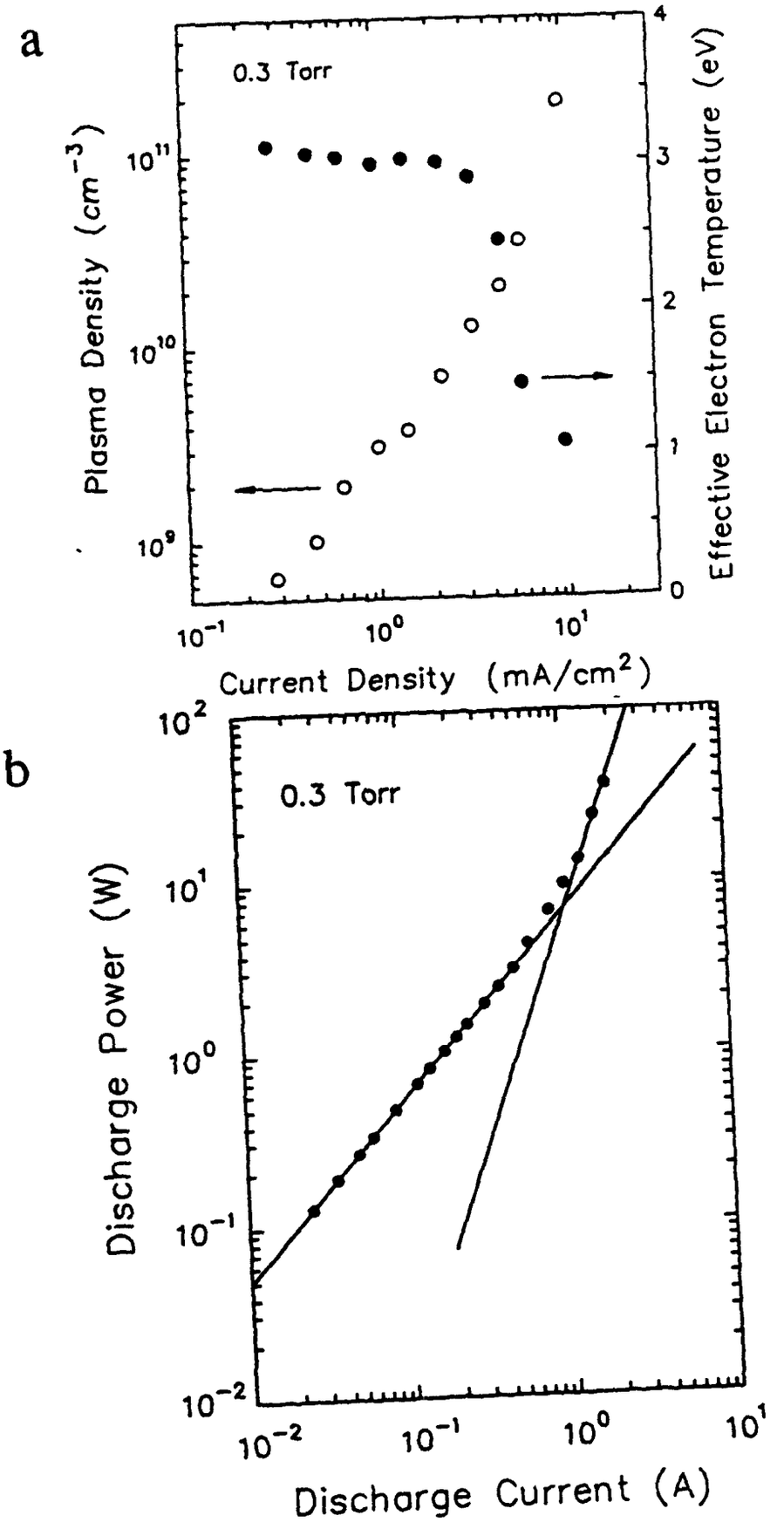
a
0.3 Torr
Plasma Density (cm^{-3})
10^{11}
10^{10}
10^{9}
Effective Electron Temperature (eV)
4
3
2
1
0
10^{-1}
10^{0}
10^{1}
Current Density (mA/cm^2)
b
0.3 Torr
Discharge Power (W)
10^{2}
10^{1}
10^{0}
10^{-1}
10^{-2}
10^{-2}
10^{-1}
10^{0}
10^{1}
Discharge Current (A)

Figure 2.7

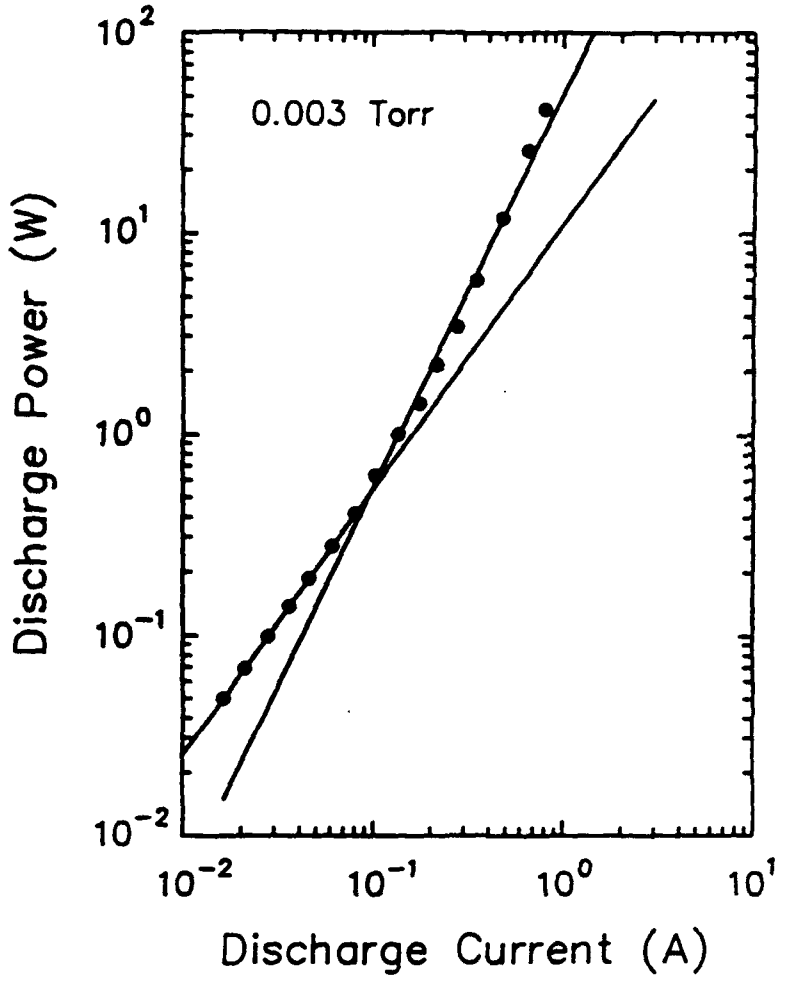
0.003 Torr
Discharge Power (W)
Discharge Current (A)
10^{2}
10^{1}
10^{0}
10^{-1}
10^{-2}
10^{-2}
10^{-1}
10^{0}
10^{1}

Figure 2.8

a

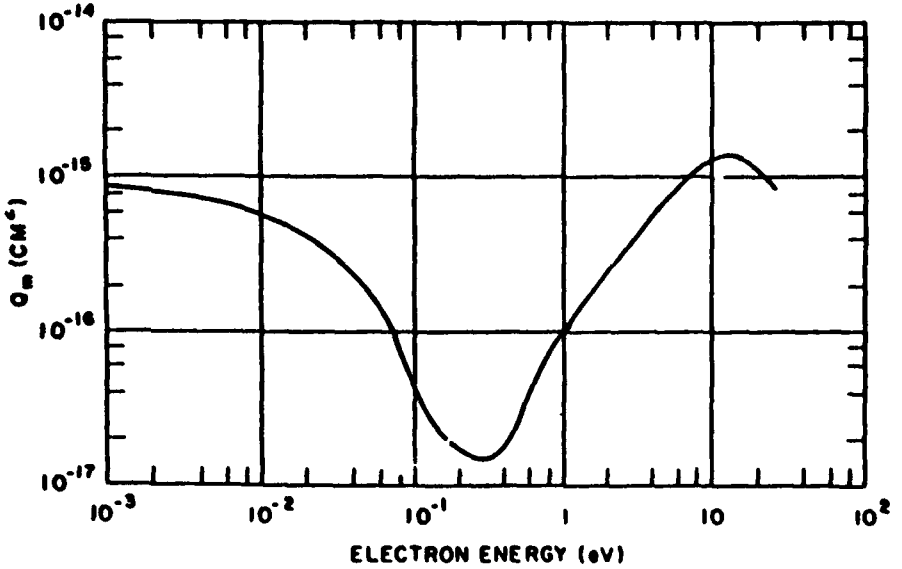
10^{-14}
10^{-15}
10^{-16}
10^{-17}
σ_m (cm^2)
10^{-3}
10^{-2}
10^{-1}
1
10
10^2
ELECTRON ENERGY (eV)

b

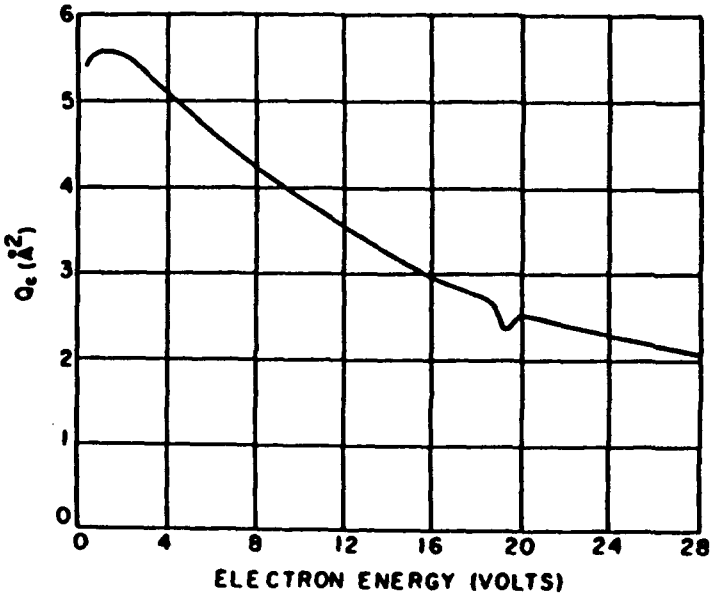
6
5
4
3
2
1
0
σ_c (Å^2)
0
4
8
12
16
20
24
28
ELECTRON ENERGY (VOLTS)

Figure 3.1

a

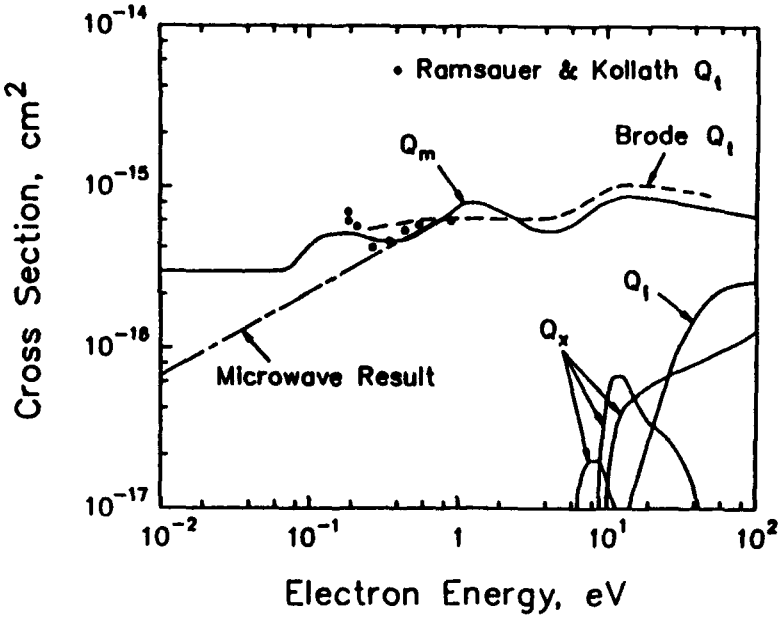
Cross Section, cm^2
10^{-14}
10^{-15}
10^{-16}
10^{-17}
• Ramsauer & Kollath Q_t
Q_m
Brode Q_t
Q_t
Q_x
Microwave Result
10^{-2}
10^{-1}
1
10^{1}
10^{2}
Electron Energy, eV

b

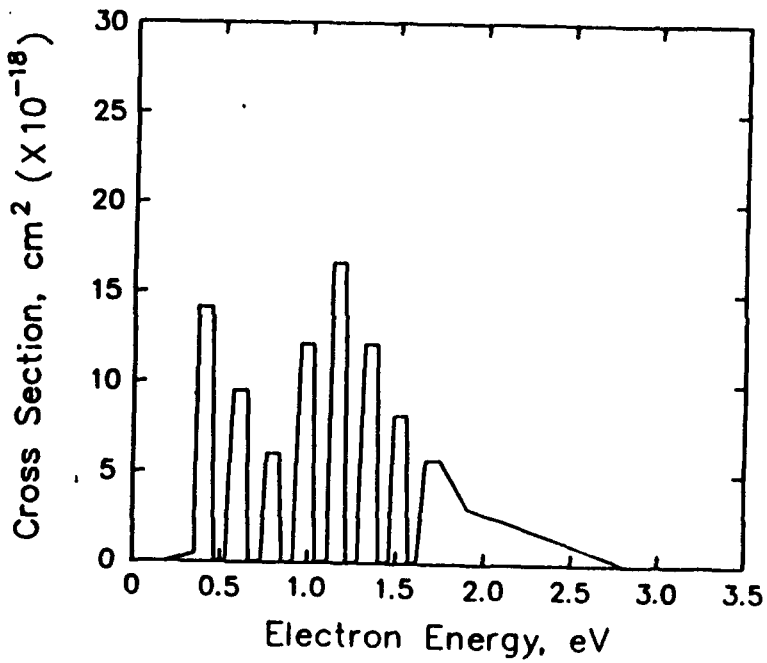
Cross Section, cm^2 ($\times 10^{-18}$)
30
25
20
15
10
5
0
0
0.5
1.0
1.5
2.0
2.5
3.0
3.5
Electron Energy, eV

Figure 3.2

a

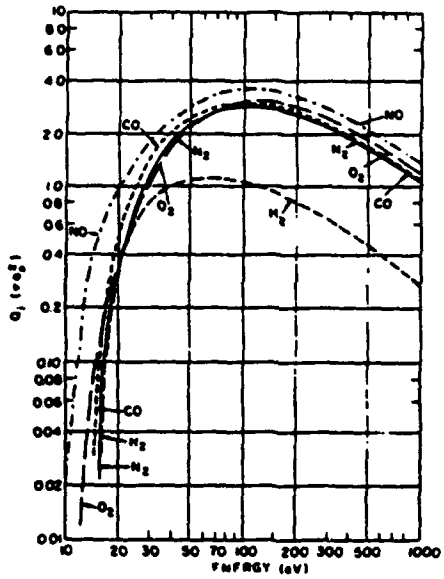
CO
NO
N_2
O_2
H_2
ENERGY (eV)

b

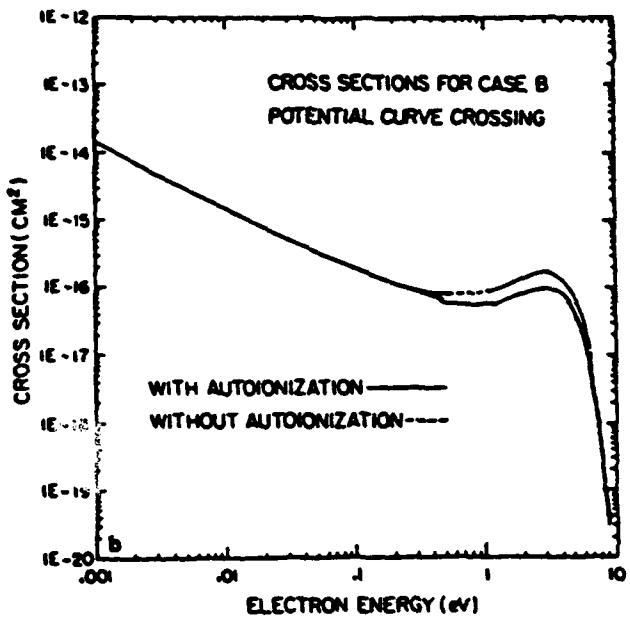
CROSS SECTIONS FOR CASE B
POTENTIAL CURVE CROSSING
WITH AUTOIONIZATION
WITHOUT AUTOIONIZATION
CROSS SECTION (CM²)
ELECTRON ENERGY (eV)
b

Figure 3.3

a

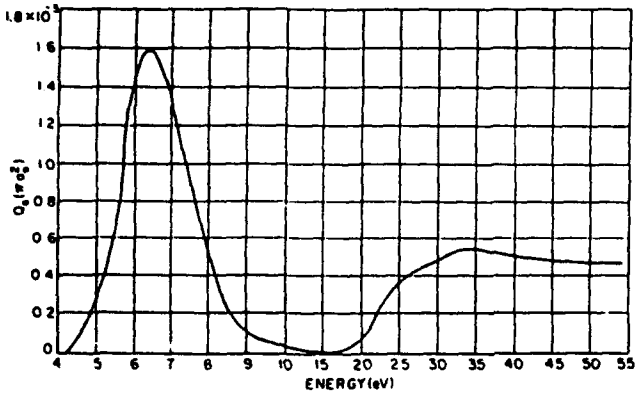

b

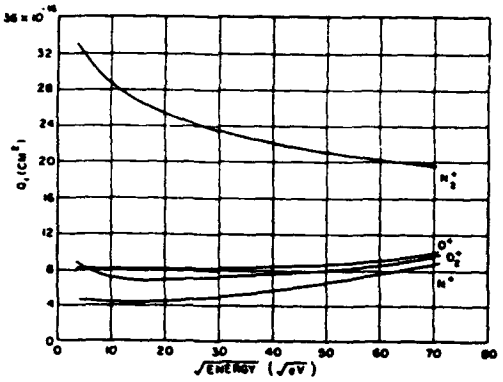

c

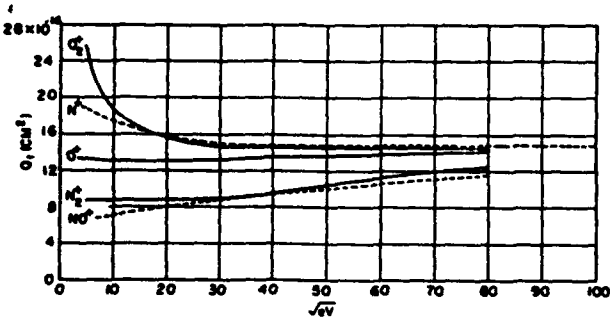

d

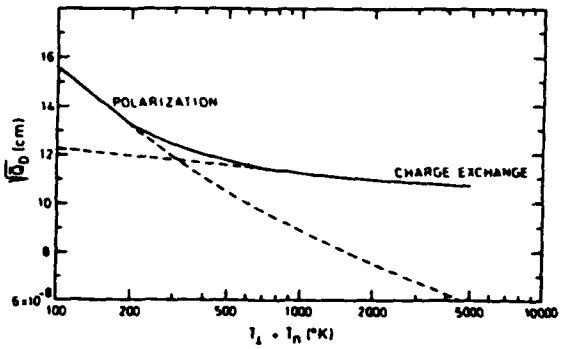

e

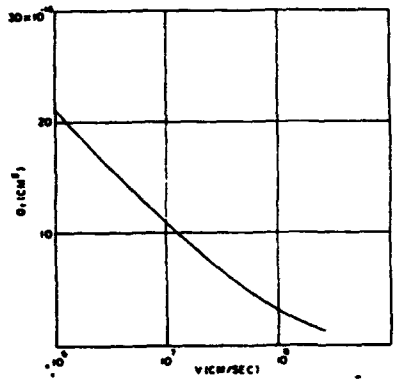

f

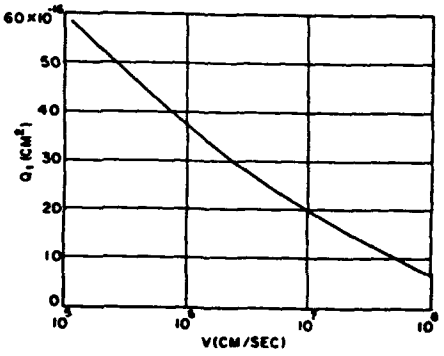

Figure 3.4

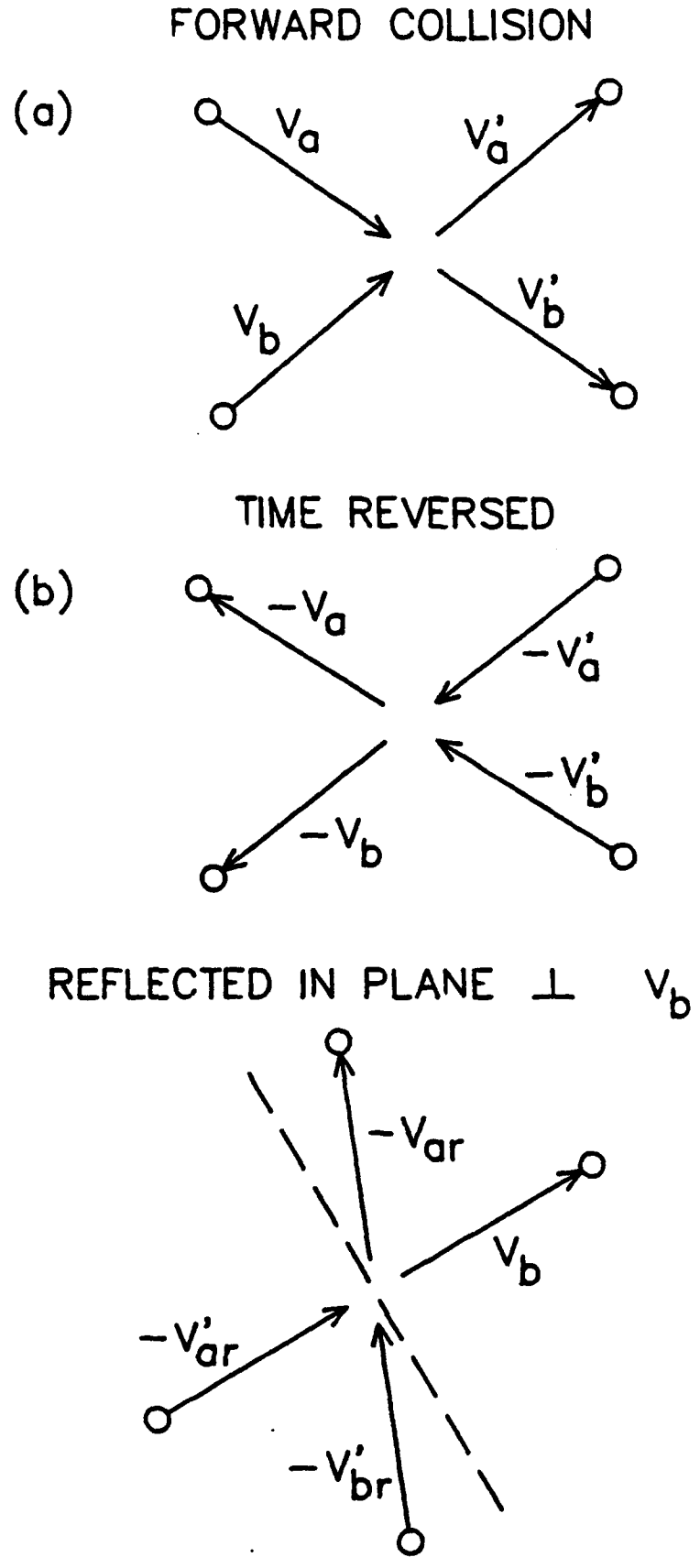
FORWARD COLLISION
(a)
V_a
V_a'
V_b
V_b'
TIME REVERSED
(b)
$-V_a$
$-V_a'$
$-V_b'$
$-V_b$
REFLECTED IN PLANE ⊥ V_b
$-V_{ar}$
V_b
$-V_{ar}'$
$-V_{br}'$

Figure 4.1

a

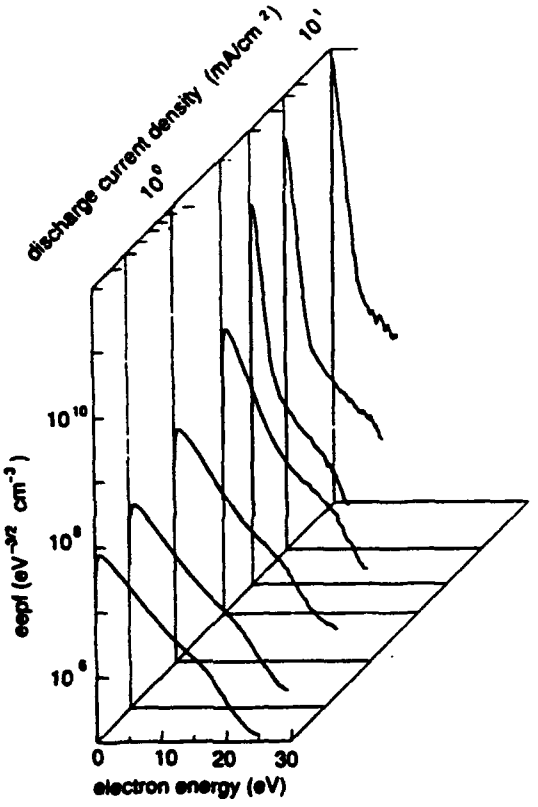
discharge current density (mA/cm²)
10⁰
10¹
10¹⁰
10⁸
10⁶
eepf (eV⁻³/² cm⁻³)
0
10
20
30
electron energy (eV)

b

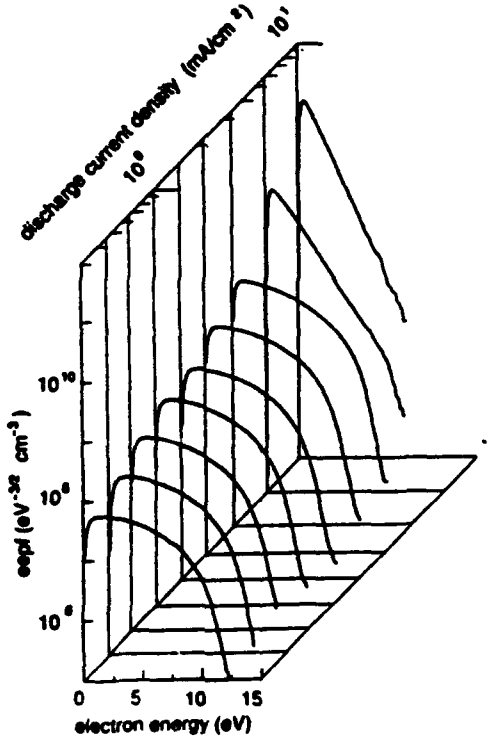
discharge current density (mA/cm²)
10⁰
10¹
10¹⁰
10⁸
10⁶
eepf (eV⁻³/² cm⁻³)
0
5
10
15
electron energy (eV)

Figure 7.1

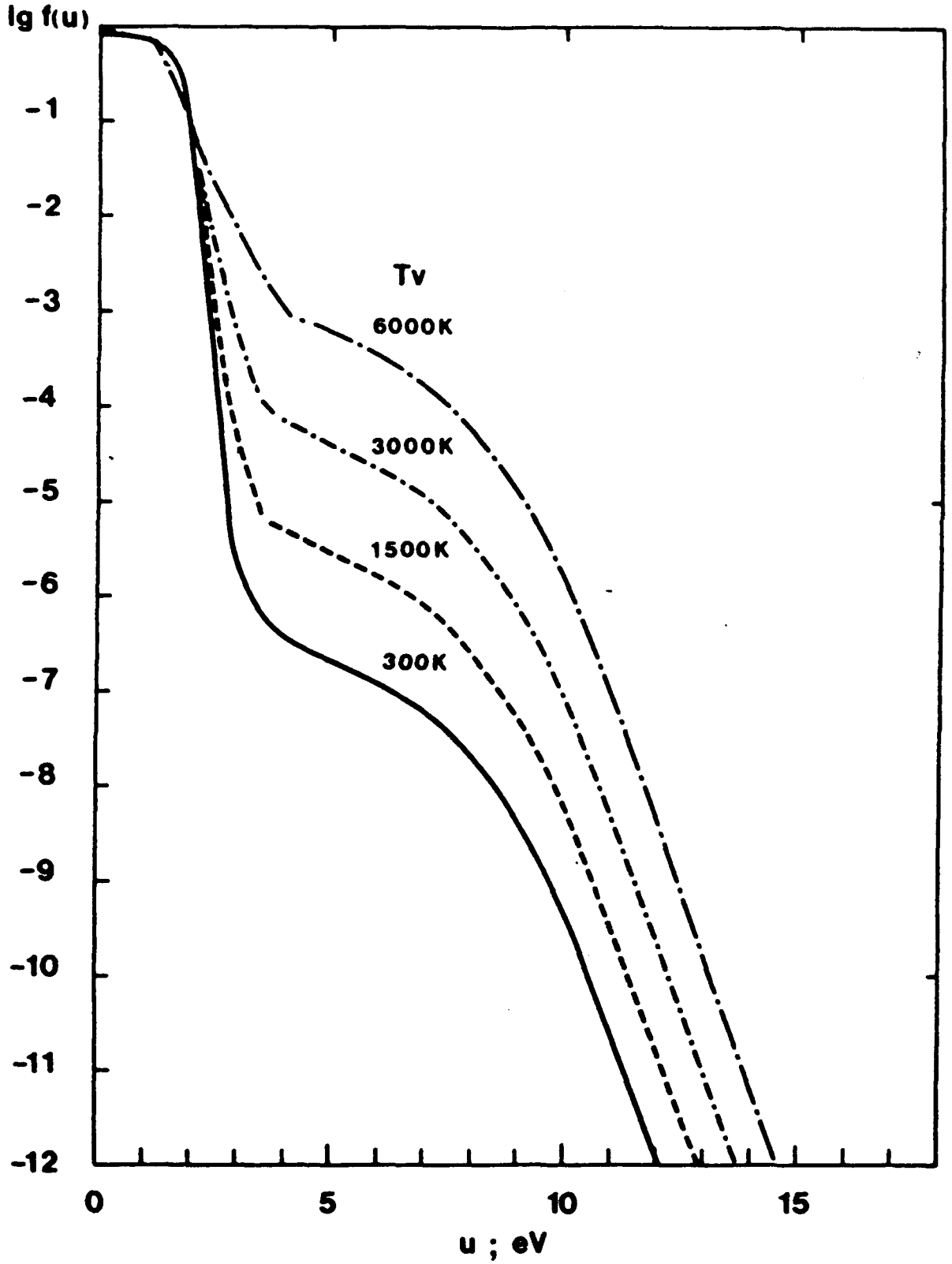

Figure 7.2